RESEARCH AND DEVELOPMENT TECHNIQUE FOR ESTIMATING AIRFLOW AND DIFFUSION PARAMETERS RELATED TO THE ATMOSPHERIC WATER RESOURCES PROGRAM

Final Report

Prepared by

M. M. Orgill

J. E. Cermak

L. O. Grant

Period September 1969 to September 1971

Prepared for

Division of Atmospheric Water Resources Management

Bureau of Reclamation

Denver Federal Center

Denver, Colorado 80521

Contract No. 14-06-D-6842

Fluid Dynamics and Diffusion Laboratory

Department of Civil Engineering, and

Department of Atmospheric Science

College of Engineering

Colorado State University

Fort Collins, Colorado 80521

CER71-72-MMO-JEC-LOG-20

PREFACE

The realization of quantitative information on transport-dispersion over irregular terrain presents a complex theoretical and operational problem for weather modification and air-pollution programs. To date most of the information on this subject has been collected from limited field programs located in the Western States.

In this study physical modeling in a special meteorological wind tunnel was investigated as a possible tool for assisting field programs with this complex problem. The results from this study reveal that physical modeling, even with its inherent limitations, can provide useful and practical data for assisting operational weather modification and other diffusion-oriented programs, especially during the pre-operational or research stages.

The complexity of a joint laboratory and field program required the assistance of several people and groups. We would like to acknowledge the assistance received from the following persons and groups: Western Scientific Services, Inc., Fort Collins; EG and G, Durango; Mee Industries, Inc.; Dr. G. Langer and The Flight Facility of the National Center of Atmospheric Research; Natural Resources Research Institute, University of Wyoming; staff and students of the Fluid Dynamics and Diffusion Laboratory; staff and students of the Department of Atmospheric Science and the Colorado State University Flight Facility.

TABLE OF CONTENTS

Section		Page
I	INTRODUCTION	12
	Statement of Problem	12
	Background	12
	Purpose, Goals and Method	13
	Procedures for Completing Objectives	14
II	LABORATORY SIMILITUDE AND DISPERSION MODELS	15
	Transport and Dispersion Over Irregular Terrain	15
	Types of Laboratory Airflows	18
	Restrictions on Laboratory Airflows	18
	General Similitude Requirements	20
	Laboratory Airflow Models	21
III	EAGLE RIVER VALLEY - CLIMAX STUDY	24
	Field Experimental Program	24
	1. Network of generators	24
	2. Criteria for experimental day	24
	3. Special field programs	26
	4. Field results	28
	Laboratory Experimental Program	30
	1. Topographic model	30
	2. Laboratory simulation facility	30
	3. Boundary conditions	40
	4. Experiments	40
	Comparison of Laboratory and Field Data	40
	1. Verification of similarity criteria	40
	2. Dispersion similarity	43
IV	ELK MOUNTAIN STUDY	49
	Field Data	49
	Laboratory Experimental Program	50
	1. Topographic model	50
	2. Laboratory simulation facility	50
	3. Boundary conditions	50
	4. Experiments	50
	Comparison of Laboratory and Field Data	55
	1. Neutral airflow	55
	2. Barostromatic airflow	57
V	SAN JUAN MOUNTAIN STUDY	64
	Field Experimental Program	64
	1. Generator network	64
	2. Criteria for experimental day	64
	3. Field data	64
	Laboratory Experimental Program	67
	1. Topographic model	67
	2. Laboratory simulation facility	70
	3. Boundary conditions	70
	4. Experiments	70

TABLE OF CONTENTS - (Continued)

Section		Page
	Results of Wind-Tunnel Laboratory Experiments	73
	1. Similitude conditions	73
	2. Dispersion results	77
VI	SUMMARY, CONCLUSIONS AND RECOMMENDATIONS	92
	Summary	92
	Conclusions	95
	Recommendations	96
	APPENDIX - REVIEW OF SIMILITUDE CRITERIA	98
	Basic Equations	98
	Boundary Conditions	99
	Similitude Criteria	99
	Partial Similitude	103
	Scale Distortion	104
	GLOSSARY OF TERMS	105
	REFERENCES	107
	BIBLIOGRAPHY - List of Reports and Papers Written in Relation to This Project	110

LIST OF FIGURES

Figure		Page
2-1	Schematic illustration of atmospheric motion and transport-dispersion over irregular terrain	17
3-1	Eagle River Valley-Climax topography and boundaries of topographic model	25
3-2	Square of the total vector separation R^2 versus time. Dual flight #4 in the Camp Hale area	29
3-3	Potential and equivalent potential temperature distributions with height at Camp Hale, Colorado. December 12 and 15, 1970	32
3-4	Silver-iodide concentration distribution over three different regions of the Eagle River Valley-Climax area. December 12, 1970	33
3-5	Silver-iodide concentration distribution over different regions of the Eagle River Valley-Climax area. December 15, 1970	34
3-6	Silver-iodide concentration distribution over different regions of the Eagle River Valley-Climax area. December 15, 1970	35
3-7	The approximate horizontal dispersion of silver-iodide seeding material at 13,000 feet m.s.l. as released from Minturn and Redcliff sources. March 12, 1970	36
3-8	Eagle River Valley topographic model during construction and in wind tunnel	37
3-9	Colorado State University low-speed recirculation wind tunnel.	39
3-10	Laboratory experimental arrangement for measuring radioactive Krypton-85 concentration	41
3-11	Laboratory experimental arrangement for obtaining measurements of the radioactive Krypton-85 concentration over the model for the barostromatic airflow	42
3-12	Comparison of selected field potential temperature vertical profiles with a barostromatic model temperature profile	44

LIST OF FIGURES - (Continued)

Figure		Page
3-13	Comparison of field and model bulk Richardson numbers at the Camp Hale location	45
3-14	Comparison between the vertical rise of model and field tracer plumes	47
3-15	Comparison of normalized surface-release axial-concentration measurements for models, Pasquill categories and non-mountainous experimental data . . .	48
4-1	Elk Mountain and surrounding topography modeled in wind tunnel	51
4-2	Colorado State University meteorological recirculation wind tunnel	52
4-3	Schematic illustration of the wind tunnel experimental setup for barostromatic airflow	53
4-4	Upstream boundary conditions for the barostromatic airflow. Elk Mountain study	54
4-5	Surface wind directions and streamlines in neutral airflow over Elk Mountain model	56
4-6	Surface distribution of radioactive Krypton-85 gas around Elk Mountain. Neutral airflow	58
4-7	Vertical cross-section of radioactive Krypton-85 gas over Elk Mountain. Neutral airflow	59
4-8	Comparison of bulk Richardson number height profiles for barostromatic airflow and field. Elk Mountain study	60
4-9	Surface distribution of radioactive Krypton-85 gas around Elk Mountain. Barostromatic airflow	62
4-10	Vertical cross-section of radioactive Krypton-85 gas over Elk Mountain. Barostromatic airflow	63
5-1	Potential and equivalent potential temperature and horizontal wind distribution at Durango, Colorado. April 22, 1970	66
5-2	Location of field generator sites that were modeled for the San Juan topographic model	68
5-3	Types of sources designed and utilized on the model for emitting radioactive gas	71

LIST OF FIGURES - (Continued)

Figure		Page
5-4	Schematic diagrams of the Colorado State University environmental wind tunnel and upstream boundary conditions	72
5-5	Vertical cross-sectional view of the airflow and turbulence fields over the topographic model.	75
5-6	Comparison of the model wind velocity profiles for different upstream conditions and a field velocity profile	76
5-7	Pictures illustrating time variation of smoke plume in the wind tunnel	79
5-8	Turning of the wind direction and speed changes as measured in the west fork of the San Juan River Valley.	80
5-9	Ground deposit as the result of chemical smoke from different simulated sources	81
5-10	Distribution of radioactive concentration for two lateral cross-sections over the model. Source: Pagosa Springs.	82
5-11	Distribution of radioactive concentration for two lateral cross-sections over the model. Source: Oak Brush Hill.	83
5-12	Distribution of radioactive concentration for two lateral cross-sections over the model. Source: Carracas Mesa	84
5-13	Distribution of radioactive concentration over Wolf Creek Pass cross-section as the result of multiple sources	87
5-14	Distribution of radioactive concentration over Wolf Creek Pass cross-section as the result of multiple sources	88
5-15	Ground level plumes as affected by the airflow over Oak Brush Hill.	89
5-16	Distribution of radioactive concentration over Wolf Creek Pass cross-section. Barostromatic airflow. Sources: Oak Brush Hill and Eight Mile Mesa	90

LIST OF TABLES

Table		Page
3-1	Special Field Program Dates for the Eagle River Valley-Leadville Area	27
3-2	Estimates of the Vertical and Horizontal Transport and Maximum Elevation of Seeding Material as Determined by Aircraft Sampling Over the Eagle River Valley	31
3-3	Performance Characteristics of Colorado State University Low-Speed Wind Tunnels	38
4-1	Elk Mountain Study-Horizontal and Vertical Dispersion of Radioactive Gas From Source #6	61
5-1	EG and G Project Generator Sites for the San Juan Mountain Area and Sites Modeled on the San Juan Topographic Model	69
5-2	Approximate Plume Widths and Heights at Two Downstream Cross-Sections for Different Groups of Sources. San Juan Study	85

LIST OF SYMBOLS

Symbol	Definition
C	Concentration of a diffusing material, e.g., silver iodide and Krypton-85
C_D	Drag coefficient
C_p, C_{p_d}	Specific heat at constant pressure (dry air)
$\mathcal{D}$	Depletion and deposition mechanisms acting on a particulate plume
D_y	Lateral transport or dispersion of a particulate plume
D_z	Vertical transport or dispersion of a particulate plume
f	Coriolis parameter $2\Omega\sin\phi$
g	Acceleration of gravity
H	Planetary boundary layer thickness
h_s	Height of source above the ground
i_x, i_y, i_z	Longitudinal, lateral and vertical intensity of turbulence
K_H	Coefficient of exchange of heat
K_M	Coefficient of exchange of momentum
$K_x, K_y, K_z; K_i$	Coefficients of eddy viscosities in the x , y and z directions
K_{ii}	Coefficients of turbulent diffusivities for mass in x , y and z directions
K	Coefficient for thermal diffusivity
K_c	Constant coefficient for mass diffusivity
k	Coefficient of thermal conductivity and von Karman constant
k_m	Coefficient of molecular diffusivity
L	Reference length
P	Atmospheric pressure
Q	Source strength; time rate of material emission from a continuous point source; also, heat flux

LIST OF SYMBOLS - (Continued)

Symbol	Definition
Q_E	Latent heat of evaporation and evapotranspiration
Q_G	Transfer of heat through the ground
Q_H	Turbulent transfer of sensible heat to the atmosphere
$Q_{L\uparrow}$	Long-wave radiation emitted by the surface
$Q_{L\downarrow}$	Long-wave radiation received by the surface from the atmosphere
Q_R	Short-wave radiation reflected from the earth
Q_T	Short-wave radiation from sun and sky
R_d	Specific gas constant for dry air
$\vec{r}$	Three dimensional vector for position
T	Temperature; travel time
T_s	Temperature of source material
$t;t_s$	Time; sampling time
U	Reference velocity
$\overline{U}$	Mean wind speed effecting a dispersing tracer plume
U_∞	Freestream velocity
U_i	Velocity components in x , y and z directions
$\vec{U}$	Total velocity vector
$\vec{U}_g$	Geostrophic or freestream velocity
U_*,u_*	Friction velocity
u_i'	Velocity fluctuations in x , y and z directions
w_s	Source efflux velocity
x,y,z	Distances along longitudinal, lateral and vertical directions
$X;Z$	Reference lengths; height of terrain
$\vec{Z}$	Three dimensional terrain

LIST OF SYMBOLS - (Continued)

Symbol	Definition
z_o	Surface roughness length
α	Distortion factor indicating degree of scale exaggeration
β	Stability parameter
$\Delta T, \Delta\theta$	Vertical temperature change
ε	Eddy energy dissipation
θ	Potential temperature
θ_e	Equivalent potential temperature
Λ	Size of mean eddies
λ	Height of roughness features; e.g., trees, large rocks, etc.
ν	Coefficient of kinematic viscosity
ρ	Air density
$\sigma_u, \sigma_w, \sigma_v; \sigma_i$	Standard deviation of the velocity components
σ_θ	Standard deviation of lateral (horizontal) wind-direction distribution
σ_{ij}	Reynolds stresses
$\overline{\sigma}_{ij}$	Viscous stresses
τ	Shear stress
τ_o	Surface shear stress
$\overline{\Phi}$	Energy dissipation function
Ω	Angular rotation of the earth
δ_{ij}	Kronecker delta $\delta_{ij} = \begin{matrix} 1 & i=j \\ 0 & i\neq j \end{matrix}$
ε_{ijk}	Permutation symbol $\varepsilon_{123} = \varepsilon_{231} = \varepsilon_{312} = +1$ $\varepsilon_{321} = \varepsilon_{213} = \varepsilon_{132} = -1$ all others = 0

LIST OF SYMBOLS - (Continued)

Symbol	Definition
Subscripts	
$]_M$	Pertain to model
$]_F$	Pertain to field
o	Reference quantity
Superscripts	
'	Indicates fluctuation quantity
—	Indicates average quantity
→	Vector quantity

I. INTRODUCTION

Statement of Problem

Several weather modification field programs are now in progress to augment water resources in the western states by artificially seeding wintertime orographic cloud systems. Artificial ice nuclei in the form of silver-iodide smoke are released from ground-based, air-borne or rocket-borne generators in the natural airstream where wind transport, mechanical turbulence and convection currents are expected to carry and disperse the seeding material into supercooled water clouds and thus, initiate precipitation by the Bergeron ice-crystal process.

One of the greatest areas of uncertainty within a winter orographic cloud-seeding program is that of obtaining the optimal distribution of seeding material within the cloud system. The complexity and variability of airflow over mountains is well known. The seeding material may be trapped, channeled and forced to flow over as well as around mountain barriers. Plume width, depth and direction may change as atmospheric stability, wind speed and direction change. In addition, the number of effective nuclei may change as the result of temperature variations and depletion mechanisms.

Successful cloud seeding of orographic clouds depends upon the introduction of sufficient artificial nuclei (e.g., silver iodide) into supercooled clouds to obtain optimum crystal concentrations. If the concentration of crystals in the cloud should be less than the optimum concentration, then not all of the vapor provided by the orographic updraft can be readily condensed upon the snow crystals. When the concentration of crystals is above the optimum number, overseeding may occur and the resultant precipitation may be less than would have occurred naturally.

The realization of the delivery of the optimal distribution of seeding material to orographic cloud systems presents a complex theoretical and operational problem. In order to help solve this complex problem several questions need to be answered in a quantitative manner. Such questions are:

1) Under given storm conditions, will artificial freezing nuclei reach the target area?
2) How much of the cloud volume will be covered (i.e., horizontal and vertical dimensions of seeding plume), and in what concentration?
3) What are the effects of stability, wind shear, orographic features and other natural factors in dispersion of the seeding material?

Background

The physical basis for modifying cold orographic clouds by artificial seeding has been discussed by Bergeron (Ref. 3), Ludlam (Ref. 23), Grant et al., (Ref. 18) and Chappell (Ref. 7). The orographic clouds which form along and windward of the mountain ranges over the western United States are frequently composed of supercooled liquid droplets. The temperature activation spectrum of natural nuclei is such that the number of effective natural ice-nuclei does not meet cloud requirements for converting the cloud water to ice form at the warmer cloud

temperatures and higher condensation rates. In such cases snow may not develop or the precipitation process may be inefficient.

If artificial ice nuclei can be activated in the saturated orographic stream far enough upwind of the mountain barrier, a more efficient conversion of cloud water to ice crystals should result in increased snowfall. Otherwise, the unconverted cloudwater evaporates to the lee of the mountain barrier. The modification potential associated with these microphysical processes has been designated as "static modification potential" by Chappell (Ref. 7). A "dynamic modification potential" may also exist when seeding alters buoyancy effects within the cloud system by changing the latent heat release in ascending air parcels. This may result in warming of the cloud system, increase cloud tops or alter the vertical motion field over the orographic barrier. The overall result could be to change the rate of condensation or cloud geometry during seeded conditions (Ref. 7).

Grant et al., (Ref. 17) have developed a simple model for showing the variation of optimum ice-nuclei concentration as a function of cloud system temperatures. The optimum ice-nuclei concentration was defined as that which enabled the cloud system to grow ice by diffusion at a given condensation rate. Chappell (Ref. 7) has derived a physical model of the cold orographic cloud system in a climatological mode suitable for testing with results from cloud seeding experiments at Climax and San Juan mountain areas in Colorado. A parameterized numerical model for simple two-dimensional representation of orographic precipitation has been derived by Willis (Ref. 35). The latter two models consider the physical effects of artificial seeding but not the transport and dispersion aspect.

The early literature on the delivery of seeding material to orographic cloud systems has been summarized by Orgill et al., (Ref. 30). Current research efforts on this subject are under investigation in Wyoming (Ref. 2), Colorado (Refs. 30 and 31), Montana (Ref. 32) and other western states.

Purpose, Goals and Method

The overall purpose of this research is to develop laboratory physical models as a tool for modeling the atmospheric planetary boundary-layer over mountainous terrain and the transport-dispersion of a passive tracer material simulating the silver-iodide seeding material. A second phase of the research involves obtaining limited field data that will assist in enlarging our understanding of the transport-diffusion process in the field and also providing relevant data to check on the laboratory physical models. The more specific objectives for the research were as follows:

1) Investigate and review the mathematical aspects of similarity for atmospheric transport and dispersion of particulate material, such as silver-iodide, over complex terrain.
2) Determine the full capability for laboratory simulation of airflow over complex roughness features.
3) Evaluate the use of laboratory simulation of airflow and transport for various types of orographic terrain as related to weather modification operations.
4) Obtain field information on the relative dispersion and transport characteristics of tracers with particle sizes ranging from meter to molecular sizes.

5) Establish modeling criteria for future operational programs in weather modification.

The laboratory or wind tunnel method consists of obtaining concentration measurements of a dispersing tracer material over a scale model of selected terrain placed in a simulated atmospheric flow. Standard field measurements of temperature, wind direction and velocity and measurements of tracer concentrations by ground stations and aircraft for selected meteorological conditions are used to confirm and/or evaluate the physical model's results.

The laboratory program involves three selected topographic regions where operational cloud seeding is in progress. These areas are:

1) Eagle River Valley-Climax area of Central Colorado,
2) Elk Mountain area of southern Wyoming, and
3) The San Juan Mountain area of southern Colorado.

The field program is limited to the Climax-Eagle River Valley area; the availability of field data for the other areas were dependent on private contractors and the University of Wyoming's Natural Resources Research Institute.

Procedures for Completing Objectives

In order to fulfill the stated objectives the following procedures were completed. First, the various parameters influencing the transport and spread of a particulate plume downstream from a source are categorized under four principal headings: 1) source characteristics, 2) depletion mechanisms, 3) atmospheric motions, and 4) boundary conditions. The existing laboratory airflow types are reviewed along with their restrictions.

The general mathematical aspects of two laboratory airflow models and the relevant similarity parameters governing their airflow characteristics were developed from existing similarity theory and information on past studies of modeling.

Second, to satisfy the basic requirement of geometric similarity scaled topographic models of the three topographic areas were constructed and arranged in wind-tunnels for the necessary experimental work.

Third, several laboratory experiments were conducted on the simulation of the atmospheric planetary boundary layer and transport-dispersion of a passive (radioactive) tracer over the scaled topographic models. Two model airflow types were explored, a neutral and barostromatic. Three different wind tunnels were utilized for the various experiments.

Fourth, field observations of temperature, wind velocity with height, surface concentrations, dispersion and transport estimates from constant-volume balloons and aircraft sampling of silver-iodide were obtained, analyzed and interpreted to provide information on the weather conditions and how these conditions affected the dispersion of the seeding material.

Fifth, the laboratory simulation results for each topographic area were compared with the available field data for geometric, kinematic, thermal and dynamic similarity. For the most part, this was accomplished by utilizing the relevant similitude criteria. The model's dispersion results were also compared with the available field data to evaluate how well the models approximate actual field conditions. In addition, the model and field results were used to assess the value of the laboratory experiments for assisting weather modification field programs in cloud seeding.

II. LABORATORY SIMILITUDE AND DISPERSION MODELS

Transport and Dispersion Over Irregular Terrain

The problem of atmospheric transport and dispersion of fine particulate material (e.g., silver iodide) and gaseous material is most easily approached by considering the factors that influences the transport and spread of the material from the source. These factors are 1) source characteristics, 2) depletion mechanisms, 3) atmospheric motions, and 4) lower boundary conditions.

The source characteristics consider the strength, height, efflux velocity and temperature, and dissemination time of the source. These characteristics as well as the source location can be varied in an effort to obtain specific operational objectives. The depletion mechanisms enhance the fall in concentration of suspended matter with downwind distance.

Atmospheric motions can be separated into two components, turbulence and mean motion. An examination of the turbulent diffusion equation indicates the manner which these two motions enter into the transport mechanism. For material with negligible fall velocity, the time averaged diffusion equation may be written as follows:

$$\frac{\partial \overline{C}}{\partial t} + \overline{U}_i \frac{\partial \overline{C}}{\partial x_i} = k_m \frac{\partial^2 \overline{C}}{\partial x_i^2} - \frac{\partial (\overline{u_i' c'})}{\partial x_i} \quad . \qquad 2\text{-}1$$

The various terms may be interpreted as follows:

$\overline{U}_i \frac{\partial \overline{C}}{\partial x_i}$ --- convective transport by mean flow

$k_m \frac{\partial^2 \overline{C}}{\partial x_i^2}$ --- molecular diffusion

$- \frac{\partial (\overline{u_i' c'})}{\partial x_i}$ --- turbulent diffusion.

In the field, molecular diffusion is neglected since it is small in comparison to the turbulent diffusion term on the time scale considered. Turbulence governs the diffusion of airborne material and is a function of atmospheric stability, directional and speed wind-shear, and surface roughness. The large-scale mean motions govern the direction in which the diffusing cloud of airborne material will be transported. Motions of the convective (advective) transport scale are governed by general synoptic flow-patterns, mesoscale circulations, and the nature of the terrain.

The lower boundary conditions, especially if they are irregular, may act to enhance the effects of depletion of a plume and increase the effects of turbulence and mean motion. Irregular terrain is difficult to generalize but nevertheless three types can be recognized: 1) blocking ridge or mountain range, 2) valley channeling, and 3) isolated mountain. The only avenue for the oncoming airflow approaching a

blocking ridge is to ascend the blocking topography. A plume of seeding material approaching the ridge may have portions of its material trapped in the lower layers while other portions are caught in the ascending airflow and transported over the ridge. With valley channeling the oncoming airflow may be channeled by the surrounding walls of the main valley, yet, interacting with the airflow from minor tributary valleys. In this case, a plume of seeding material may be trapped and channeled in the valley but with portions of it escaping the top of valley due to mechanical and convective turbulence and stability. With the isolated or singular mountain, a substantial portion of the oncoming airflow is forced to diverge and flow around the obstacle instead of over it. A plume of seeding material may be affected in the same manner but with portions of the material ascending the summit of the mountain.

All three terrain types may be found in the western United States. In Colorado, the Eagle River Valley and Climax-Leadville area located in the Central Rocky Mountains and the San Juan Mountains in southern Colorado are good examples of all three types. The Elk Mountain area of southern Wyoming is a good example of a singular mountain.

The previous discussion indicated that the spatial distribution of a particulate plume over mountainous terrain is affected by numerous variables, e.g.,

$$\overline{C}(\vec{r}) = f(Q, w_s, T_s, h_s, \mathcal{D}, H, \vec{Z}, \lambda, f, \vec{U}(z), \vec{U}_g, \beta, K_i, t, T) \qquad 2\text{-}2$$

These variables can be categorized under the four previous principal headings as follows:

Source characteristics

Q, w_s, T_s, h_s

Depletion mechanisms

$\mathcal{D}$

- Gravitational settling
- Precipitation scavenging
- Surface impaction
- Electrostatic attraction
- Adsorption
- Coagulation
- Chemical interaction
- Ultraviolet decomposition
- Resuspension and redeposition

Atmospheric motions

Mean flow	Turbulence
$f, \vec{U}(z), \vec{U}_g, T$	β, K_i, t

Boundary Conditions

$\vec{Z}, H, \lambda$

A schematic illustration of these various parameters and the role they play in transport and dispersion over irregular terrain is shown in Fig. 2-1.

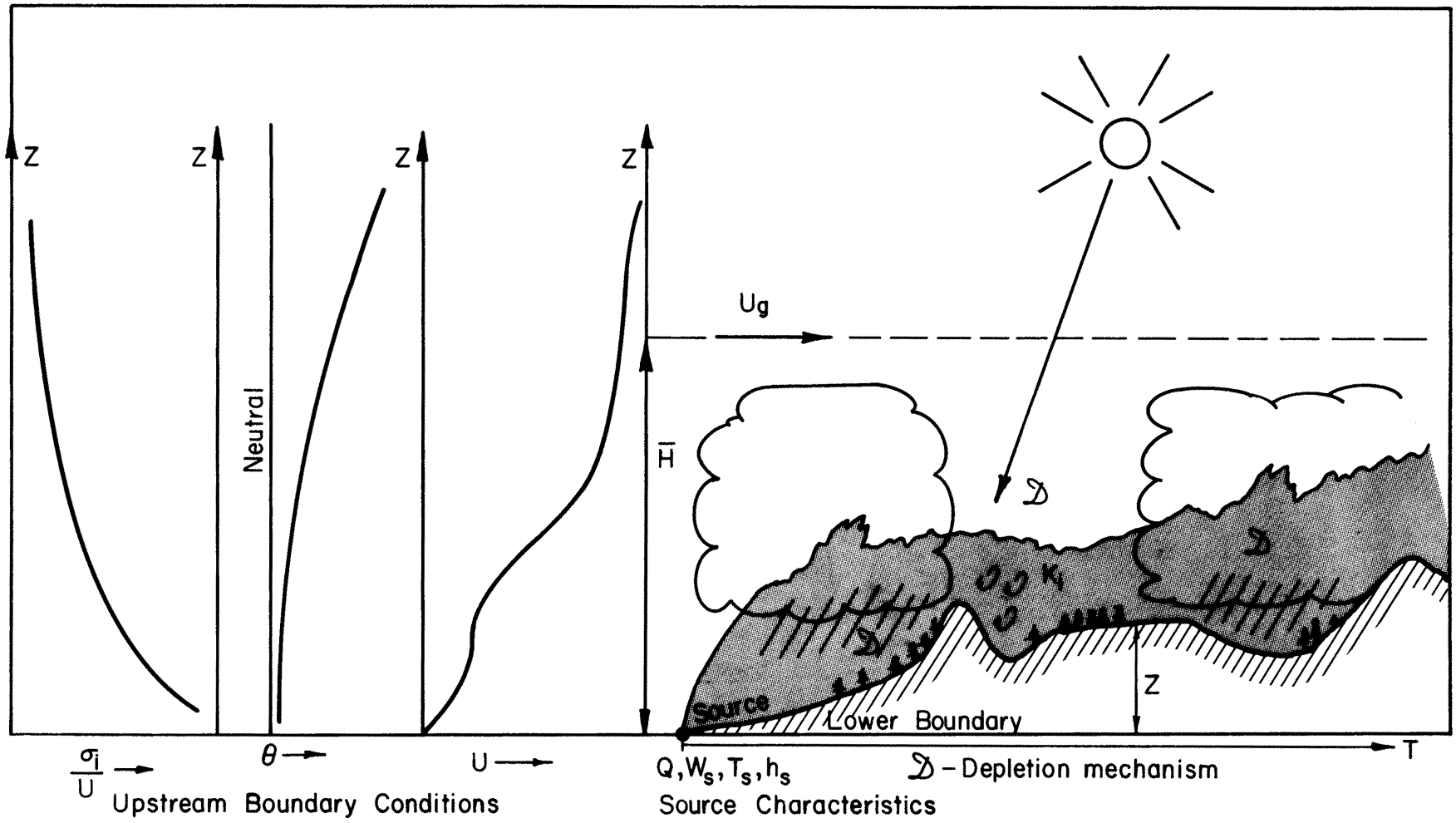

Fig. 2-1 Schematic illustration of atmospheric motion and transport-dispersion over irregular terrain.

Types of Laboratory Airflows

The laboratory simulation of transport and dispersion over irregular terrain presents several problems which may be generalized as follows:

1) The physical limitations of the laboratory facilities necessitate adopting certain restrictive assumptions,
2) the problem of similitude between model and prototype,
3) the problem of obtaining proper measurements of the pertinent parameters in the laboratory facility as well as the field, and
4) the problem of verifying the model results with actual field measurements.

Three general types of airflow can be generated in a laboratory facility:

1) Neutral airflow, where static stability is assumed neutral and the pressure field is determined by the geometry of the terrain features. If the terrain features are sharp, the flow patterns are not influenced by viscous forces and Reynold's number differences between the model and prototype. Irreversibility in the flow (as well as turbulence) is usually the result of separation eddies, which appear on the lee side of obstacles.
2) Barostromatic* airflow, where the air is stably stratified due to density or temperature stratification. This type of airflow is generally quasi-laminar and with proper density stratification gravity waves and "hydraulic" jumps occur. Large vertical temperature gradients and low flow velocities are required in order to produce this type of flow in a laboratory facility.
3) Unstable airflow, where the air is heated from below producing thermal convection cells throughout the flow medium (Ref. 12).

Restriction on Laboratory Airflows

In order that the flow in any laboratory model should be of value in interpreting or predicting the observed flow in the atmosphere, it is essential that the two flow systems should by dynamical, thermally and kinematially similar. This means that it must be possible to describe the flow in the two systems by the same equations after appropriate adjustments of the units of length, time and other variables.

Several difficulties arise in attempting to generate a physical model which will be similar to the actual atmosphere. The difficulties are principally due to the limitations of the laboratory facility in reproducing a scaled-down model atmosphere. The problem requires a simplification of the basic equations of the atmosphere** by a set of restrictive assumptions. In this study the following restrictions were placed upon the atmospheric flow and boundary conditions in order to make laboratory simulation possible:

---

* Word derived from Greek and adopted by R. S. Scorer as representing an airflow which exhibits density stratification. For the purpose of this study it represents airflow with stable thermal stability in the upper levels and near-neutral thermal stability in the lower levels.

** See Appendix

1) Coriolis forces - The effects of coriolis acceleration on air motion were neglected on the basis that the field or prototype regions were relatively small (L~40 to 50 km). In this case the inertial effects of the air motion were expected to predominate over coriolis effects. Local terrain effects were expected to contribute in decreasing the effect of the earth's rotation.

This assumption was not strictly valid for the San Juan Mountain area which covered a larger areal extent.

2) Steady-state conditions - In the physical models it was assumed that velocity, temperature or density fields were in steady-state. This was a good approximation for the neutral airflow but in the case of the barostromatic airflow the temperature and velocity fields over the topographic models were unsteady with time.

3) Uni-directional upper-level flow - In the physical models the upper-level flow above the terrain was considered uni-directional or that little directional wind shear occurs due to a thermal wind or horizontal temperature gradients. However, in the barostromatic airflow this assumption was not totally valid because of horizontal and vertical temperature gradients. In addition, directional wind shear could occur due to irregular terrain.

4) Radiation and cloud system effects - The weather situation of interest is storm periods with fairly extensive cloud cover over the region. Therefore, the various heat fluxes due to the sun, atmosphere and earth were assumed negligible. However, in the case of the barostromatic airflow the turbulent transfer of sensible heat was of some importance. Thermodynamic and compressibility effects due to cloud systems could not be simulated.

In the Elk Mountain study, field data were generally obtained under cloudless sky conditions but there was no systematic attempt to model the various heat fluxes in the laboratory airflow of this study.

5) Source characteristics - A particulate plume, e.g., silver-iodide particles, quickly attains the wind speed in the horizontal plane, while its rise is determined by its vertical momentum and buoyancy due to heat and molecular-weight difference. Rise of the plume is impeded by entrainment with air, which at first is due to turbulence generated by the relative motion of the plume. As this dies out, atmospheric turbulence dominates the mixing. Buoyancy of the plume may be altered by the atmospheric stability. Stable air acts as a restoring force on the plume, but in unstable air the plume may rise to large heights.

The sources in the field are silver-iodide generators which burn approximately 20 gms of silver-iodide per hour (Q) at a flame temperature (T_s) around 1200°C. The material emits at a few meters per sec (w_s) from the orifice.

For a wind-tunnel model of 1:9600 scale ratio it is not feasible to scale or simulate Q , T_s , h_s and w_s for prototype silver-iodide generators. The sources on the models correspond approximately to a field virtual source elevated some 50-60 meters from the surface. For the model airflows it was assumed that the effects of dissimilarity due to T_s , Q , h_s and w_s were quickly masked by the effects of turbulent mixing as the material moves downstream after release.

6) Deposition and depletion mechanisms - The mechanisms causing deposition and depletion are numerous and often not well understood. These include gravitational settling (fallout), precipitation scavenging (washout, snowout, and rainout), surface impaction (storage), electrostatic attraction, adsorption (coagulation) and chemical interaction. A further complication is the possibility of ultraviolet decomposition of the silver-iodide crystals. A third process is the possibility of resuspension and redeposition of the material.

No attempt was made to model any of the depletion variables on the model scale. Some of the variables such as the fallout velocity of silver-iodide particles (dia~.02μ) is very small and can be neglected. Grant et al., (Ref. 16) suggests that precipitation scavenging, coagulation, ultraviolet decomposition and electrostatic attraction have a small effect in depleting the seeding material in the Eagle River Valley and Climax area. However, information does not exist for the other areas.

The problem of resuspension and redeposition exists for the field as discussed by Grant (Ref. 15), but it appears that the time scale for this mechanism is somewhat longer than the one of interest in this study. Surface impaction may be an important deposition variable in the case of ground-based sources because of the possible interception by dense stands of trees.

General Similitude Requirements

Complete similarity between two flow systems of different length scales require geometrical, kinematical, dynamical and thermal similarity. In addition, certain boundary conditions should also be duplicated.

The following outline shows, in general, what requirements are necessary to consider for complete flow similarity:

1) Boundary conditions
   a. Upstream conditions - initial velocity, turbulence, temperature profiles, etc.
   b. Upper-level conditions
   c. Lower boundary conditions - surface topography
   d. Side boundary conditions - topography and wind-tunnel wall effects
2) Geometric similarity
   a. Modeling of terrain features, roughness, trees, etc.
   b. Boundary-layer thickness
3) Kinematic similarity
   a. Rossby number (Coriolis effects)
   b. Streamlines
   c. Velocity profiles
4) Dynamic and thermal similarity
   a. Reynolds number
   b. Richardson number
   c. Froude number
   d. Prandtl number
   e. Euler number
5) Dispersion similarity - Peclet number

The similitude parameters (Reynolds numbers, etc) governing the airflow and dispersion patterns may be derived by dimensional analysis, similarity theory or inspectional analysis. Complete derivations may

be found in various publications and books such as McVehil, et al., (Ref. 25), Nemoto (Refs. 28 and 29), Bernstein (Ref. 4) and Cermak et al., (Ref. 5). The Appendix gives a review of the present status on obtaining similarity criteria for planetary and surface boundary-layer studies.

Laboratory Airflow Models

The physical limitations of the present laboratory experimental facilities requires the relaxation of certain similitude requirements as listed under the section on laboratory restrictions. Thus, complete similitude between field and model cannot be totally satisfied. However, past studies have indicated that partial similarity* may be adequate for obtaining reasonable results.

The following statements summarizes the principal similarity aspects of the two airflow models that have been used to obtain diffusion results in this study:

1. Neutral airflow model
   a. Thermal similarity

      The atmospheric stability is assumed to be in a neutral state or adiabatic equilibrium. Under these conditions an air parcel displaced adiabatically will continue to possess the same temperature and pressure as its surroundings, so that no restoring force acts on a parcel displaced vertically. The state of adiabatic equilibrium is approached in a layer of air in which there is strong vertical mixing, e.g., when the sky is thickly covered with cloud and there is a moderate or high wind velocity.

      In a neutral state the environmental lapse rate of temperature is equal to the dry-adiabatic lapse rate or the saturation-adiabatic lapse rate. When expressed in terms of the potential temperature and air density one can write the approximation,

$$\frac{1}{\bar{\theta}} \frac{\partial \theta}{\partial z} \sim 0]_F \equiv - \frac{1}{\bar{\rho}} \frac{\partial \rho}{\partial z} \sim 0]_M \quad . \qquad 2.3$$

      The main limitation in this approximation is that it must be possible to treat the atmosphere like an incompressible fluid. Generally, this limitation (Ref. 10) has been accepted but the full consequences of such an assumption have not been fully explored for modeling flow over irregular terrain.

   b. Airflow and dispersion similarity

      In this type of airflow the concentration at any location downstream from a source is assumed a function of the following variables,

$$\bar{C}(\vec{r}) = f(Q, \vec{Z}, H, \vec{U}(z), \vec{U}_g, K_i, t_s, T) \qquad 2\text{-}4$$

      Now according to similarity or dimensional analysis (Appendix) one can write the relevant nondimensional variables which are important in the neutral airflow model as,

---

* See Appendix

$$\frac{\overline{C}\,\overline{U}\,X^2}{Q} = f\left(\frac{Z}{H}\,,\ Re_t\,,\ \frac{U(z)}{U_g}\,,\ \frac{t_s}{T}\right) \qquad 2\text{-}5$$

where Z , H are parameters depending on geometric similarity. Re_t depends upon turbulence similarity and $U(z)/U_g$ depends upon kinematic or flow similarity. t_s/T refers to time similarity.

These nondimensional variables along with the appropriate upstream boundary conditions, such as, a proper velocity and turbulence profile make up the essential elements of the neutral airflow model.

In this physical model the airflow was aerodynamically rough which allows relaxing the requirement for Reynolds number duplication (Refs. 30 and 33). Usually the turbulent Reynolds or Peclet numbers cannot be evaluated because of the lack of proper field data. However, a test of the similarity of turbulent Reynolds number between field and model airflow was evaluated in the Eagle River Valley-Climax study (Ref. 30).

Since the field and laboratory measurements were seldom obtained for all three space dimensions, i.e., x , y , z , the vector notation was dropped and the similarity relations were evaluated in terms of one or two dimensions.

2. Barostromatic airflow model

a. Thermal similarity

In this particular physical model one attempts to simulate the normal temperature stratification observed in the atmosphere, i.e., an increase of potential temperature with height. The similarity relation can be written in terms of the potential temperature and air density, as

$$\frac{1}{\overline{\theta}}\frac{\partial \theta}{\partial z} > 0\Big]_F \equiv -\frac{1}{\overline{\rho}}\frac{\partial \rho}{\partial z} > 0\Big]_M \ . \qquad 2\text{-}6$$

The above statement infers that the physical model requires temperature or density stratification.

b. Airflow and dispersion similarity

The principal difference between this airflow and the neutral airflow is the temperature stratification and low airflow velocities. An examination of the similarity criteria (Appendix) indicated that the relevant nondimensional variables would be,

$$\frac{\overline{C}\,\overline{U}\,X^2}{Q} = f\left(\frac{Z}{H}\,,\ Re\ ,\ Ri\ ,\ Pr\ ,\ \frac{U(z)}{U_g}\,,\ \frac{t_s}{T}\right) \qquad 2\text{-}7$$

where the Richardson and Prandtl numbers are required for dynamic or thermal similarity. These variables, along with the upstream boundary conditions, such as velocity and temperature profiles, constitute the principal elements of the barostromatic airflow model.

The present airflow models only attempted to simulate the gross features, therefore, many of the variables representing the fine

structure of the flow have been neglected because of the difficulties in reproducing these aspects in a laboratory facility and also due to the lack of field data in which to check the laboratory results and similarity criteria.

III. EAGLE RIVER VALLEY-CLIMAX STUDY

The general purpose of the first study was to develop laboratory airflow models which would be adequate in estimating airflow and atmospheric transport-dispersion characteristics during winter storms (northwest winds) over the Eagle River Valley-Climax topographic complex. Both barostromatic and neutral airflow models were investigated because detail information on the meteorological characteristics associated with the winter storms were not established at the outset.

The study was different from the other two research efforts in that 1) the topography is principally a long narrow valley, but complicated by singular and blocking ridges and 2) the availability of field data made field and model data comparisons more complete than the other two studies.

The contents of this section have been condensed from reports submitted by Orgill et al., (Refs. 30 and 31).

Field Experimental Program

The basic features of the Climax weather modification experiment have been discussed by Grant et al., (Ref. 18) and Chappell (Ref. 7). Only information pertinent to this study will be summarized.

1. Network of generators

   Six silver-iodide ground generators are used in the project. These are Colorado State University modified sky-five, acetone, needle-type ground generators. The seeding rate of the generators may vary from 2 gm/hr to 200 gm/hr of silver-iodide, but are usually set at 15-20 gm/hr which produces about 10^{14} particles per gm silver-iodide effective at -12°C and 4×10^{15} particles per gm silver-iodide effective at -20°C.

   Two of the six generators are located in the Eagle River Valley which is oriented in a northwest-southeast direction from the primary target area (Chalk Mountain). Only northwest wind flow has been used for topographic modeling (Fig. 3-1).

   The two generators located in the Eagle River Valley were placed near the towns of Minturn and Redcliff. Both generators are deep in the valley but the location of the Minturn generator is upwind from Battle Mountain.

2. Criteria for experimental day

   The decision to turn on the generators during normal operations was made with a randomization scheme. The sampling period was a 24-hour interval of time.

   The weather criteria used for selecting the experimental days to be used for the prototype studies were:

   a) deep northwest (270-360°) airflow (5-15 mps) over the area, and

   b) overcast to broken orographic clouds with some precipitation but of light intensity.

Fig. 3-1 Eagle River Valley-Climax topography and boundaries of topographic model.

These weather conditions, although typical for the area during wintertime, were only observed five or six times during special field program dates. In addition, some field measurements were made during southwest (270-180°) airflow situations.

3. Special field programs

The primary objective of the special field programs were to collect sufficient imformation to check on the laboratory results. The programs were not large scale and therefore their objectives were quite limited. On occasion the field programs of the study benefited from other active programs in the same area such as the National Science Foundation's Rocky Mountain orographic cloud precipitation and modification program and the State of Colorado weather modification program.

The principal objectives of the field program were as follows:

a) Obtain sufficient radiosonde, pilot balloon (rawin) and near surface data to define the vertical structure of the atmosphere in orographic terrain, especially during weather conditions when cloud seeding would most likely be in operation.

b) Obtain data on the trajectory of air parcels by means of the superpressure balloon technique and also make estimates on the atmospheric dispersion from these same measurements.

c) Obtain surface samples of tracer material (e.g., silver-iodide, zinc sulfide, sulfur hexafloride) downwind from generator sites in order to determine the dimensions of the tracer plume.

d) Obtain upper-level samples of particulate material using a kite system and aircraft. Primary emphasis was on obtaining measurements on the vertical depth of the tracer plume by using an aircraft as a sampling platform.

Seven periods of field data collection were implemented to attain the four objectives listed above (Table 3-1). During these periods, especially those for 1969-70, the following tasks were at least partially completed:

a) Collection of radio-and rawin-sonde data at Minturn (upwind), Camp Hale (upwind, near the Ridge), and Fairplay (downwind).

b) Collection of pilot balloon data taken at four different locations from Minturn to Chalk Mountain. However, low cloud ceilings limited the vertical extent of the data.

c) Realization of dual and single super-pressure balloon runs in the Camp Hale, Leadville and Redcliff areas. Eight of the balloon releases were tracked by a double-theodolite technique and six releases were tracked by a M-33 radar and transponder system. Six of the eight releases tracked by the double theodolite technique were done under general northwest wind conditions and have provided additional data on the local dispersion characteristics in the Camp Hale area.

d Sampling of silver-iodide tracer material near the surface was accomplished at Chalk Mountain and Tennessee Pass.

e Seven aircraft sampling flights were completed in the Climax-Leadville and Eagle River Valley area. Four of the flights were made in weather conditions comparable to conditions

Table 3-1

Special Field Program Dates for the Eagle River Valley-Leadville Area

Date	Data			
	Pilot Balloon	Radio - or Rawinsonde	Constant-Volume Balloon	Ground Ice Nuclei Data
16-20 Dec. 1968	Camp Hale Fish Hatchery	Camp Hale Fish Hatchery, Chalk Mountain	Arkansas River Valley near Leadville	Chalk Mountain HAO
8-16 Dec. 1969	Eagle River Valley, Chalk Mountain	Minturn Camp Hale Fairplay	Camp Hale	Chalk Mountain HAO Tennessee Pass
13-16 Jan. 1970	None	Minturn Camp Hale Fairplay	Redcliff Camp Hale Arkansas River Valley near Leadville	Chalk Mountain HAO Tennessee Pass
*12, 13 & 16 March, 1970	None	Camp Hale	None	Chalk Mountain HAO Tennessee Pass
30 April, *1 May 1970	None	Camp Hale	None	Chalk Mountain HAO Tennessee Pass
*11, 12 Dec. 1970	None	Camp Hale	Redcliff (12th)	Chalk Mountain HAO Tennessee Pass
*15, 16, 17 Dec. 1970	Near Leadville	Camp Hale Avon	Minturn; near Leadville	Chalk Mountain HAO Tennessee Pass

* 12, 13, 16 March; 1 May 1970; 11, 12 and 15 December, 1970 aircraft sampling days.

expected for cloud seeding operational days. One of the flights was made as stable atmospheric conditions prevailed in the valley.

The particulate materials used for tracing was silver-iodide, fluorescent zinc-sulfide particles and sulfur hexa-fluoride gas. All three of the tracers were released for sampling during the flight of December 15, 1970.

The tracer materials were released from two sites, Minturn and Redcliff during four of the flights, and from Minturn during the last three flights.

The aircraft used for the sampling flights was the Aero-commander 500-B. The instrumentation consisted of the NCAR ice-nucleus counter, a Mee Industries model 110 automatic fluore-scent particle counter, millipore filter sampling system for ice nuclei and a simple sampling tube and bottle system for collecting sulfur hexafluoride.

4. Field Results

On the basis of these limited field data some tentative generalizations can be made regarding the atmospheric conditions which prevail during storm periods selected for cloud seeding and how these atmospheric conditions may effect the dispersal of the seeding material.

Storm events associated with the northwest winds exhibited a strong orographic effect in the Eagle River Valley area. Visual observations of the local weather conditions supported these conclusions.

A diurnal variation in static stability was observed during the storm events. Neutral or unstable stability conditions existed in the lower 1000 meters during the late morning and afternoon hours. More stable conditions existed during the night-time hours. However, there may be storm situations that have quasi-steady state stability conditions for 12 hours or more. The field sampling was not frequent enough to make any definite conclusions concerning the duration of specific stability regimes.

The wind direction and speed was typically variable. The ridge-top wind speeds (~13000 ft/msl) varied between 1 to 16 m/s but the most frequent wind speed was between 8 to 12 m/s.

Significant cross-valley flow was observed several times and may occur quite frequently during the winter. Yet, events with little ($<30^{o}$) directional shear were also observed a number of times.

The dual constant-volume balloon flights showed that the total dispersion rate approached and exceeded t^3 and t^4 for short periods during the flights (Fig. 3-2).

Calculations of the eddy diffusivities from the super-pressure balloon data showed that on this particular day (December 12, 1969) the vertical eddy diffusivity changed with height, from 10^4 cm^2 sec^{-1} within the valley to 10^6 cm^2 sec^{-1} near the surrounding mountain summits. This indicated a strong vertical eddy flux out of the valley due to a strong shear flow at ridge level. Zonal and meridional eddy diffusivities were on the order of 10^5-10^6 cm^2 sec^{-1} (Ref. 30).

Aircraft sampling flights of the silver-iodide seeding material showed that the range of vertical transport of seeding material was of the order

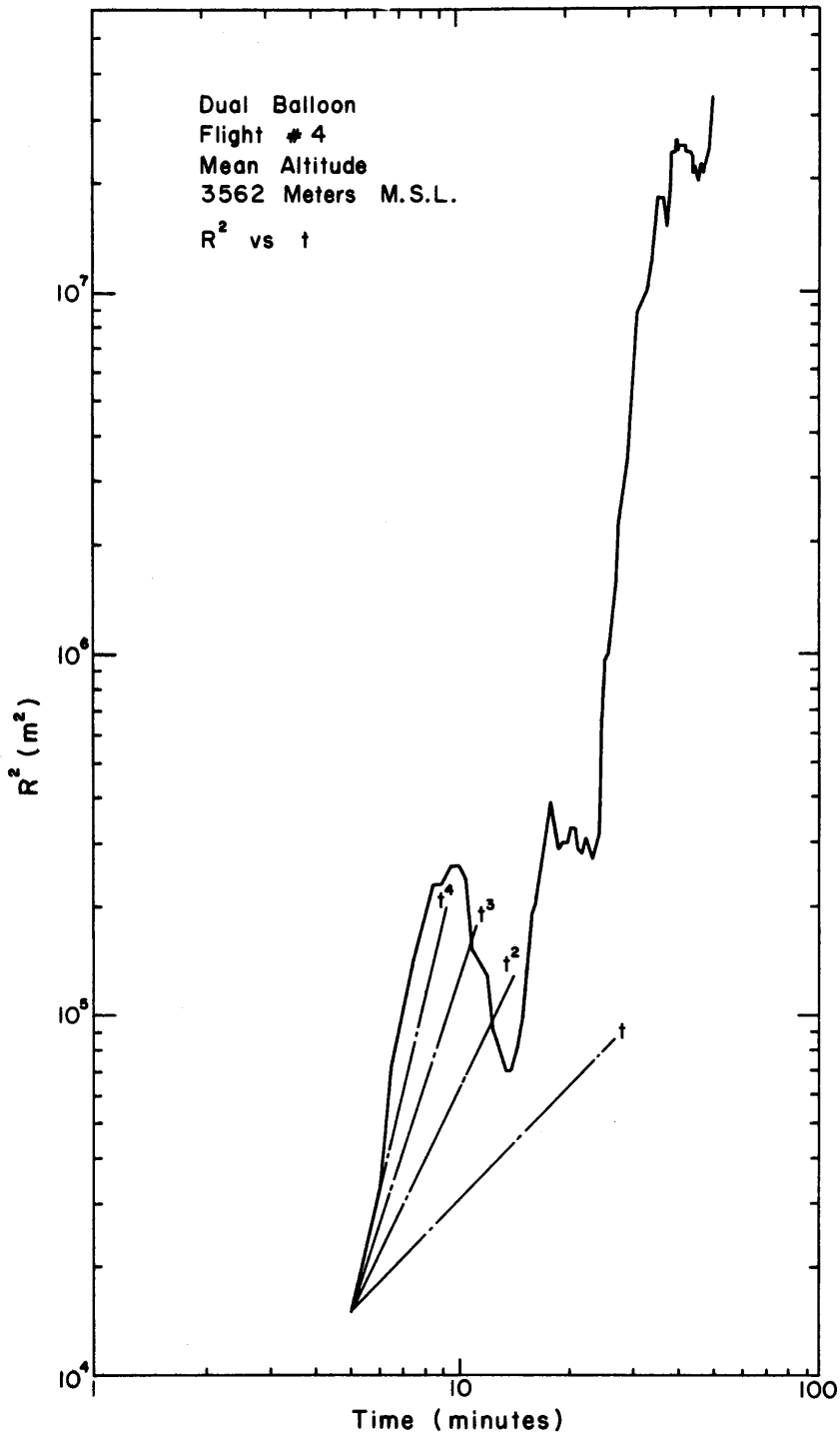

Fig. 3-2 Square of the total vector separation R^2 versus time. Dual floght #4 in the Camp Hale area.

D_z ~ 975-1740 meters agl of generator/10 kms of horizontal transport

with the larger values observed during near-neutral stability events (Table 3-2). These vertical transport values exceeded the natural mean slope of the terrain which is

Valley Slope ~ 280 meters/10 km .

The lowest value of vertical transport was not observed during the afternoon of greatest stability (December 12, 1970), but for one of the days (December 15, 1970) when considerable snow showers were occurring over the area. Utilization of the silver-iodide by low clouds may have been responsible for the lower transport value since the more unstable stability conditions on December 15 (Fig. 3-3) should have favored a larger vertical transport value.

The last two sampling flights confirmed the results from the previous three flights (Ref. 30) in that the valley channels the airflow and seeding material quite strongly along the valley towards the Tennessee Pass area. When the seeding material reaches the higher elevations above the ridge it then spreads out in the horizontal (Figs. 3-4, 3-5, 3-6 and 3-7). Unfortunately, the direction and horizontal dispersion of the seeding plume from the generators was not determined very precisely because the aircraft sampling was frequently limited by inclement weather conditions on the mountains next to the valley.

The sampling of fluorescent zinc-sulfide and sulfur hexafluoride was not successful. Only traces of the zinc sulfide could be found over the area even at the lowest altitudes (8-9,000 ft msl). It is speculated that very shallow trapped air and surface impaction of this large and cold tracer material may have been partially responsible for these results.

The aircraft sampling indicated that the atmospheric dispersion during orographic storm events is large enough to transport the seeding material from ground generators to orographic cloud systems. Mechanical turbulence enhanced by near-neutral stability conditions and orographically induced eddies are principal physical mechanisms for dispersing the seeding material from the generators.

Laboratory Experimental Program

1. Topographic model

The topographic model of this study simulated the Eagle River Valley area and topography surrounding Climax, Colorado (Fig. 3-8). The direction of the freestream (or geostropic) wind is approximately 320° or northwest. The length scale of the model is nondistorted with a scale ratio of 1:9600. Overall dimensions of the model is approximately 25 ft 6 in x 5 ft 10 in. The lowest and reference elevation is 7,800 ft (2379 m) msl and the highest is Mt. Lincoln at 14,284 ft (4350 m) msl. The maximum height difference in the model is 8 in. Further details of the model construction are found in Ref. 30.

2. Laboratory simulation facility

All the experimental work was conducted in the Colorado State University low-speed recirculating wind tunnel. Specifications of this facility is found in Table 3-3 and a schematic view of the wind tunnel is shown in Fig. 3-9.

Table 3-2

Estimates of the Vertical and Horizontal Transport and Maximum Elevation of Seeding Material as Determined by Aircraft Sampling Over the Eagle River Valley

Date	Vertical Transport meters agl/10 km of Horizontal Transport	Horizontal Transport km/10 km of Horizontal Transport	Maximum Elevation (ft msl) of Seeding Material Detected Above Background (~10 nuclei/liter)
March 12, 1970	1740	~15	~14,000
March 13, 1970	1220	--	>12,000 (clouds)
March 16, 1970	1340	--	>12,500 (clouds)
December 12, 1970	1280	~ 7	~13,000
December 15, 1970	975	--	~12,000 (clouds)

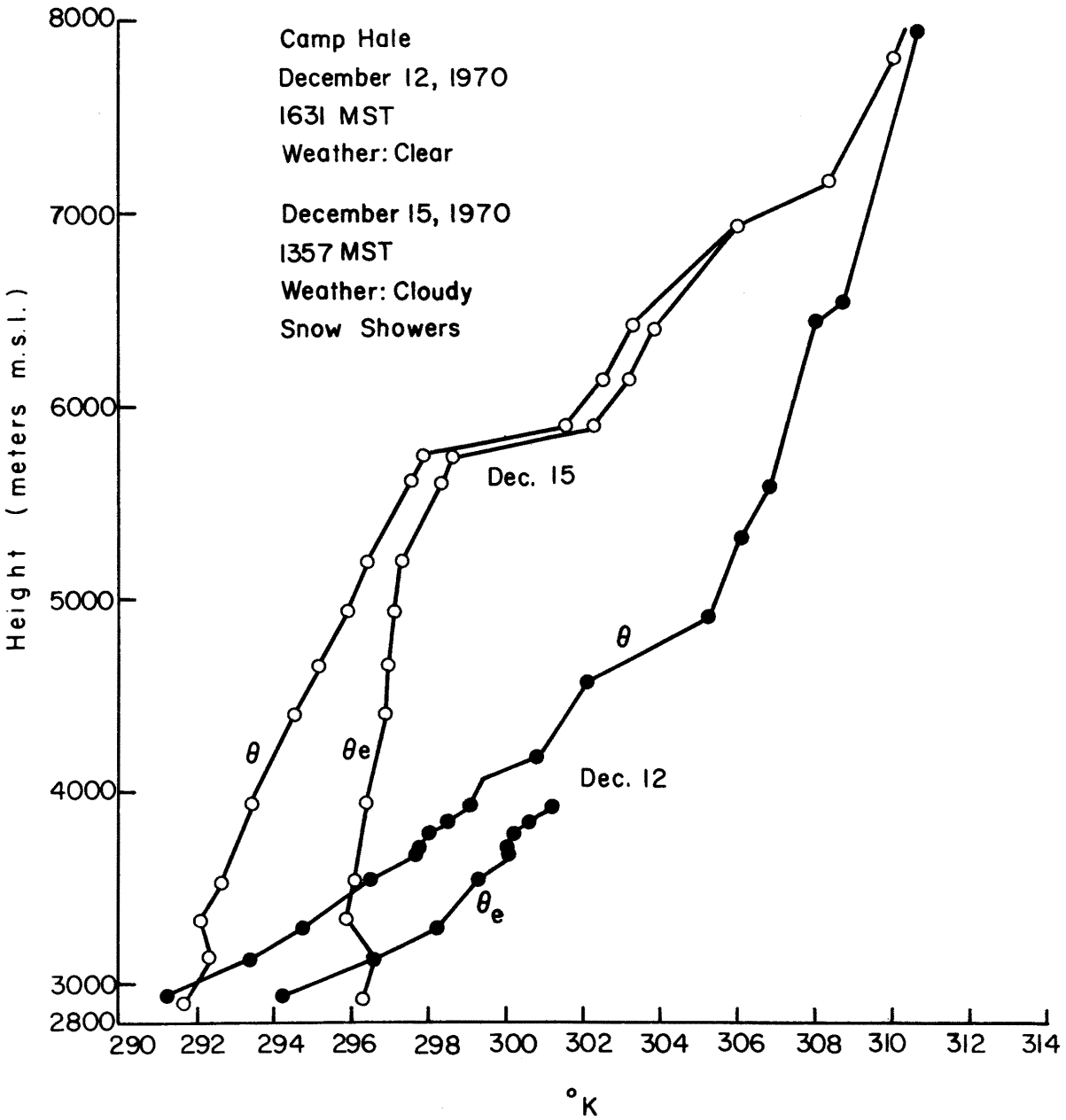

Fig. 3-3 Potential and equivalent potential temperature distributions with height at Camp Hale, Colorado. December 12 and 15, 1970.

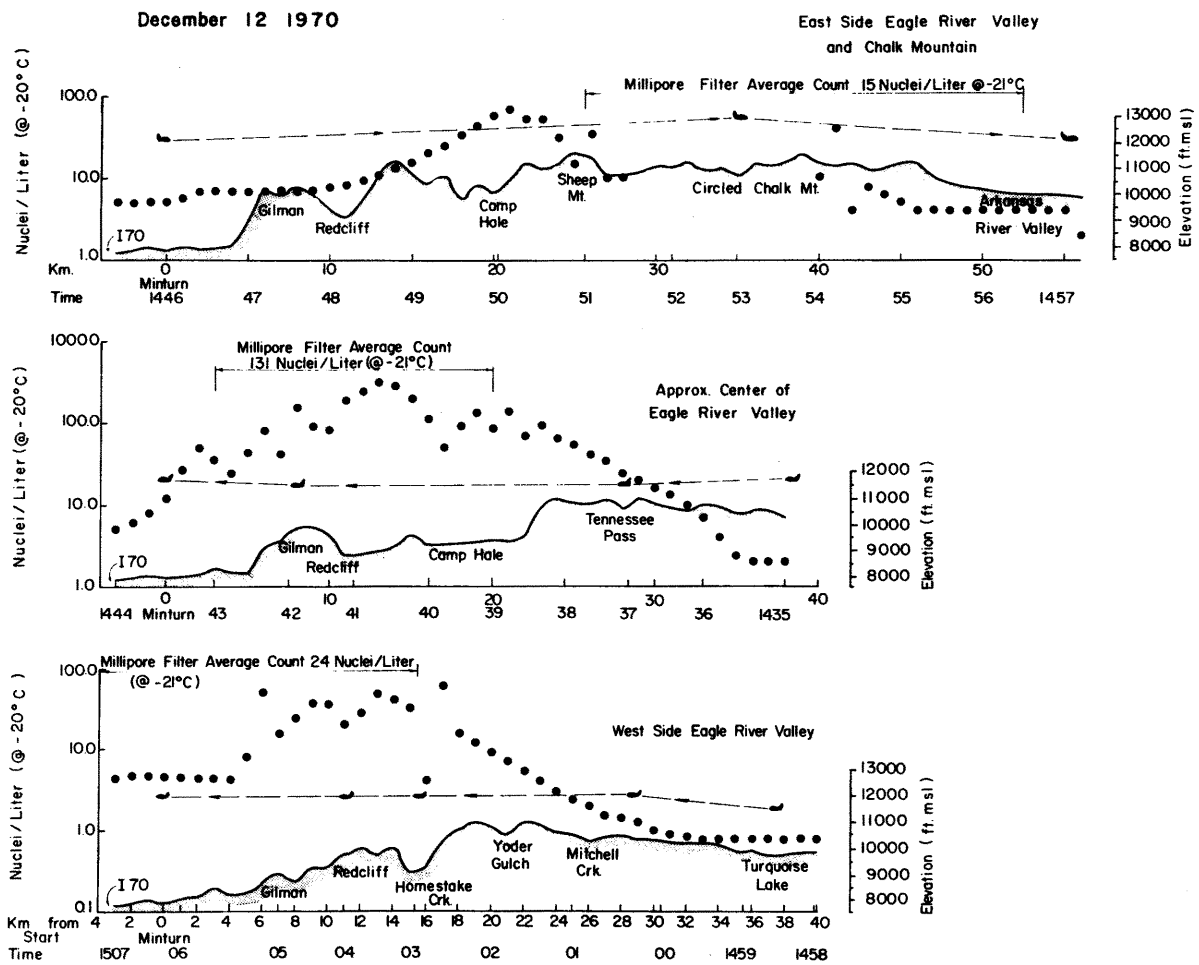

Fig. 3-4 Silver-iodide concentration distribution over three different regions of the Eagle River Valley-Climax area. December 12, 1970.

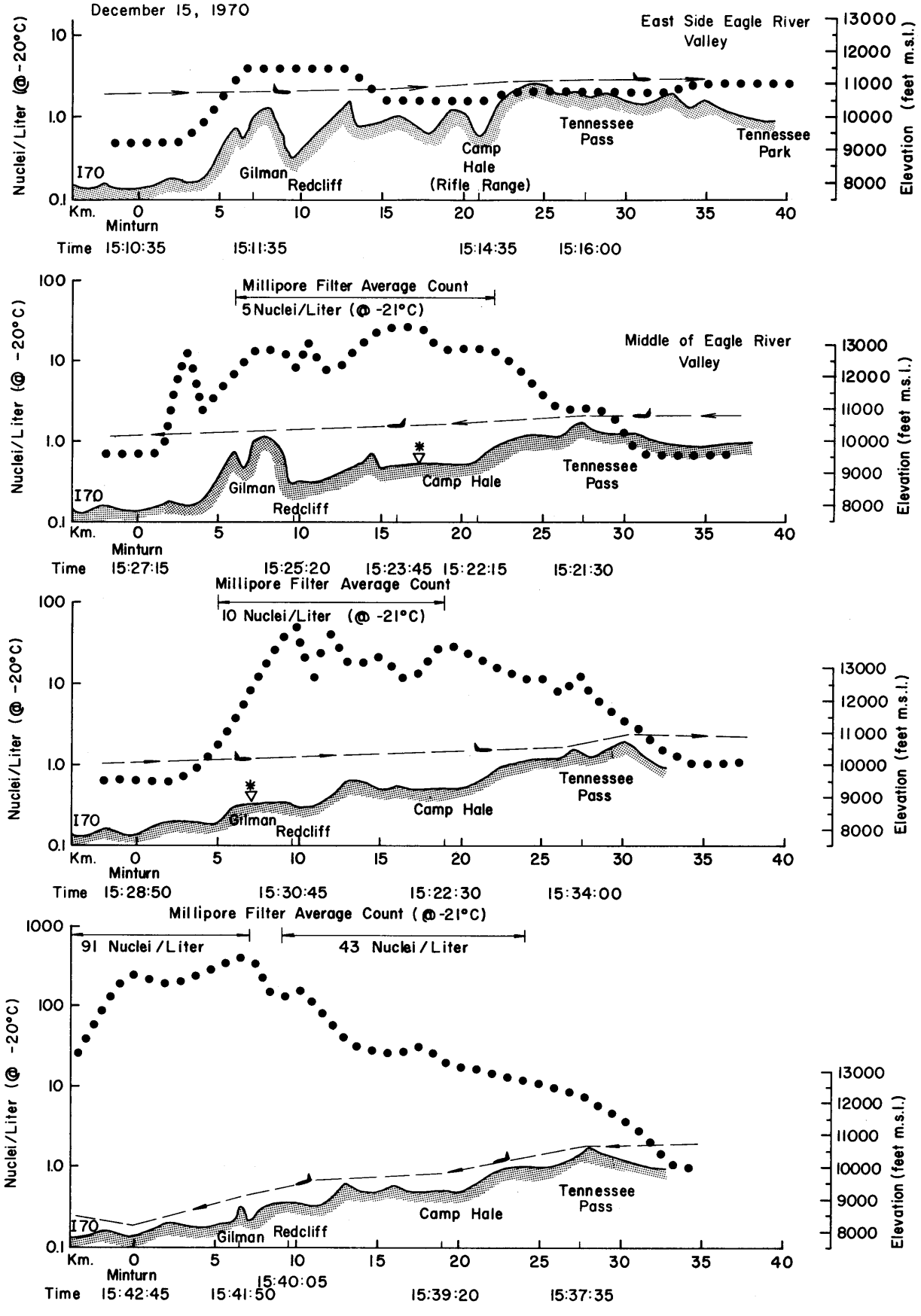

Fig. 3-5 Silver-iodide concentration distribution over different regions of the Eagle River Valley-Climax area. December 15, 1970.

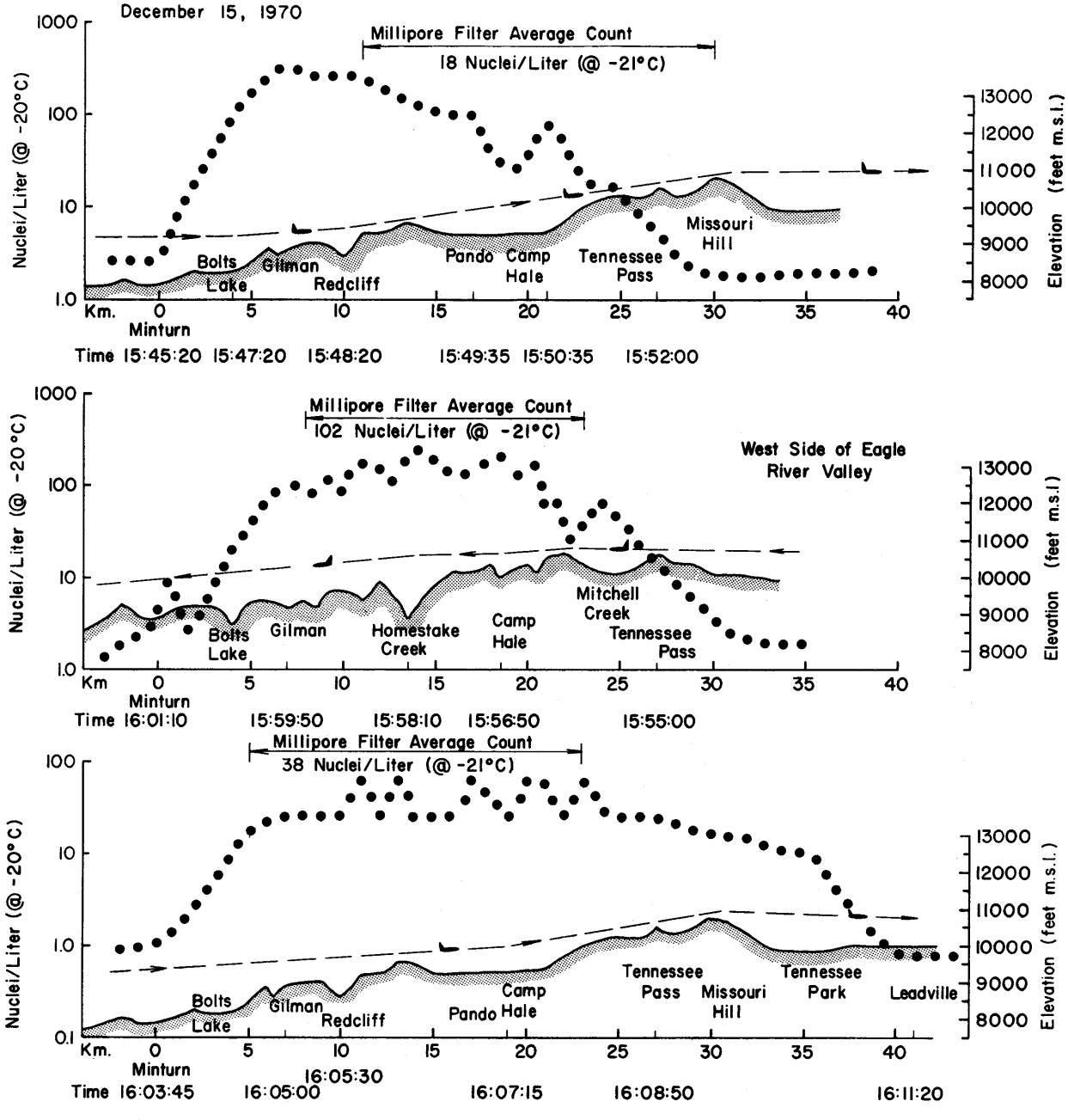

Fig. 3-6 Silver-iodide concentration distribution over different regions of the Eagle River Valley-Climax area. December 15, 1970.

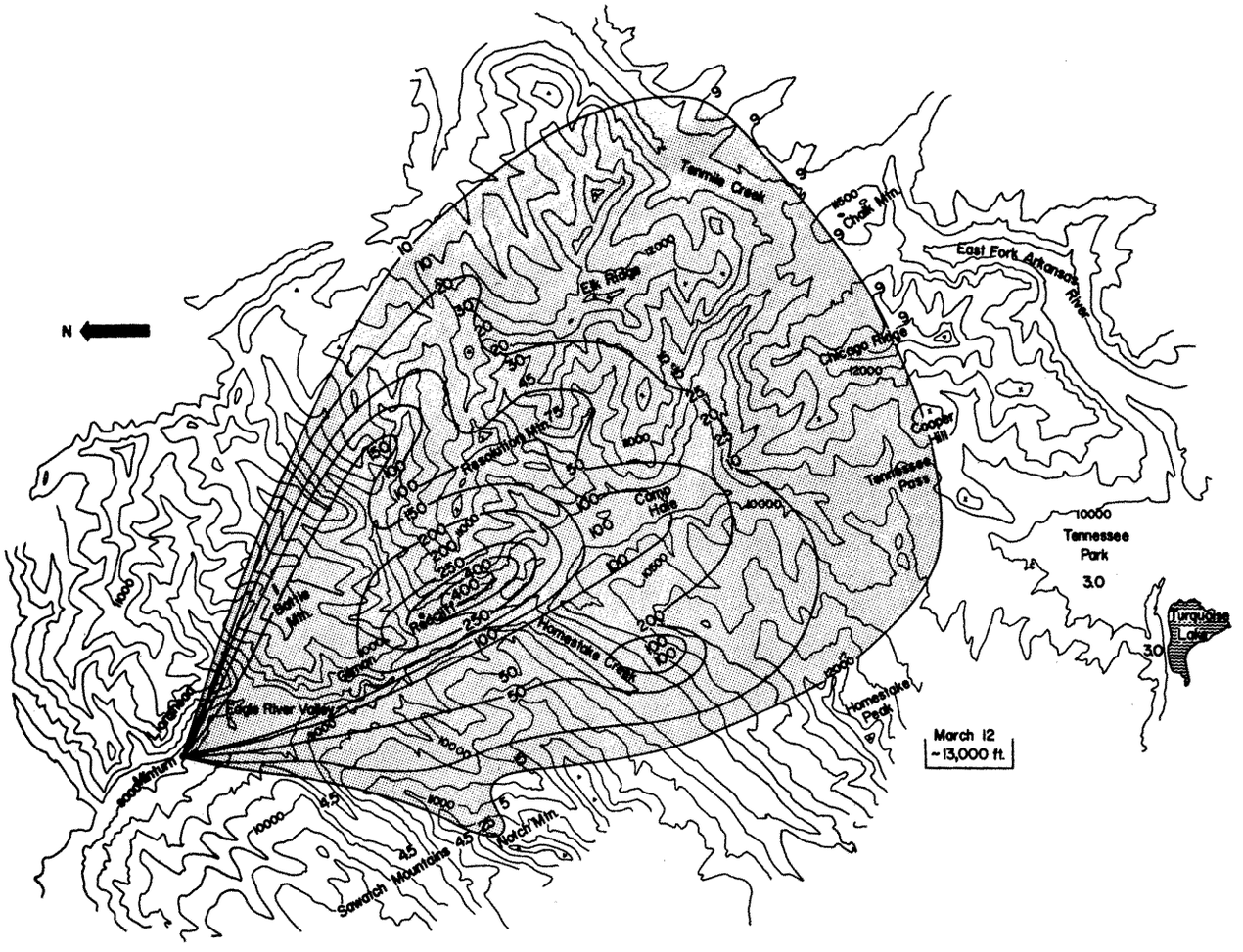

Fig. 3-7 The approximate horizontal dispersion of silver-iodide seeding material at 13,000 feet m.s.l. as released from Minturn and Redcliff sources. March 12, 1970.

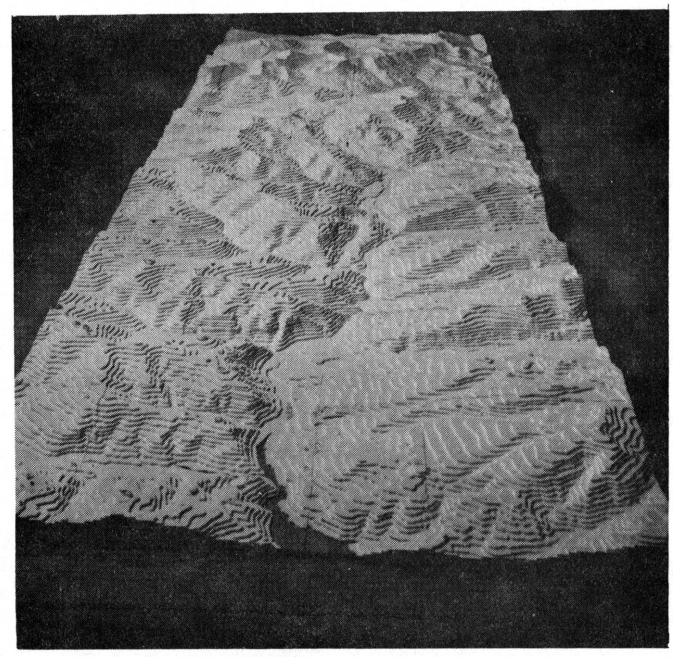

Looking downstream

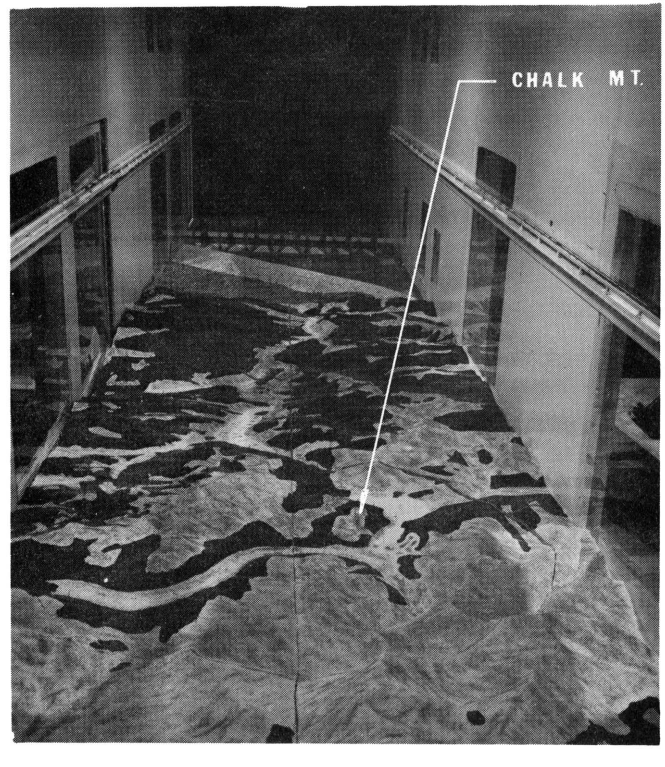

Looking upstream

Fig. 3-8 Eagle River Valley topographic model during construction and in wind tunnel.

Table 3-3

Performance Characteristics of Colorado State University Low-Speed Wind Tunnels

Characteristics	Army Meteorological Wind Tunnel	Low-Speed Wind Tunnel	Environmental Wind Tunnel
1. Dimensions			
Test-section length	88 ft	30 ft	54 ft
Test-section area	36 ft^2	36 ft^2	84 ft^2
Contraction ratio	9:1	4:1	2.78:1
Length of temperature controlled boundary	40 ft	10 ft	None
2. Wind-Tunnel Drive			
Total power	400 hp	75 hp	150 hp or 10 hp
Type of drive	4-blade propeller	16-blade axial fan	6-blade axial fan
Speed control: coarse	Ward-Leonard DC control	single speed induction motor	single-speed induction motor
Speed control: fine	pitch control	pitch control	pitch control
3. Temperatures			
Ambient air temperatures	40°F to 200°F	not controlled	not controlled
Temperature of controlled boundary	40°F to 400°F	ambient to 200° F	not controlled
4. Velocities			
Mean velocities	approx. 5 fps to 120 fps	approx. 3 fps to 60 fps	0 fps to 60 fps
Boundary layers	up to 16 inches	up to 8 inches	up to 20 inches
Turbulence level	low (about 0.1 percent)	low (about 0.5 percent)	1-2 percent
5. Pressures	adjustable gradients	not controlled	not controlled
6. Humidity	controlled from approx. 20% to 80% relative humidity under average ambient conditions	not controlled	not controlled

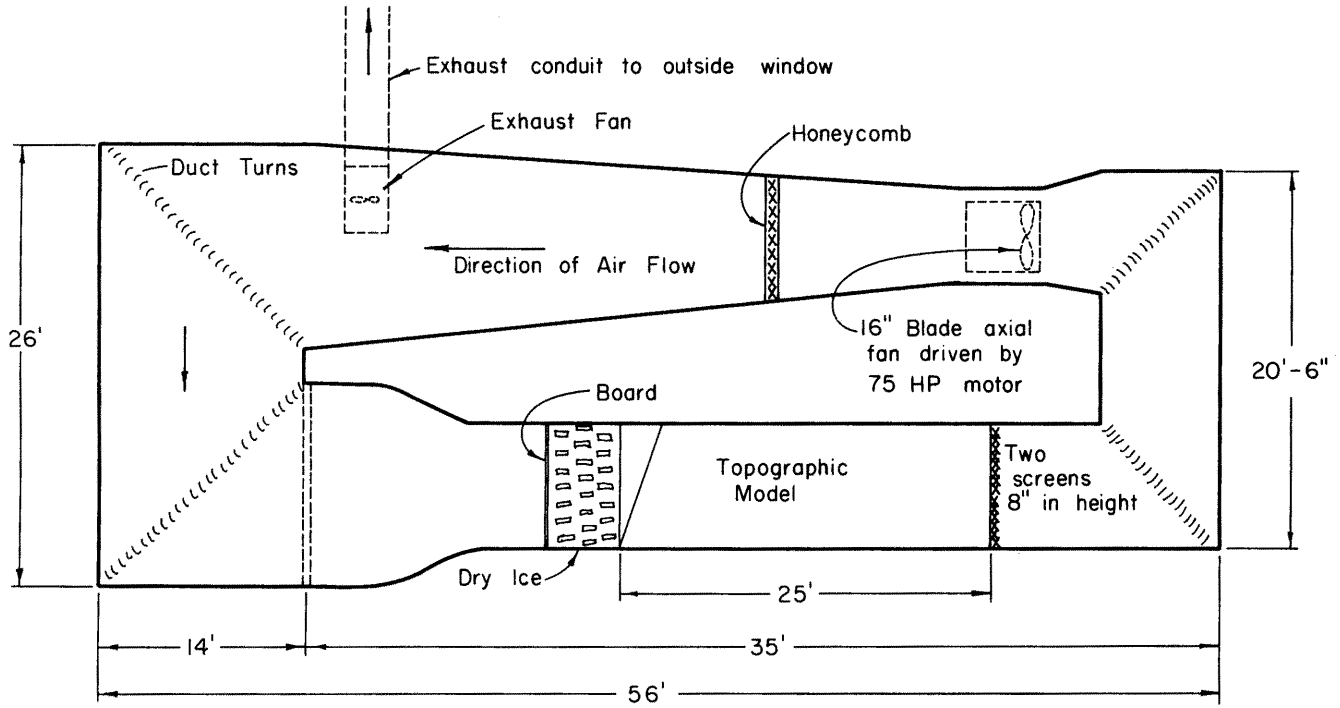

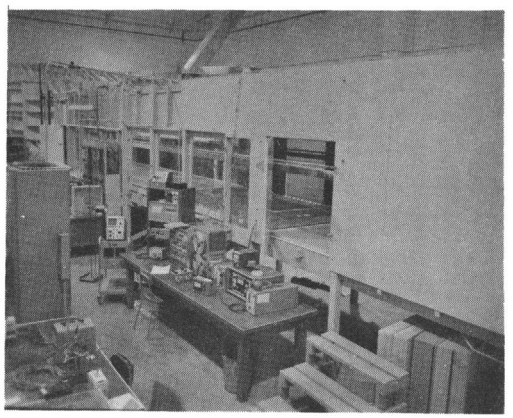

Fig. 3-9 Colorado State University low-speed recirculation wind tunnel.

3. Boundary conditions

The lower boundary conditions were provided by the topographic model. In order to approximate the velocity, turbulence and temperature profiles over the model, the upstream section of the wind tunnel was modified with artificial devices. In case of the neutral airflow a momentum boundary layer was developed by using screens and the topographic model. The experimental setup is shown in Fig. 3-10. In the case of the barostromatic airflow a thermal boundary layer was produced by placing several hundred pounds of solid carbon dioxide (dry ice) in the upstream section of the wind tunnel (Fig. 3-11)

The upper-boundary conditions (roof) was not adjusted or modified. Therefore a longitudinal pressure gradient existed along the topographic model.

The side walls and irregular configuration of the model was observed to effect the side flow patterns up to 12 inches on each side. Therefore, the effective width of the model which was not affected seriously by the side wall boundary conditions was approximately four feet.

4. Experiments

In the case of the neutral airflow, six experimental periods in the wind tunnel were required in order to obtain data on the static-pressure distribution, surface streamlines, velocity, turbulence (turbulent intensities and shear stress) and concentration.

Two sets of concentration data were obtained; one, simulating a single source at the location of Minturn and two, simulating a dual source at the location of Minturn and Redcliff.

Concentration measurements over the topographic model were obtained by releasing radioactive Krypton-85 from sources located in the model and using Geiger-Mueller tubes to determine the relative amount of Krypton in samples of the gas-air mixture. The sampling method was developed by Chaudhry. Details on the operation of this equipment was reported in previous reports (Refs. 8 and 9).

In the case of the barostromatic airflow the limitations of the dry ice method required conducting a series of experimental programs to obtain data on velocity, temperature, density and radioactive concentration measurements. Altogether, approximately eight separate dry-ice experiments were conducted in order to obtain acceptable measurements of the above quantities. Laboratory setup and conditions were kept the same as much as possible.

Two sets of concentration measurements were made over the topographic model. In one case, a single source at the location of Minturn was simulated while the second, simulated a single source at the location of Redcliff. The sampling was done by the radioactive gas method.

Comparison of Laboratory and Field Data

1. Verification of similarity criteria

a. Neutral airflow

In the case of the neutral airflow the concentration distribution over the model and prototype depends on 1)

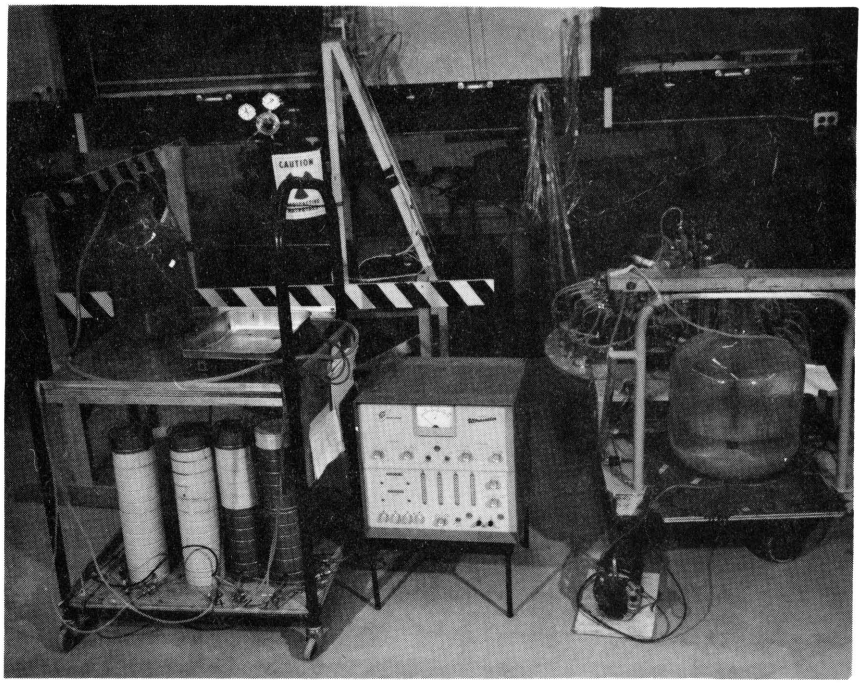

Fig. 3-10 Laboratory experimental arrangement for measuring radioactive Krypton-85 concentration.

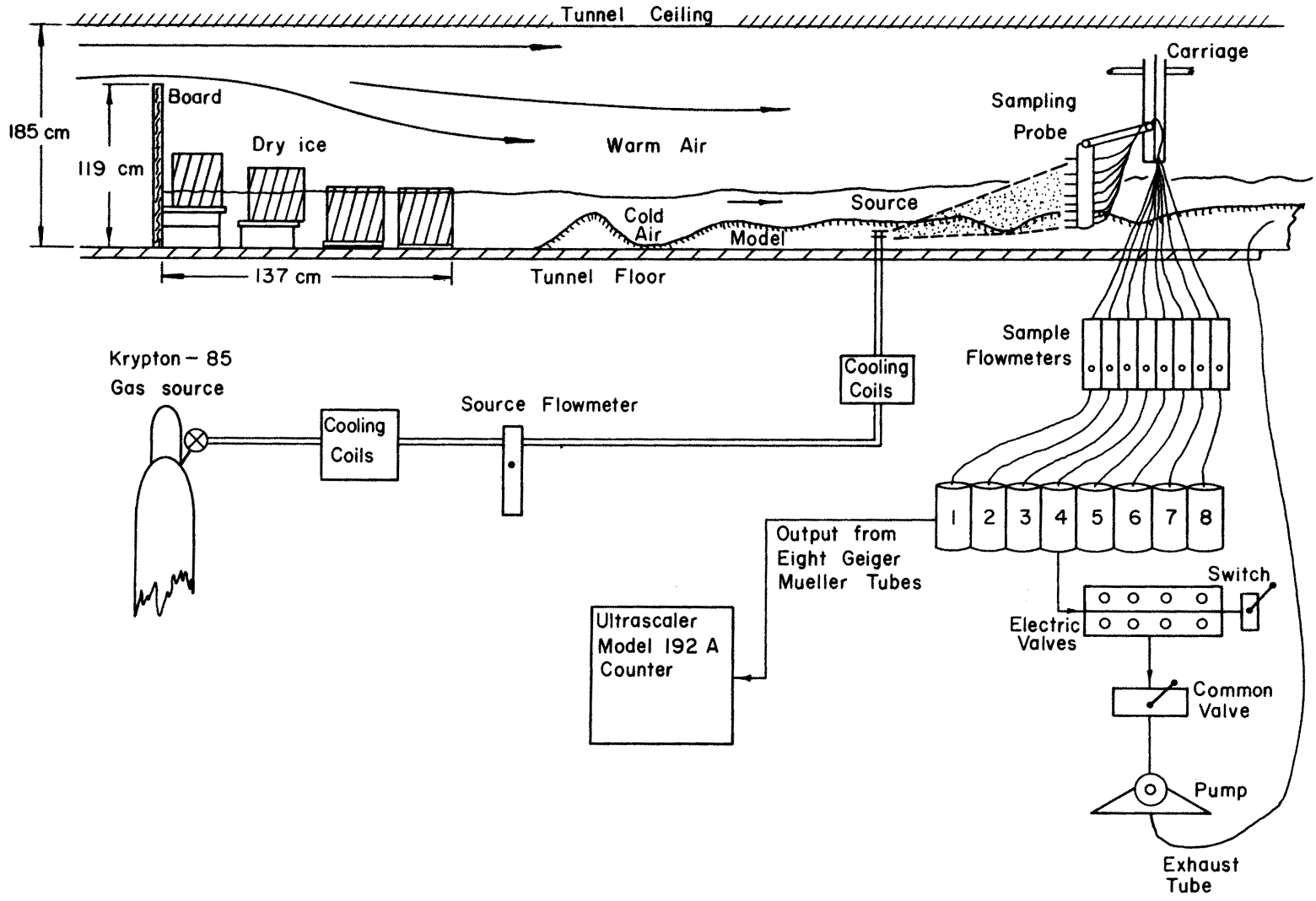

Fig. 3-11 Laboratory experimental arrangement for obtaining measurements of the radioactive Krypton-85 concentration over the model for the barostromatic airflow.

geometric, 2) turbulence, 3) kinematic, and 4) time similarity viz

$$\frac{\overline{C}\,\overline{U}\,X^2}{Q}(r) = f\left(\frac{Z}{H}, Re_t, \frac{U(z)}{U_g}, \frac{t_s}{T}\right) \qquad 3\text{-}1$$

Each of these nondimensional variables were evaluated for the model airflow and the prototype (Ref. 30, p. 96). In general, it was found that geometric and kinematic similarity was achieved in an approximate way. In the case of dynamic or turbulence similarity the model airflow was probably more turbulent than the corresponding prototype atmosphere based on estimates of the turbulent Reynolds number, eddy-energy dissipation and freestream criteria. Insufficient modeling of the upstream boundary conditions may have augmented the turbulence intensities, especially in the front half of the topographic model near Minturn.

Time similarity, of course, could not be achieved, but estimates based on the sampling and travel times for model and prototype suggested that the concentration patterns for the model were equivalent to prototype time-mean plumes of approximately 4 hours.

b. Barostromatic airflow

In the case of the barostromatic airflow the concentration distribution over the model and prototype depends on 1) geometric, 2) dynamic (thermal), 3) kinematic, and 4) time similarity viz

$$\frac{\overline{C}\,\overline{U}\,X^2}{Q} = f\left(\frac{Z}{H}, Re, Ri, Pr, \frac{U(z)}{U_g}, \frac{t_s}{T}\right) . \qquad 3\text{-}2$$

Dynamic similarity was based on the Abe-Cermak approach while thermal similarity was based on matching bulk Richardson numbers for the field and model (Figs. 3-12 and 3-13). The similarity of temperature or Richardson numbers was good in the lower levels but the model airflow was more stable than the prototype atmosphere in the higher levels.

The concentration fields as obtained from the model airflow corresponds to a prototype time-mean plume of approximately 18 minutes.

2. Dispersion similarity

The comparison of model and field results on transport and dispersion over the topographic model showed the following favorable results for both barostromatic and neutral airflows:

a) Both model and field data show that the tracer material diffused throughout the principal valley.

b) The direction of the tracer plume were approximately the same for model and field.

c) Comparison of normalized field ground-level concentrations at approximately 30 km from the first source (Minturn) with equivalent normalized model ground-level concentrations showed that model results fall within the observed range of field values.

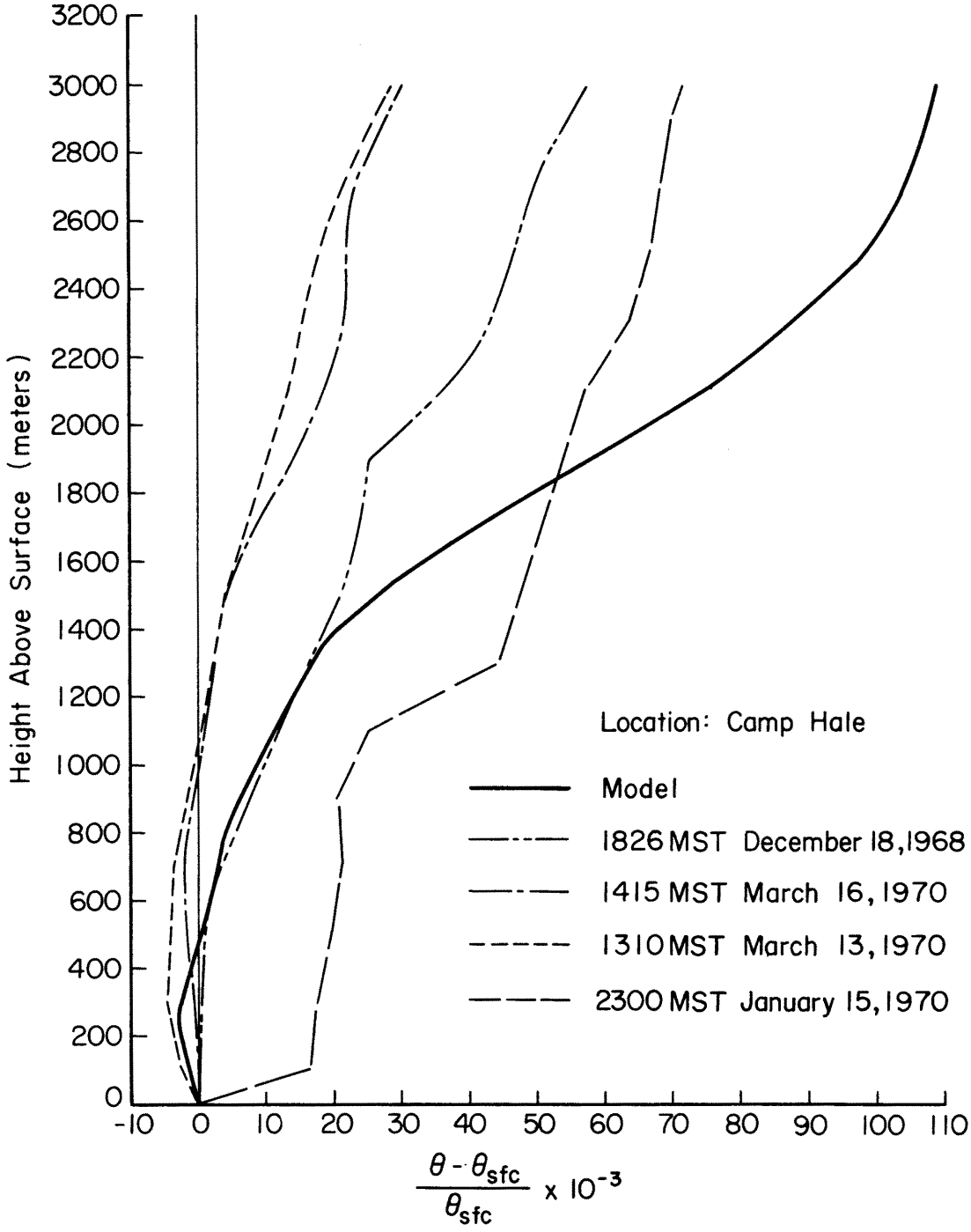

Fig. 3-12 Comparison of selected field potential temperature vertical profiles with a barostromatic model temperature profile.

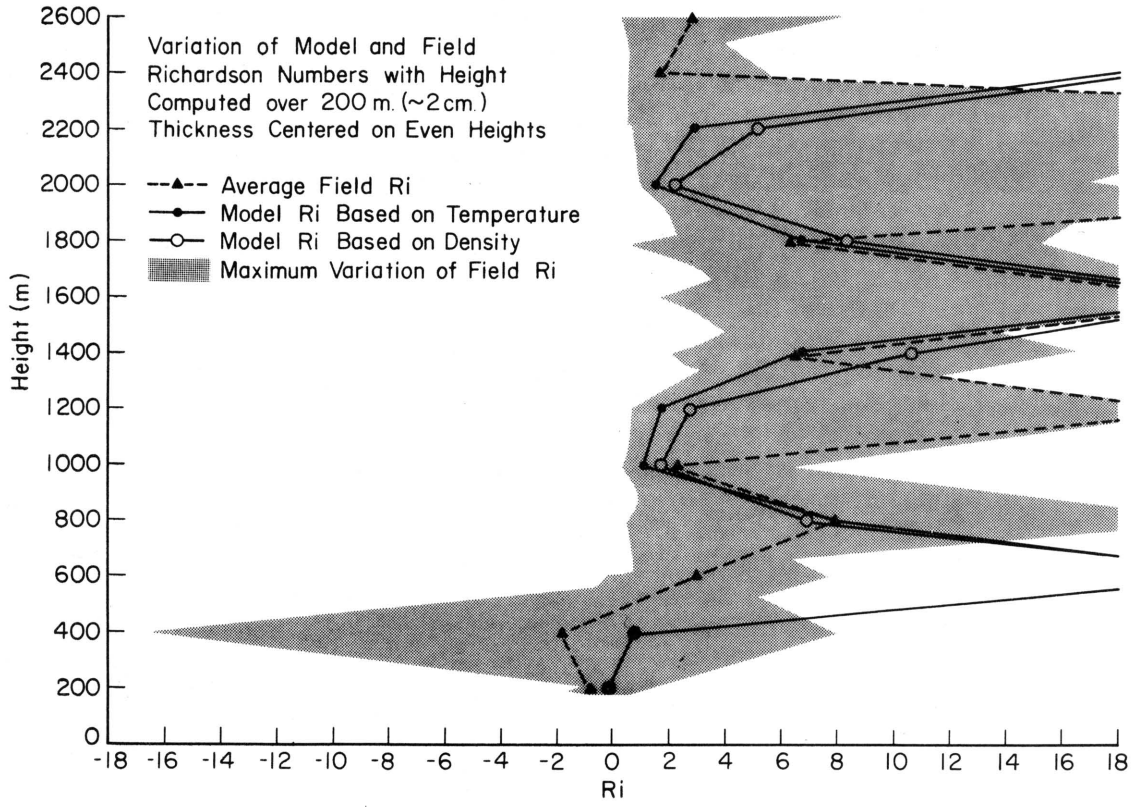

Fig. 3-13 Comparison of field and model bulk Richardson numbers at the Camp Hale location.

d) The scaled-up plume width as generated by the barostromatic airflow compared favorably with the field plume width (>12 km) near the surface at field sites approximately 30 km from the first source. However, the neutral airflow results underestimated the average field plume width by approximately 25 percent.
e) The angle-of-inclination of the plume's center of mass immediately downwind from generator sites was approximately equal for field and models. Comparison of barostromatic model-and-field plume rise rates compared favorably, however, the neutral model exaggerated the plume-rise rate by a factor of 2 to 2.5 (Fig. 3-14).
f) Comparison of normalized model axial-ground concentrations as a function of scaled-up distance with empirical methods of Pasquill and a modified Gaussian method showed that model dilution and decrease of concentration with distance were generally different from the other two methods (Fig. 3-15). Differences between model results and the other two methods were the result of topography, partial simulation of the actual airflow and dispersion and the inadequacy of the empirical and Gaussian methods for predicting dispersion in irregular terrain.
g) The comparison of the neutral and barostromatic model results with the field data showed that the barostromatic model simulated the atmospheric conditions corresponding to winter storms with northwest winds better than the neutral physical airflow model.

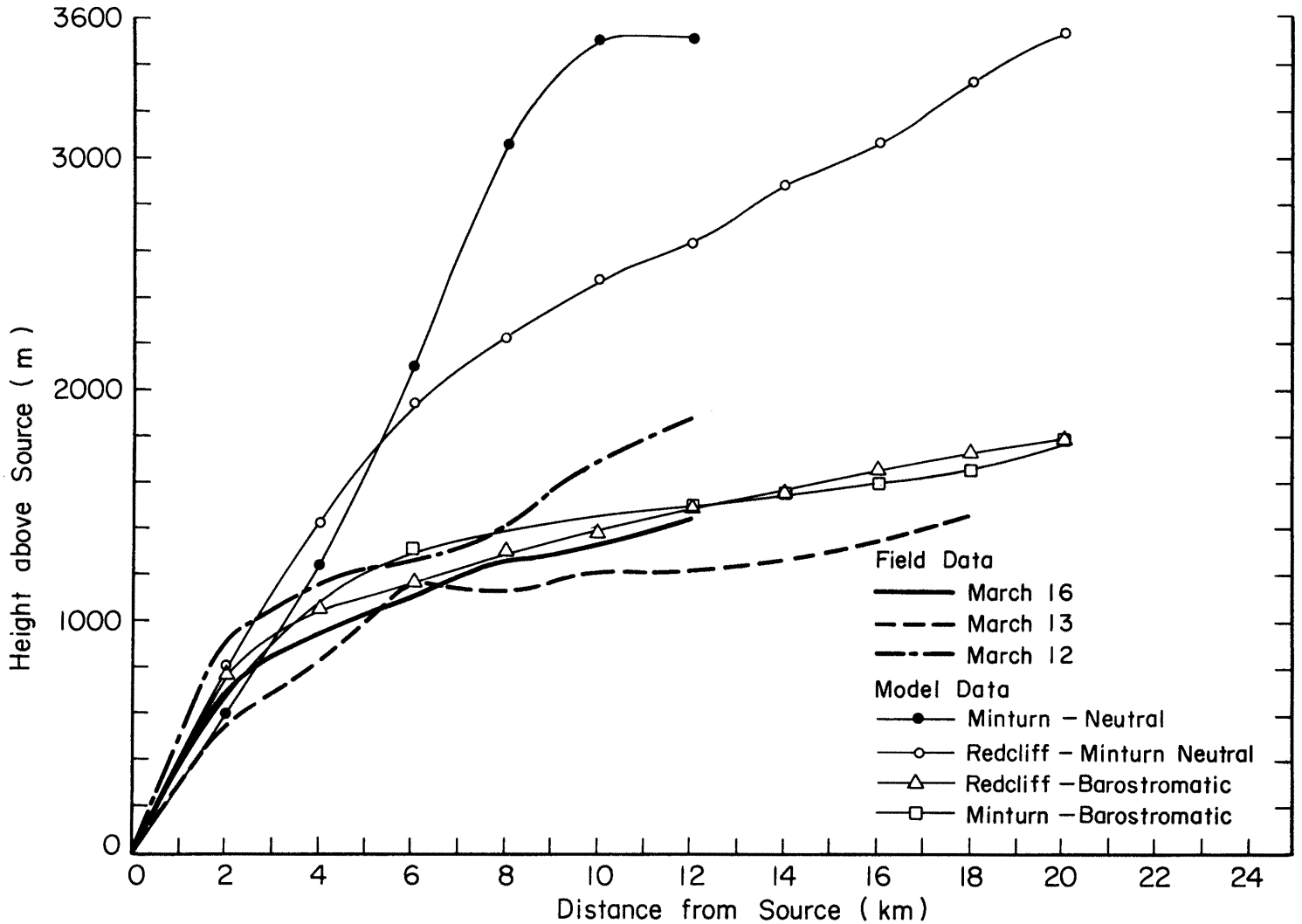

Fig. 3-14 Comparison between the vertical rise of model and field tracer plumes.

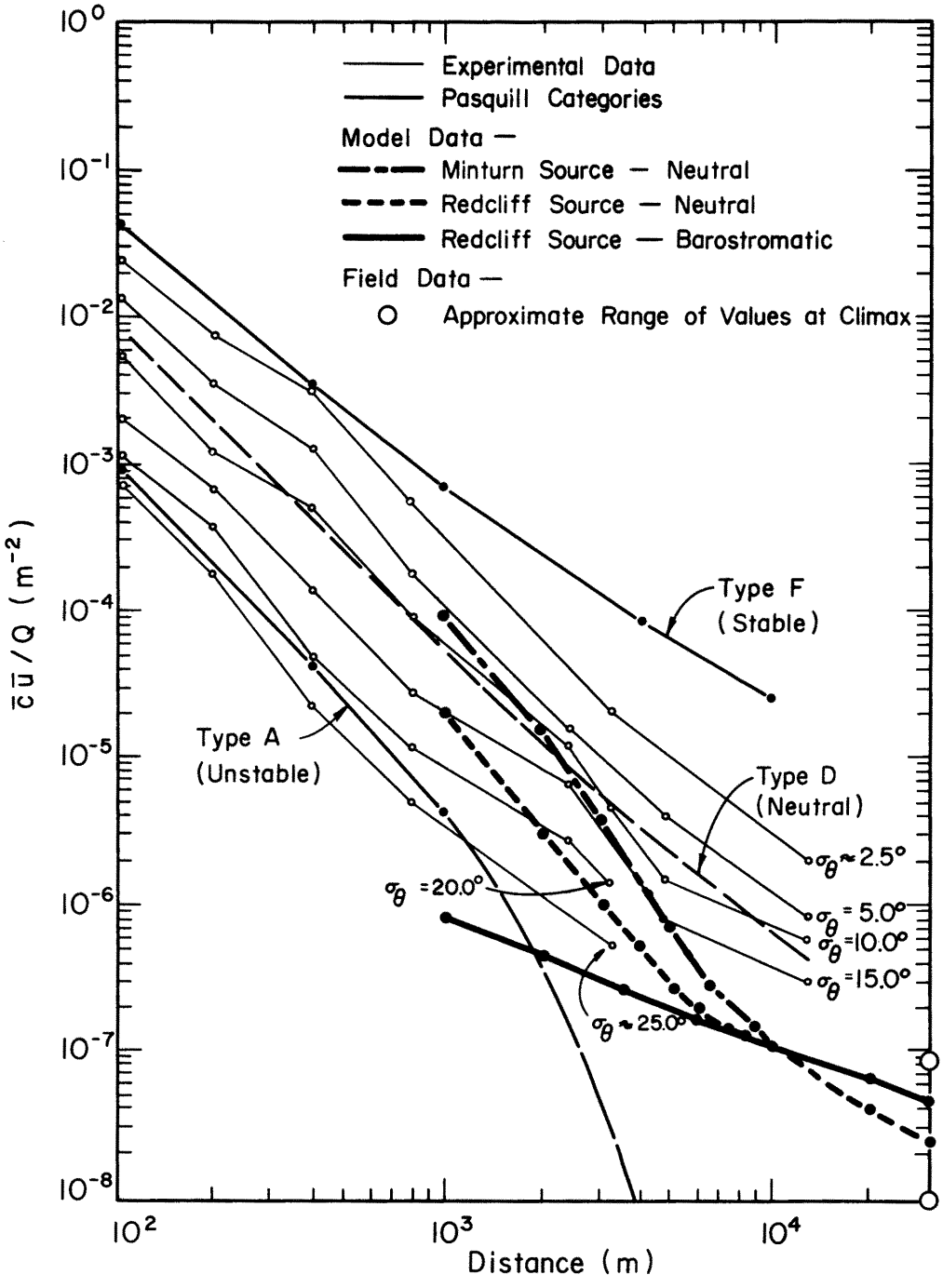

Fig. 3-15 Comparison of normalized surface-release axial-concentration measurements for models, Pasquill categories and non-mountainous experimental data.

IV. ELK MOUNTAIN STUDY

The general purpose of this study was to investigate the airflow and diffusion properties over a scaled topographic model of Elk Mountain with a laboratory physical model that possesses certain similarities to the shallow-water analogy (Ref. 21). This study was different from the other two research efforts in two ways. 1) Elk Mountain is a relatively isolated mountain as compared to the more complex terrain of the other studies and 2) a certain amount of numerical simulation work has been accomplished for Elk Mountain and was available for comparison with the laboratory physical models.

The contents of this section has been condensed from a more detailed report submitted by Kitabayashi et al., (Ref. 22).

Field Data

Field information relating to transport and dispersion of silver-iodide within the Elk Mountain Water Resource Observatory was obtained from the Natural Resources Research Institute, University of Wyoming (Refs. 2, 26 and 27).

Silver-iodide plume tracking was obtained by two NCAR ice-nucleus counters; one, in the observatory atop Elk Mountain and the other in the University of Wyoming aircraft.

Plume measurements were obtained during the winter months within the Elk Mountain Water Resource Observatory. During these studies, a silver-iodide generator was operated at a distance of 9-17 km upstream from the location of the NCAR counter atop Elk Mountain. In order to obtain an estimate of the plume width, it was assumed that the physical shape of the plume remained somewhat constant with time and for small movements of the seeding source.

During such experiments, the aircraft was flown at various positions between the silver-iodide dispensing point and the observatory atop Elk Mountain to establish the location of the plume. Also during these experiments, the temperature lapse rate and winds between the seeding source and the top of the mountain was continuously monitored. Numerous constant-volume balloons, rawinsondes and pilot balloons were released during the experiments to determine the wind flow at all levels on the windward side of Elk Mountain.

All the plume tracking experiments were conducted on cloudless days. However, the presence of the cap cloud on Elk Mountain may be accompanied by the same dynamic and stability conditions as were present during these tests.

The principal results of the plume tracking studies for the 1966-68 winter season was reported by Auer et al., (Ref. 2). The conclusions from these studies were the following:

1) The silver-iodide plume did not mix to vertical depths greater than about 450 m (~10 km from source) and that the angle of horizontal dispersion was usually about 10^{o} (plume width~ 1.0 to 3.7 km).
2) An inverse relationship between lapse rate and horizontal diffusion angle was observed, i.e., the smaller horizontal diffusion angles were associated with larger (unstable) lapse rates.
3) Concentrations of ice nuclei found within the seeding plume at the observatory some 10-17 kn downstream from the release point

varied from a few nuclei per liter at the edges of the plume to a maximum concentration of about 150 per liter, active at -20°C.

Laboratory Experimental Program

1. Topographic model

Construction methods, materials and scale (1:9,600) were essentially the same as for the other models. The direction of the freestream wind is 250° or west-southwest. The dimensions of the model are 5 ft 9 in x 12 ft. The lowest and reference elevation is 6,800 ft and the highest is Elk Mountain at 11,156 ft. The maximum height of the model is 5 1/2 in.

Generally, Elk Mountain (Fig. 4-1) is isolated but hills to the north and south complicate the topography. The windward side of the mountain rises gradually from a sagebrush plain while the leeward side descends abruptly from 11,156 ft to 8,000 ft within 3 km. The only topography upstream from Elk Mountain is an extension of the Park Range located some 65 km to the west-southwest.

2. Laboratory simulation facility

The Colorado State University low-speed recirculating wind-tunnel was used for the first measurements. The concluding series of measurements were made in the 6 ft x 6 ft meteoreological wind tunnel. Specifications of these facilities are found in Table 3-3, and a view of the meteorological wind tunnel is shown in Fig. 4-2.

3. Boundary conditions

The lower boundary conditions were provided by the topographic model. In the case of neutral airflow a momentum boundary layer was developed by the long test section and artificial devices. The freestream velocity was 9 m/s.

In the case of the barostromatic airflow a thermal and momentum boundary layer was produced by placing blocks of solid carbon dioxide (dry ice) in the upstream section of the wind tunnel and also by using the cold plates of the wind tunnel floor (Fig. 4-3). Seven I-shaped aluminum rods about 10 cm high and 1.8 m long were also placed on the cooled plate floor parallel to the airflow to increase the thermal boundary layer and to attenuate large scale (low frequency) turbulence.

The upper-boundary condition (roof) was not modified, therefore, a longitudinal pressure gradient was present along the longitudinal axis of the tunnel. There was no serious effects due to the sidewall boundary conditions. Figure 4-4 shows a upstream view of the wind tunnel setup for one of the barostromatic airflow experiments.

4. Experiments

Four experimental periods in the wind tunnel were made to obtain data on surface streamlines, velocity, turbulence and concentration for the neutral airflow case. Only one set of concentration data was obtained over the topographic model. The source was location #6 (Fig. 4-1) which is located west-southwest of Elk Mountain about 17.5 km (prototype scale) from the mountain crest. The concentration measurements were obtained by the radioactive Krypton-85 method.

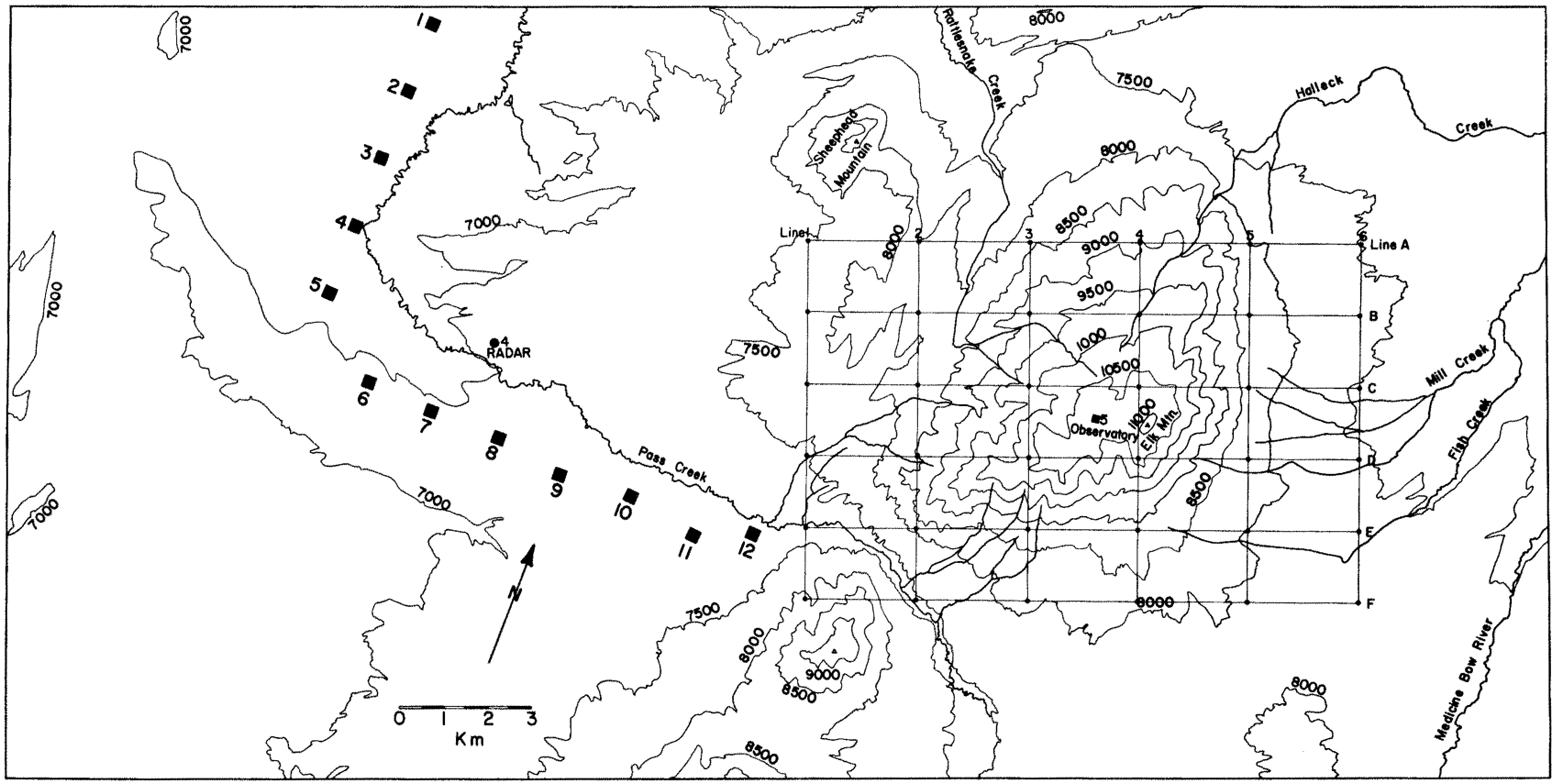

Fig. 4-1 Elk Mountain and surrounding topography modeled in wind tunnel.

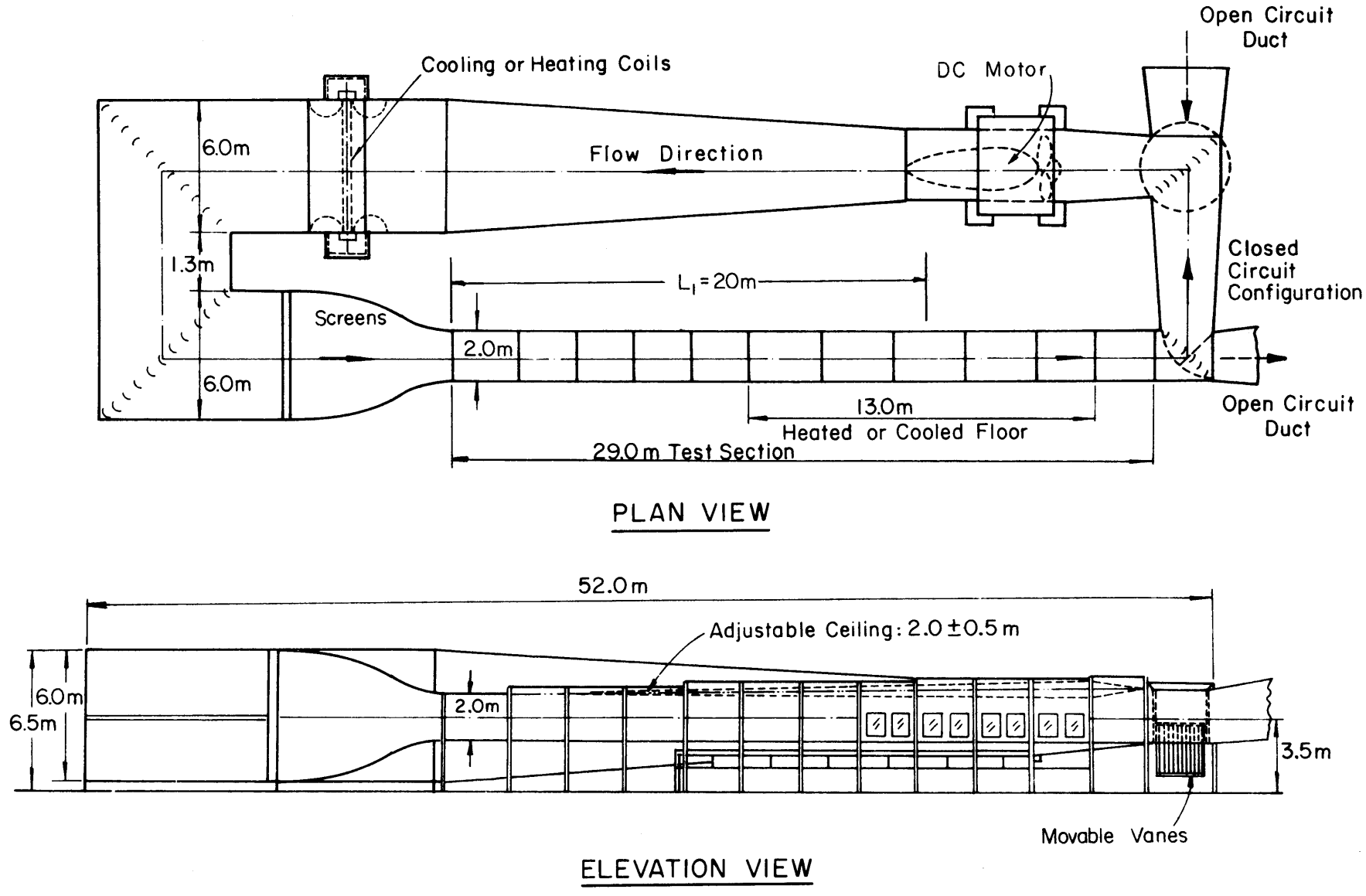

Fig. 4-2 Colorado State University meteorological recirculation wind tunnel.

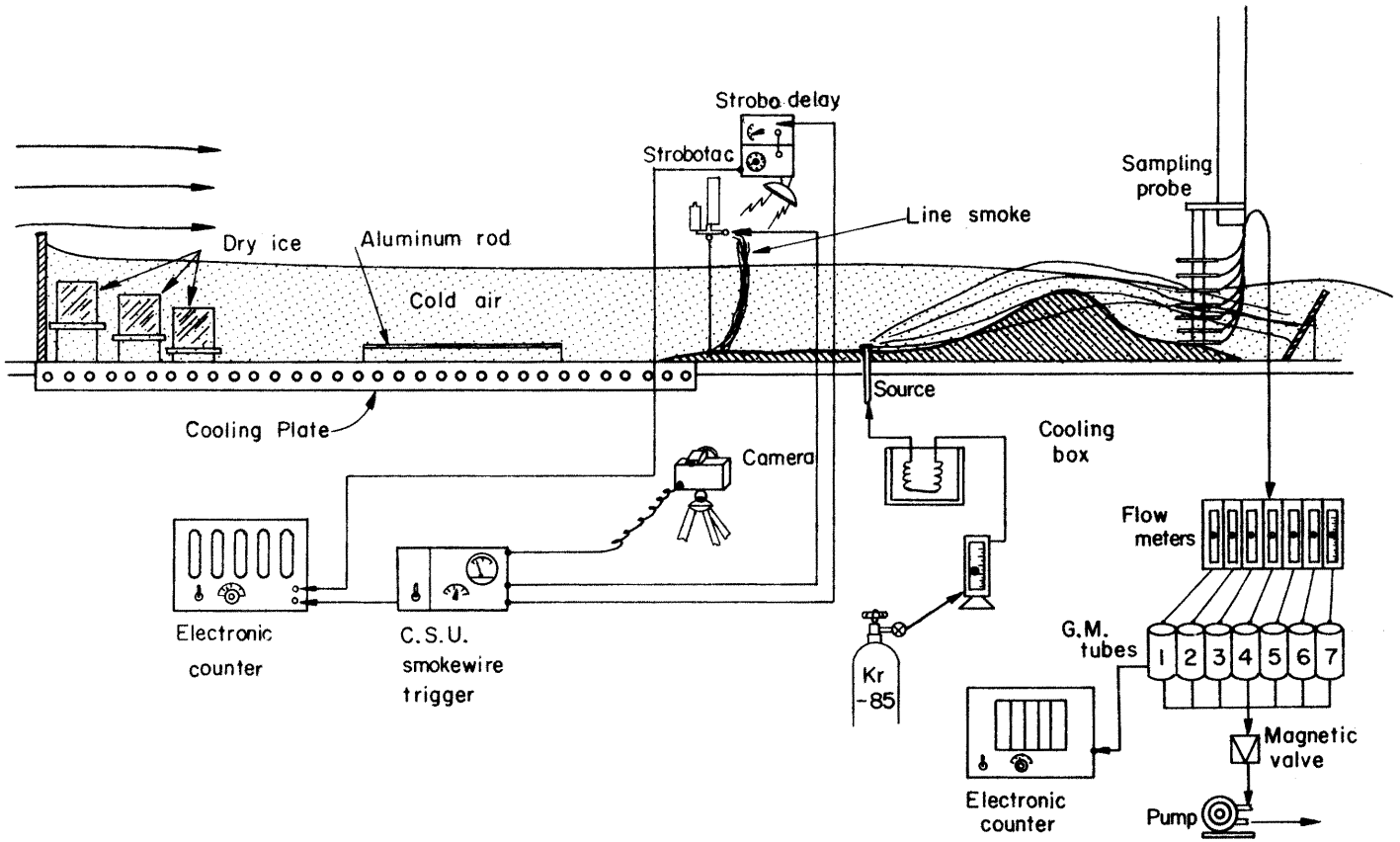

Fig. 4-3 Schematic illustration of the wind tunnel experimental setup for barostromatic airflow.

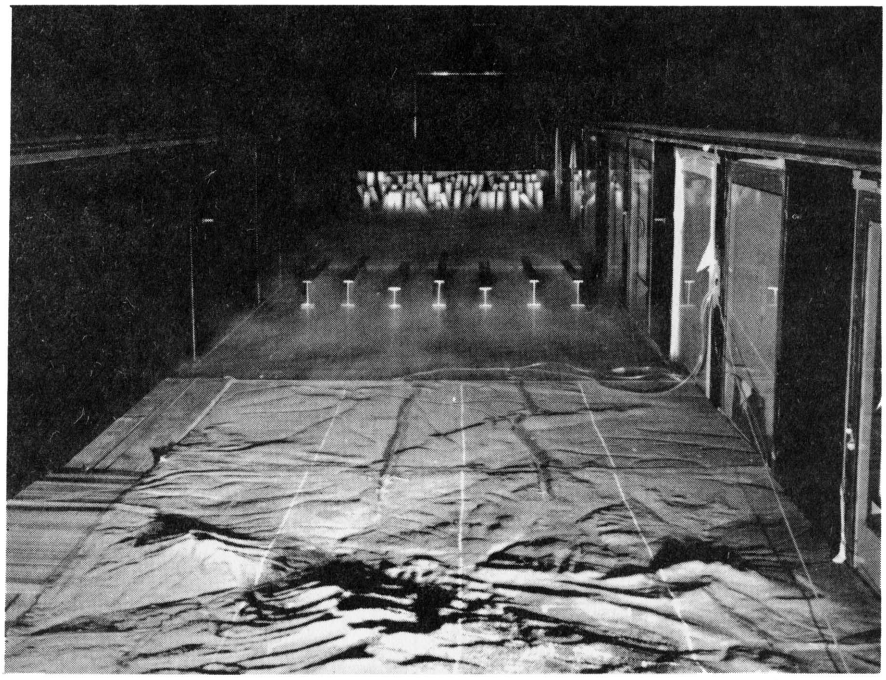

Fig. 4-4 Upstream boundary conditions for the barostromatic airflow. Elk Mountain study.

In the case of the barostromatic airflow several experiments were needed to obtain data on airflow velocity, temperature and concentration measurements. In addition to these measurements a series of experiments, both neutral and barostromatic, were conducted on visual simulation of the airflow over the topographic model.

Comparison of Laboratory and Field Data

1. Neutral airflow

a. Airflow similarity

In the laboratory a freestream velocity of 9 m/s was chosen to assure that the airflow was turbulent over the topographic model. For dynamic similarity, the Reynolds number similarity was not used since the airflow was assumed to be aerodynamically "rough" (Ref. 33).

In the wind tunnel, the boundary layer for the neutral stability case was defined as the height where the local velocity approaches the freestream value. This is similar to Hanna's (Ref. 20) definition of the momentum boundary layer as the height where the local velocity approaches the geostrophic wind. For the field, this depth was 1-1.5 km while for the wind tunnel it was approximately 1.4 km (prototype scale).

The depth of the planetary boundary layer can be estimated from an equation devised by Laikhtman and modified by Hanna (Ref. 20)

$$H = 0.75\bar{U}_g \frac{1}{\left(\frac{g}{\theta}\frac{\Delta\theta}{\Delta z}\right)^{1/2}} \qquad 4\text{-}1$$

Using Eq. (4-1) with $\bar{U}_g$ = 15 m/s , $\Delta\theta/\Delta z = 1.8\times10^{-3}\ ^{o}K/m$ and $\bar{T} = 270^{o}K$ the planetary boundary layer depth is calculated as,

$$H \sim 1500m$$

for the mean conditions of the field. This value, as well as the laboratory estimate compares favorably with the "well-mixed layer" defined by the Wyoming group for their modified numerical model.

The mean velocity and turbulent intensity profiles over the topographic model were typical for a rough wall boundary-layer with no apparent effects from the topography except near the immediate vicinity of Elk Mountain. Figure 4-5 shows the near-surface streamline pattern for this type of airflow. At the upstream slope of Elk Mountain, the upstream flow diverged due to the blocking effect of the mountain. This was more apparent on the steep southern slope of the mountain. Separation of the flow was observed on the lee side of the mountain. At this location, the wind direction flucuated strongly and high turbulent intensities (40-60%) occurred.

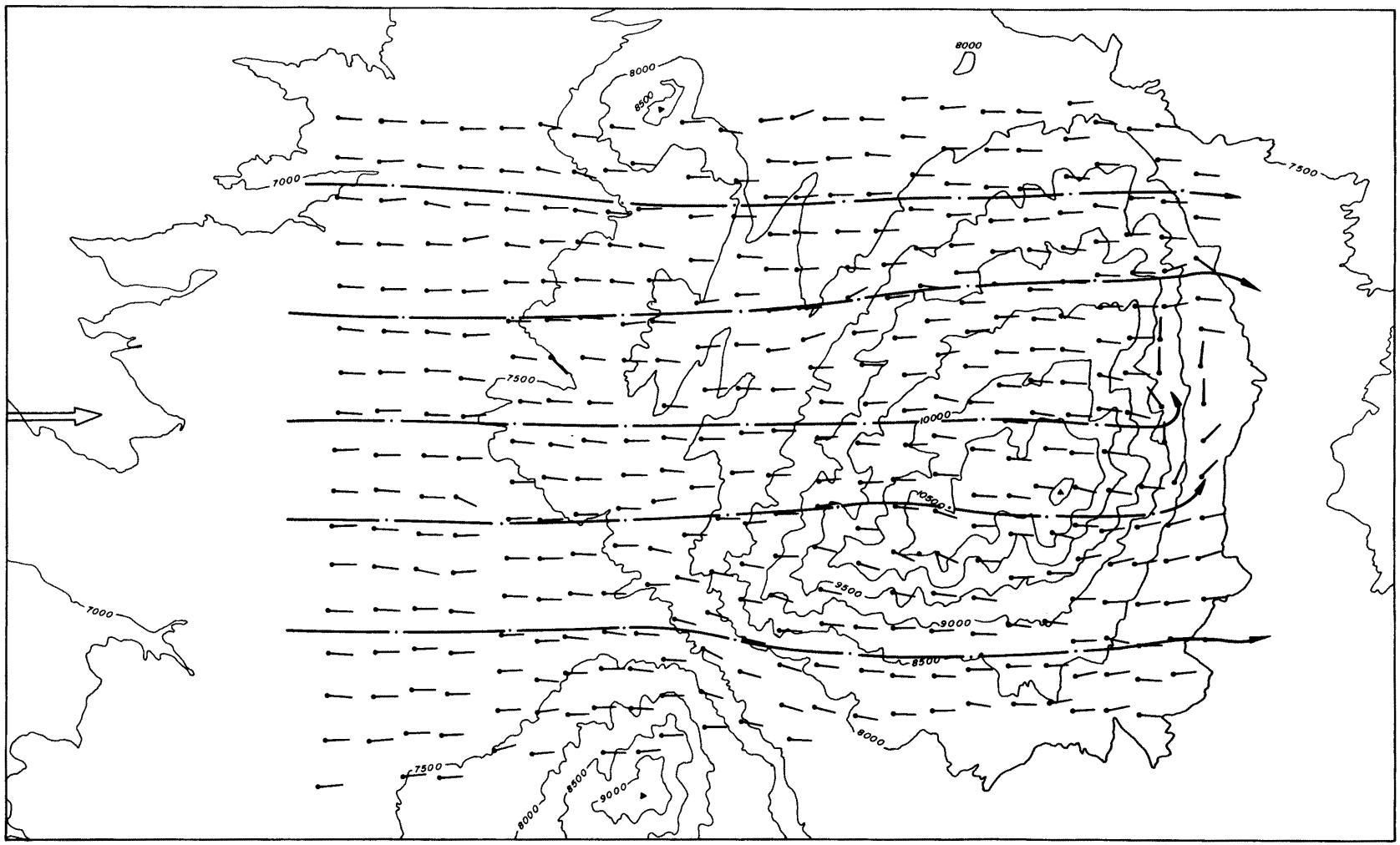

Fig. 4-5 Surface wind directions and streamlines in neutral airflow over Elk Mountain model.

A comparison between the laboratory streamlines and the vertical stream-surfaces as computed by the University of Wyoming group by a numerical model showed that the diverging flow around Elk Mountain was simulated to a high degree of correspondence (Ref. 22).

b. Dispersion similarity

The surface distribution of radioactive tracer in terms of a dimensionless concentration parameter $\overline{C}\,\overline{U}\,H^2/Q$ is shown in Fig. 4-6. The plume axis does not deviate too far from the freestream direction except near the mountain. The horizontal angle of dispersion was approximately 16^o which was a little larger than the 10^o reported by field observations (Ref. 2).

A vertical cross-section of the plume along the horizontal axis of the maximum concentration is shown in Fig. 4-7. The vertical dispersion was

$$D_z \sim 1 \text{ km/10 km of horizontal transport}$$

which was approximately two times the mean dispersion measured in the field. Differences in lapse rate stability conditions and definition of the top of the plume may explain part of the differences between field and laboratory.

2. Barostromatic airflow

a. Airflow similarity

In the wind tunnel, the airflow velocity and temperature distribution were established to give Froude and Richardson number similarity.

The Froude number similarity was based on the "well-mixed layer" height where

$$U_m = U_f \frac{H_m}{H_f} \quad . \qquad 4\text{-}2$$

Since $U_f \sim 12$ to 15 m/sec the wind tunnel velocity should be $U_m \sim 15$ to 20 cm/sec. A freestream of approximately 20 cm/sec was measured in the wind tunnel. The Froude number based on the temperature inversion height was $Fr_M \sim 0.20$ which compares favorably with a field value of $Fr_F \sim 0.15$.

A bulk Richardson number

$$Ri_b = \frac{g}{\overline{\theta}} \frac{\Delta\theta}{\overline{U}^2} \Delta z \qquad 4\text{-}3$$

was computed for laboratory and field data and the height profiles are shown in Fig. 4-8. As with the Climax study, the model and field correspondence was good in the "well-mixed layer" but in the upper layers the wind tunnel Richardson number was approximately one and one half times as large (more stable) as the field value.

The airflow and thermal characteristics of this physical model resembled certain aspects of the shallow-water

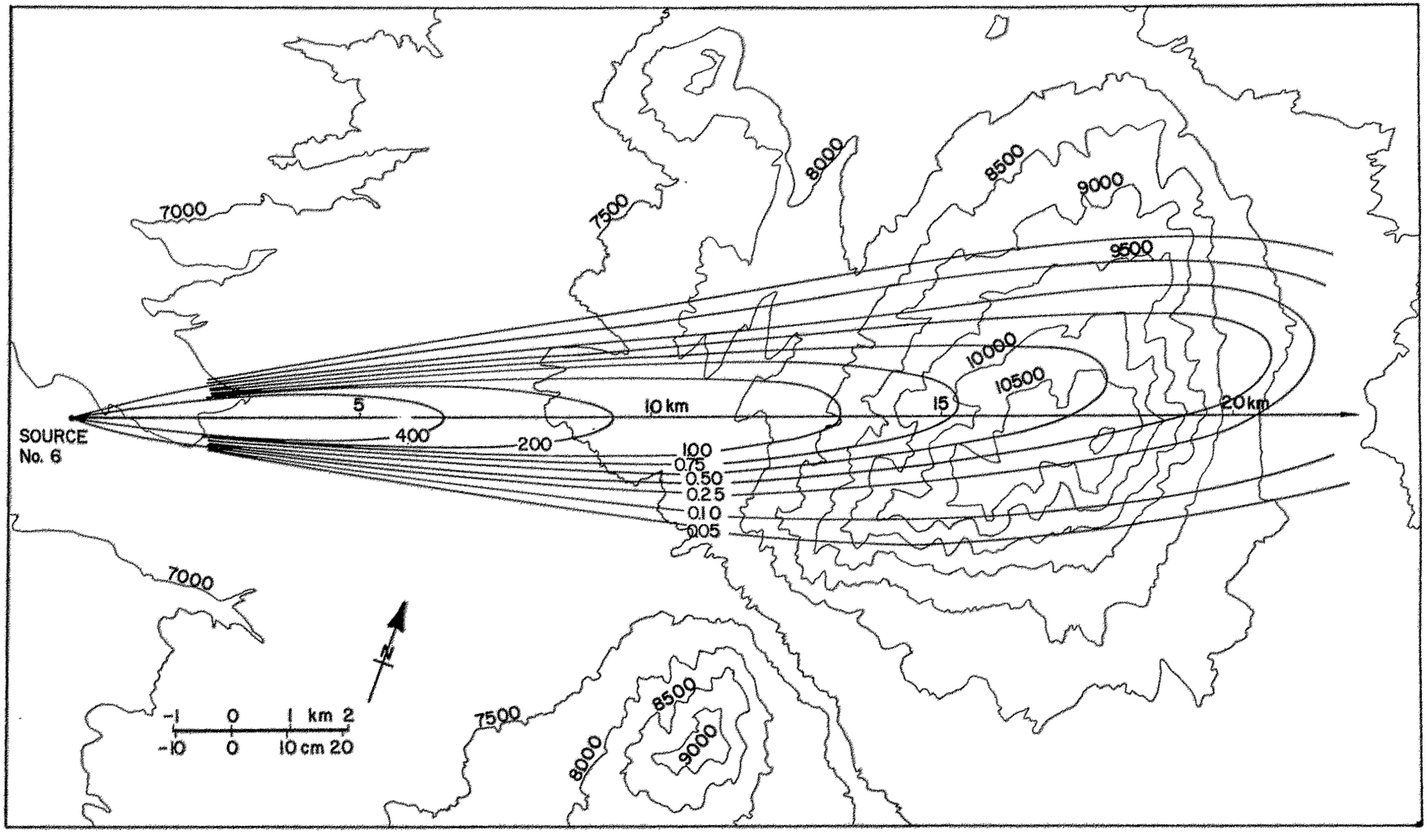

Fig. 4-6 Surface distribution of radioactive Krypton-85 gas around Elk Mountain. Neutral airflow.

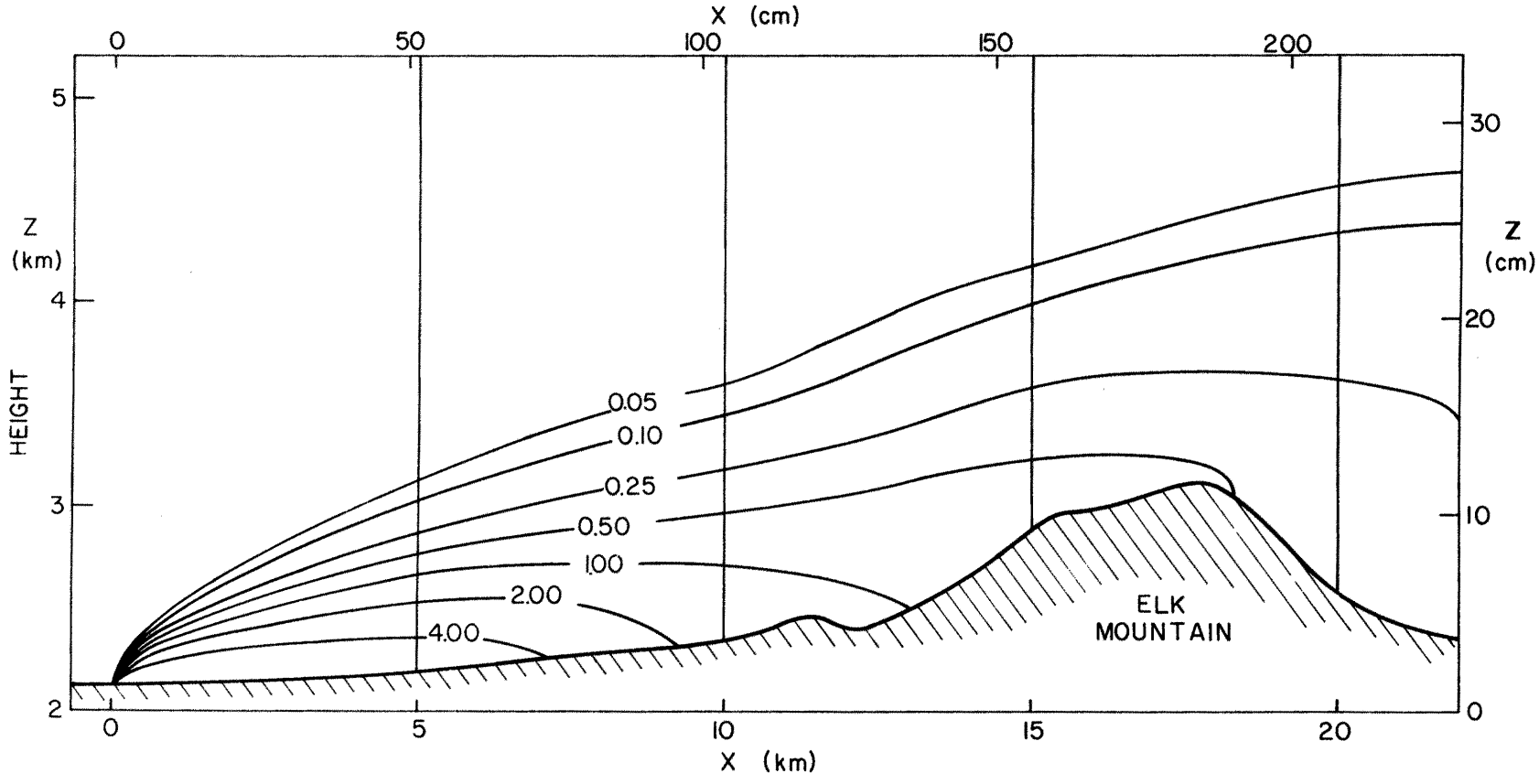

Fig. 4-7 Vertical cross-section of radioactive Krypton-85 gas over Elk Mountain. Neutral airflow.

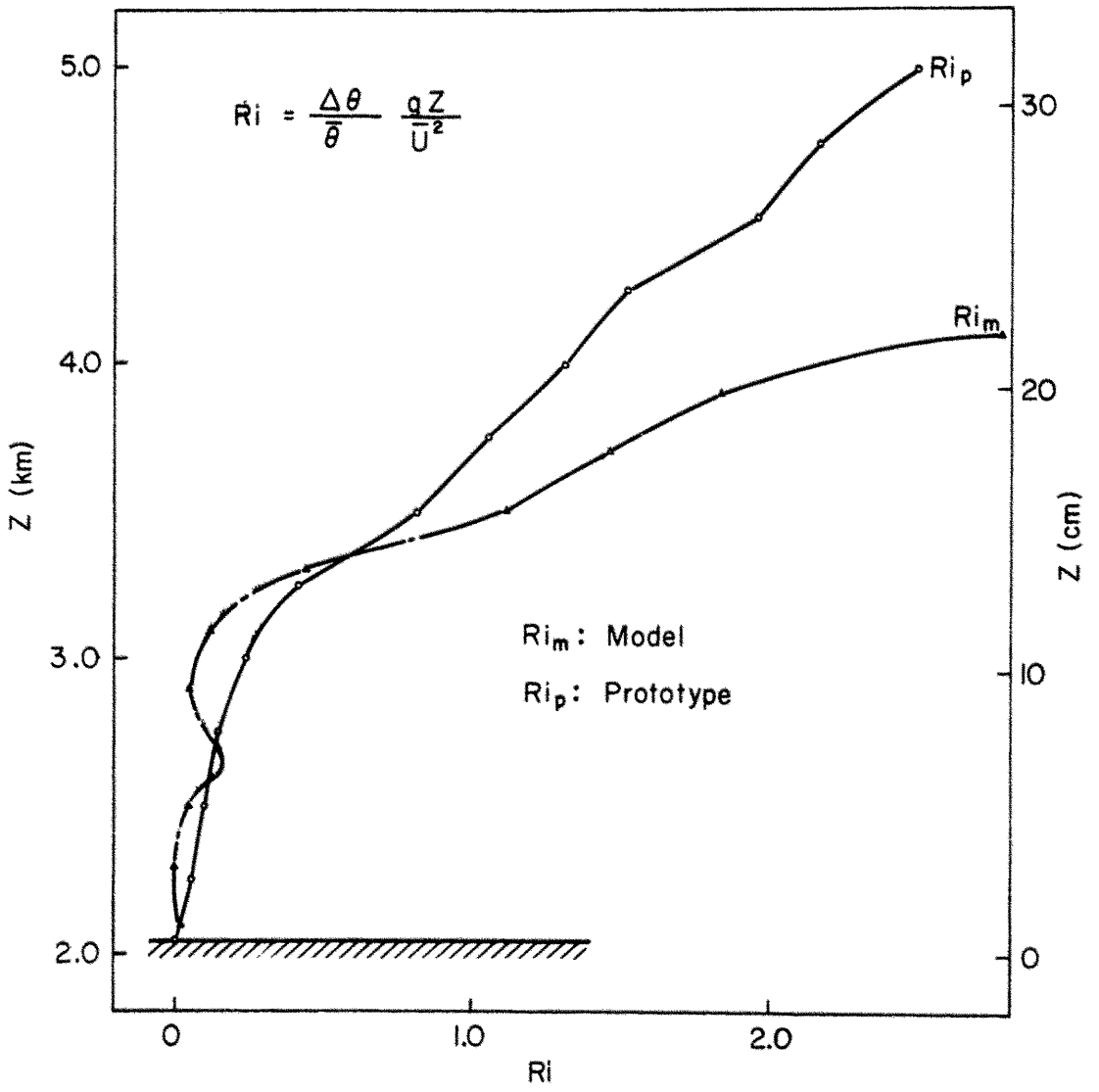

Fig. 4-8 Comparison of bulk Richardson number height profiles for barostromatic airflow and field. Elk Mountain study.

analogy. These particular aspects were the following:

(1) The velocity profiles over the topographic model were in good agreement with the vertically homogeneous flow assumed in the shallow-water analogy.

(2) The occurrence of an atmospheric "hydraulic" jump on the lee side of the mountain was observed in the laboratory airflow.

(3) Highest wind velocities were observed over the mountain crest.

(4) Height distribution of the stable thermal layer in the laboratory airflow corresponded well in the shallow-water analogy.

b. Dispersion similarity

The horizontal and vertical distribution of the radioactive gas tracer is shown in Figs. 4-9 and 4-10. The horizontal dispersion does not seem to change significantly in magnitude from the neutral case due to the existing thermal neutral-layer near the surface. However, smoke visualization pictures indicated that the blocking effect of the mountain was a little more significant than for the neutral case.

The vertical and horizontal plume widths at several downstream points are given in Table 4-1 for neutral and barostromatic airflow. The lateral plume width was defined as the distance from the plume axis to the point where the concentration decreases to 10 percent of the peak value. The vertical plume height is defined by the height where the concentration decreases to one-tenth of the ground level value.

Table 4-1

Elk Mountain Study - Horizontal and Vertical Dispersion of Radioactive Gas from Source #6. Distances and Heights Scaled to the Prototype

	Neutral		Barostromatic	
x km	Lateral km	Vertical km	Lateral km	Vertical km
5	1.3	0.57	---	----
10	2.8	0.95	3.0	0.77
15	5.0	1.20	3.7	1.15
20	5.8	2.10	7.5	0.78

Field results show that the plume width varies between 1.0 and 3.7 km (at 10 km) which corresponds well with the scaled laboratory results. However, the field vertical dispersion of 450 m (at 10 km) is somewhat less than the 770-950 m (prototype scale) observed in the physical models. Both the field and physical models indicated that significant quantities of a tracer can reach elevations exceeding the summit of Elk Mountain.

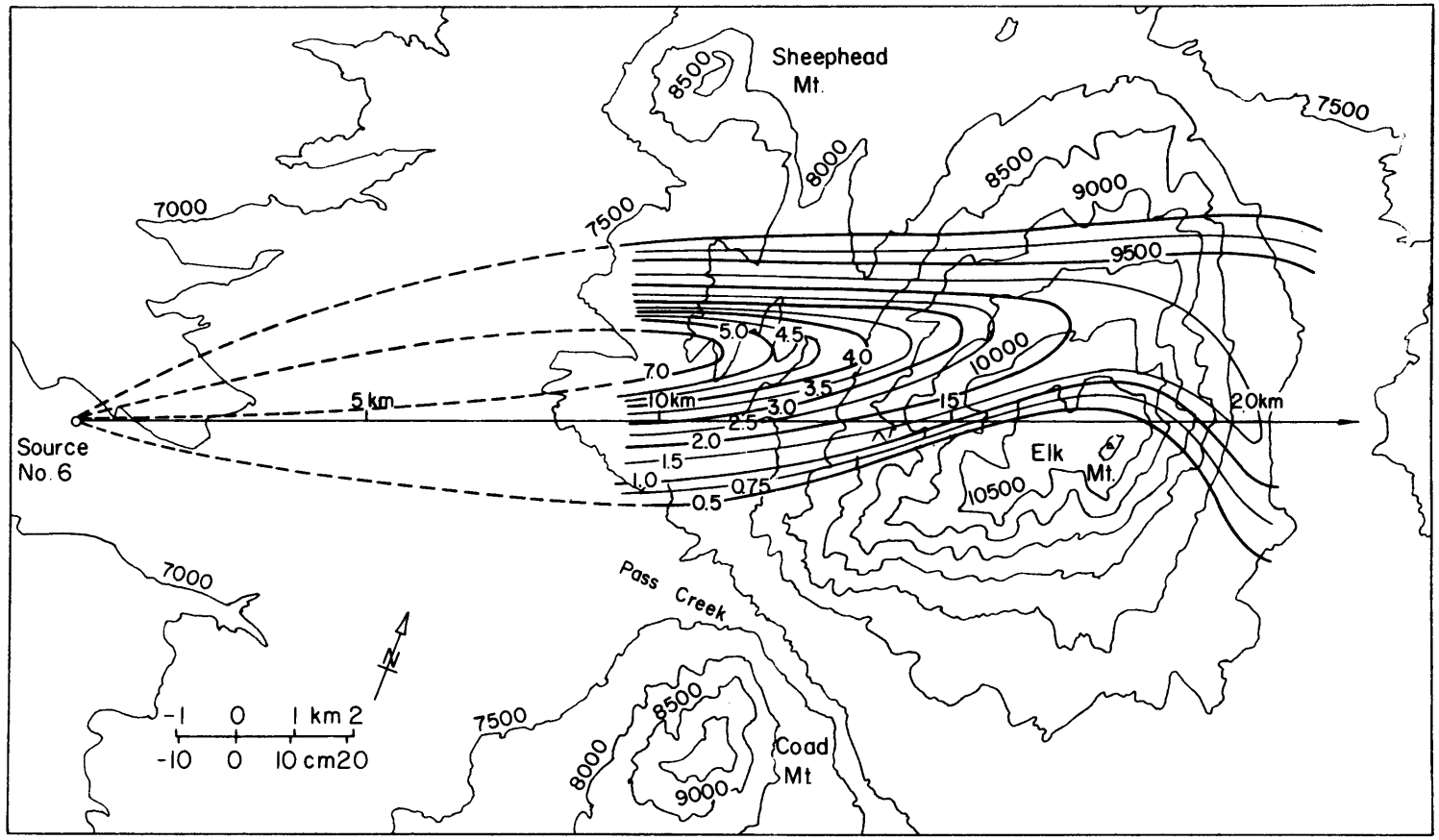

Fig. 4-9 Surface distribution of radioactive Krypton-85 gas around Elk Mountain. Barostromatic airflow.

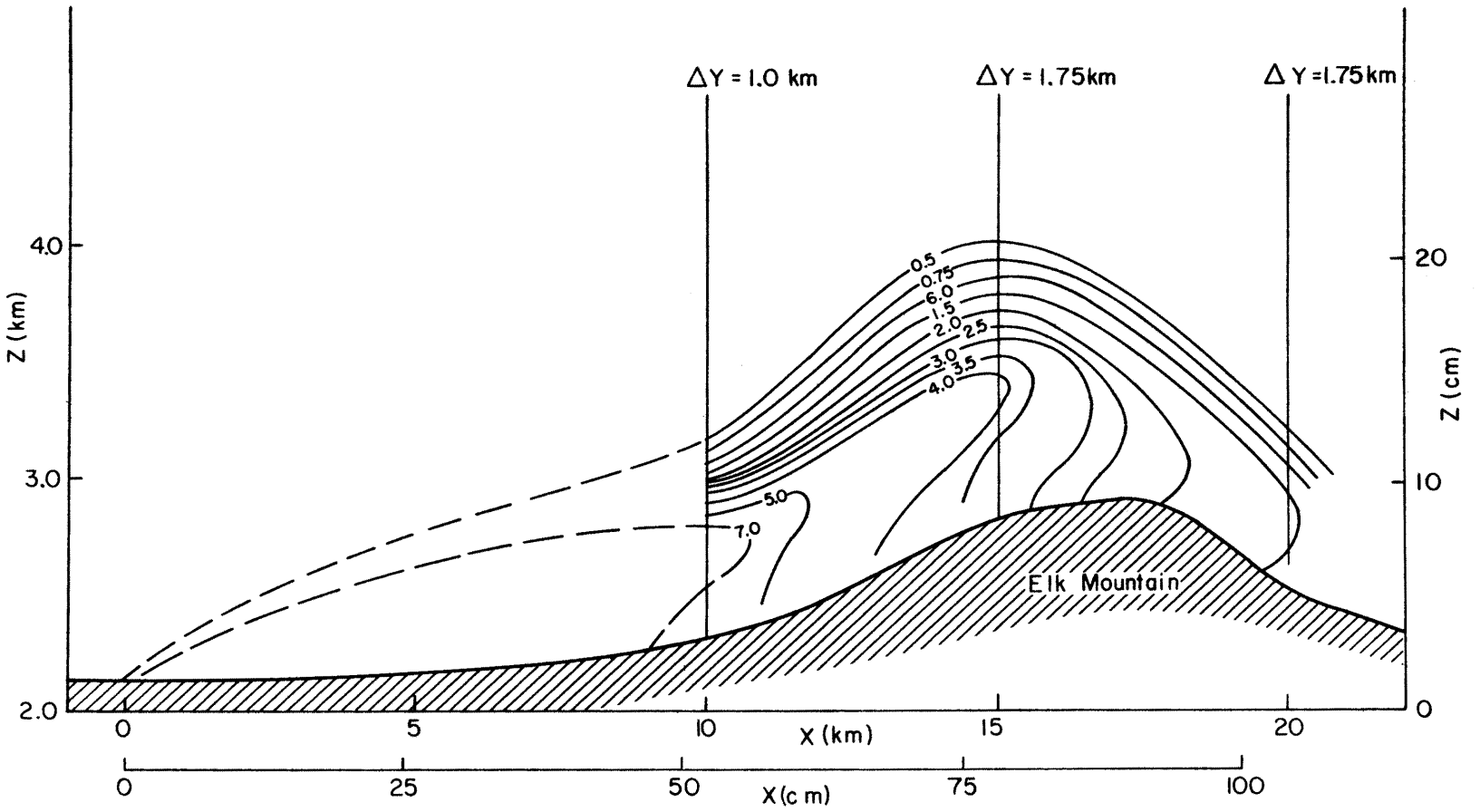

Fig. 4-10 Vertical cross-section of radioactive Krypton-85 gas over Elk Mountain. Barostromatic airflow.

V. SAN JUAN MOUNTAIN STUDY

The purpose of this last study was to develop a laboratory airflow model which would be adequate in estimating airflow and atmospheric transport-dispersion characteristics during winter storms (southwest winds) over the San Juan river drainage basin and Wolf Creek Pass region. The neutral and barostromatic airflow models were utilized again since detail information on the meteorological characteristics associated with the winter storms were not established.

This study differs from the other studies in at least three ways; 1) the modeled topographic area was twice as large than either the Climax or Elk Mountain modeled areas, thus requiring a distorted topographic model, 2) the topgraphy was typical of a large barrier mountain although complicated by river valleys and singular mountains, and 3) dispersion from multiple sources.

This section extends the material which was presented earlier in the last Interim Report (Ref. 31).

Field Experimental Program

1. Generator network

According to information published by EG and G (Ref. 11) the present silver-iodide generator network consists of 33 ground-based generator sites. Of these, 20 will be manually operated and 13 will be remote-controlled. The location of the generators are based on the Colorado State University design study (Ref. 18) which specified a primary line of generators 20-25 miles from the main mountain mass, and a secondary line 40-45 miles and several close-in generators.

2. Criteria for experimental day

An experimental day for seeding has been defined in terms of predicted precipitation, 500 mb temperatures and predicted 700 mb wind directions toward the mountain slopes, i.e., 150° through 300° of preliminary study of the frequency of experimental days to be expected showed a variation from 2 to 10 experimental days per month during the winter season (Ref. 11).

3. Field data

The available field data as acquired from Western Scientific Services, Inc., and EG and G was examined to obtain some information on the frequency of certain weather events that would be comparable to the model experiments. The acquired information was not a large quantity and not completely adequate, hence, some of the present descriptive statements about the meteorological conditions must be considered tentative until additional field data has been collected and analyzed.

Small samples of temperature and wind data were examined for the general area. Wind data were available from 15 Western Scientific Services rawinsondes released from Durango and 13 pilot-balloons releases from Chromo. Four pilot balloon releases from Pagosa Springs were obtained from EG and G. One of the reasons for the small sample of data was that only soundings with southwest wind were requested since the present model only simulates the southwest (220°) flow direction.

An examination of these data along with wind studies conducted by EG and G (Ref. 11) reveals the following wind-pattern characteristics in this area:

a. According to EG and G studies, a thermal-tidal wind regime may exist between the lower plateau areas to the southwest and the mountain mass of the Rockies to the north and east. This means that at night northwesterly or northerly wind components increase in the lower levels, while during the day, southwest or southerly components increase in magnitude. In addition, a local scale upslope and downslope circulation driven by the diurnal heating and cooling patterns of adjacent mountains and valleys has been observed from pilot-balloon data. Such wind regimes are most evident in synoptically quiescent periods within the planetary boundary layer.

b. Examination of the wind vertical profiles during deep southwest wind periods showed that a variety of wind speed and direction profiles existed. However, there were periods during southwest winds when the wind direction varied little in direction within the planetary boundary layer.

These wind data were not abundant enough to arrive at any statistics on the frequency of these occasions, but this was important information since the present model study assumes that little turning of the wind occurs at the geostrophic heights or in the lower levels except that caused by topographic relief.

c. Examination of several potential and equivalent potential temperature profiles showed that the stability conditions may vary widely even during storm periods with precipitation. An important question regarding the stability is whether events with near-neutral stability through a deep layer exists in this area during storm periods. This is of importance since the neutral model experiments were conducted under the assumption that near-neutral conditions existed in the field.

Only one or two soundings showed these near-neutral characteristics and these were not ideal. Figure 5-1 shows the temperature and wind vertical profile for April 22, 1970 at 1700 MST. This sounding exhibited temperature conditions which the laboratory experiments could approximate, but further information is needed in order to determine how long such stability periods persist.

d. Studies by EG and G (Ref. 11) have found that during precipitation conditions, trapping low-level temperature inversions were virtually nonexistent, but during fair weather with strong long-wave radiational losses from snow cover an inversion was very predominant.

The thermal-tidal, diurnal wind and temperature regimes do not pose any problem for the laboratory simulation since the wind regime of interest is large-scale storm-driven southwest winds where mountain and valley winds would only be minor modifications to the large-scale wind pattern.

Diffusion tests by means of ground generators and aircraft were conducted during the period 24 February, 1970 through 23 April, 1970. Three sites were chosen for the tests

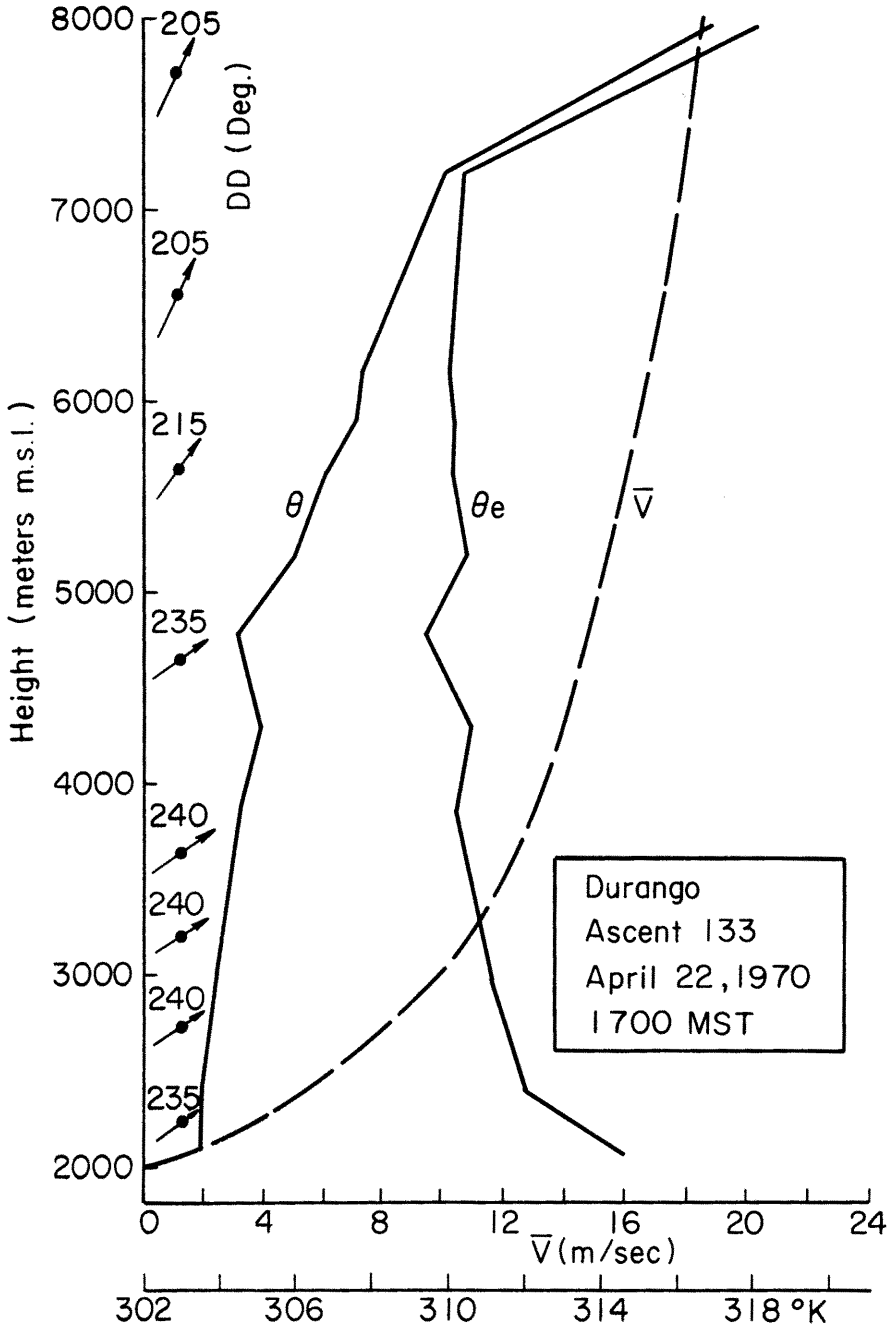

Fig. 5-1 Potential and equivalent potential temperature and horizontal wind distribution at Durango, Colorado. April 22, 1970.

one of which included the Pagosa Springs area. Due to a dry winter, the three areas were not snow-covered in December, January or early February. The diffusion results were dominated by convective days and displayed much less organized plumes than were observed in previous similar tests in the northern Colorado Rockies.

The preliminary results from these diffusion tests as reported by EG and G (Ref. 11) are the following:

a) "Ice nuclei released at the foothills site were transported vertically very swiftly. Nuclei released at 7800 feet reached 12,000 feet within five to seven miles from the release site.

b) "Most of the tests were conducted under neutral or near neutral stratification and the convective transport was dominant.

c) "The Pasquill-Gifford model fits the observed instantaneous plume width reasonably well out to two to three kilometers and over the lower terrain.

d) "At greater distances, the volume occupied by the released particulates appears much wider than that indicated by the Pasquill-Gifford diffusion model. Evidently, the mixing increases markedly as more pronounced terrain upslopes and rougher terrain elements are encountered.

e) "The Gaussian distribution with a well-defined plume axis of maximum concentration does not apply. Particularly in the vertical, the material is much more uniformly mixed through a vertical layer.

f) "The conditions of these tests were much less stable than those conducted in the northern Colorado Rockies, and convective transport was dominant. The plumes were much less steady state and less coherent.

g) "Trapping under inversions was not observed during the tests in the project area. Very little heating was required to reverse noctural drainage circulations."

Laboratory Experimental Program

1. Topographic model

The construction of the San Juan model was described in earlier project reports and details of this work will not be repeated in this report.

The overall dimensions of the model are approximately 12 ft x 28 1/2 ft. The model is divided into 14 sub-sections to facilitate placement into the wind tunnel. The model was constructed to simulate a south-southwest (220^{o}) freestream or geostrophic wind. This wind direction was selected on the basis of information from the San Juan experimental design study (Reg. 18).

Since the large extent of the geographical area to be modeled required a large scale reduction it was decided to construct a distorted scale model with a horizontal scale of 1:14,000 and a vertical scale of 1:9600. The lowest elevation is 5,800 ft and the highest is Summit Peak at 13,272 ft. The maximum model height is 9 1/4 in.

The topographic model only covers part of the area of the field generator network. Figure 5-2 and Table 5-1 shows the number of generator sites simulated on the topographic model. Fifteen

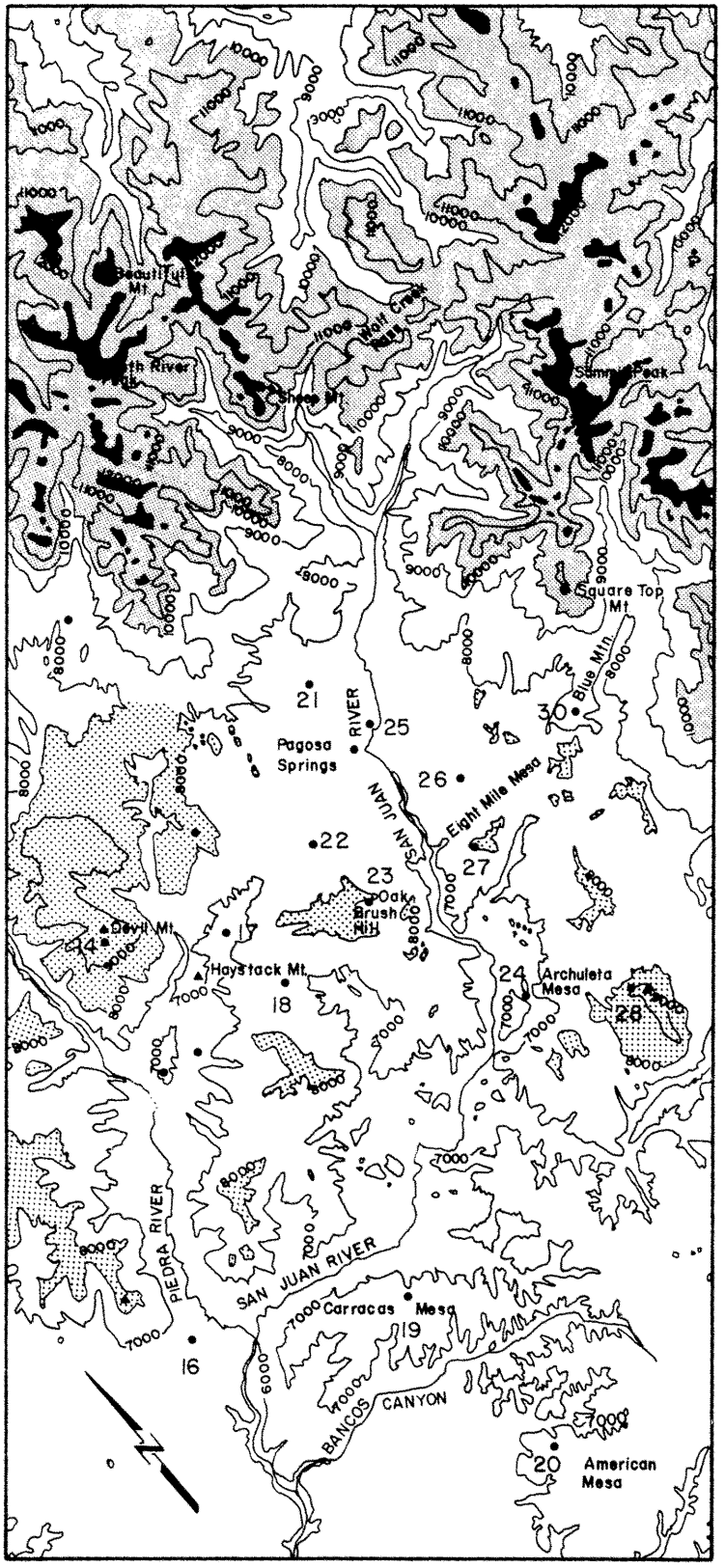

Fig. 5-2 Location of field generator sites that were modeled for the San Juan topographic model.

Table 5-1

EG and G Project Generator Sites for the San Juan Mountain Area and Sites Modeled on the San Juan Topographic Model

1. Parmley Ranch
2. Fort Lewis
3. Stocker Ranch
4. Royce Ranch
5. Sutton Ranch
6. Halliburton Ranch
7. Generator Site - Remote
8. Herrboldt Ranch
9. Ignacio Site
10. Moore Ranch
11. Sisk Ranch
12. A. T. and T. Microwave - Remote
13. Halverson Ranch
*14. Devil Mountain - Remote
15. Cooper Ranch - Remote
16. Baldamar Ranch
17. Radcliff Ranch
18. Espinosa Ranch
19. Carracas Mesa - Remote
20. American Mesa - Remote
21. Hott Ranch
22. Harris Ranch
23. Oak Brush - Remote
24. King Ranch
25. Formwalt Ranch
26. Hudson Ranch
27. Eightmile Mesa - Remote
28. Archuleta Mesa - Remote
29. Wirt Lookout - Remote
30. Blue Mountain - Remote
31. V-Mountain - Remote
32. Abeyta Mesa - Remote
33. Crowley Ranch

*Generator sites underligned were constructed on the topographic model. In addition, eight other sites were constructed for optional measurements.

of the 33 field generator sites were constructed on the model. In addition, eight other sites were constructed for optimal measurements.

Two different types of sources were designed for the model as shown in Fig. 5-3. Type I was used principally for the experiments for neutral flow with the exception of three sources located several feet from the mountain massif. For these three distant sites, Type II was utilized in the experiments. Type II source was also used for the experiments with barostromatic airflow.

2. Laboratory simulation facility

All the experimental work was conducted in the Colorado State University low-speed environmental wind tunnel. Specifications of this facility is found in Table 3-3 and a view of the wind tunnel is shown in Fig. 5-4.

3. Boundary conditions

In the case of the neutral airflow the velocity and turbulence profiles were approximated by modifying the upstream section of the wind tunnel with cardboard tubes and gravel roughness.

A schematic diagram of the Colorado State University environmental wind tunnel and the upstream modifications are shown in Fig. 5-4. At the beginning of the test section two sets of cardboard tubes were fixed into place, the first set, 36-in. long and 2 1/2 in. diameter were placed on the floor with the second set, 18 in. long and 2 1/2 in. diameter placed on top of the first.

Downstream from the tubes small gravel roughness elements were randomly scattered extending across the tunnel and for 6 ft down the tunnel. The model fills the remainder of the tunnel up to 33 ft downstream from the entrance. The upstream boundary conditions may not be the ideal arrangement but was selected after several days of experimentation with different upstream arrangements using roughness, vortex generators, etc. These present conditions appear to give approximate velocity profile similarity.

In addition to the upstream modification the upper boundary conditions (roof) was adjusted to produce an approximate zero longitudinal pressure gradient along the model. The boundary-layer development on the side walls have been measured at approximately 12 in. and with the irregular configurations of the model may affect the side flow patterns up to 18 in. Therefore, the effective width of the model which may not be affected seriously by the side wall conditions was approximately 9 ft.

In the case of the barostromatic airflow where temperature stratification was required the upstream boundary conditions consisted of 900 to 1000 lbs of dry ice. The airflow from the ice produced a thermal boundary layer which resembled that of the other two studies.

4. Experiments

Several experimental periods were required in order to obtain data on velocity, turbulence, temperature, concentration and visualization of airflow.

In the case of the neutral airflow the following experiments were completed:

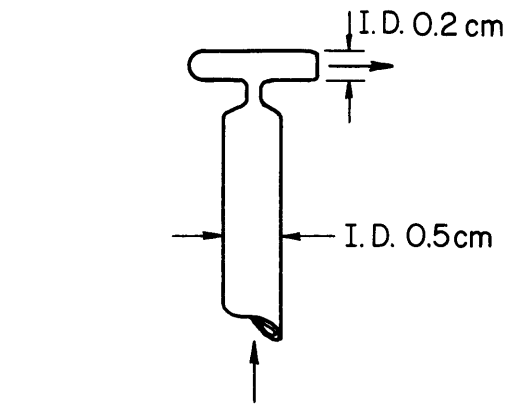

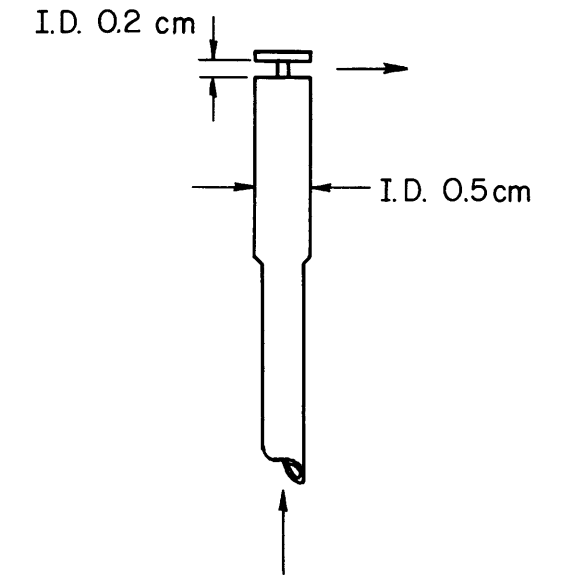

Fig. 5-3 Types of sources designed and utilized on the model for emitting radioactive gas.

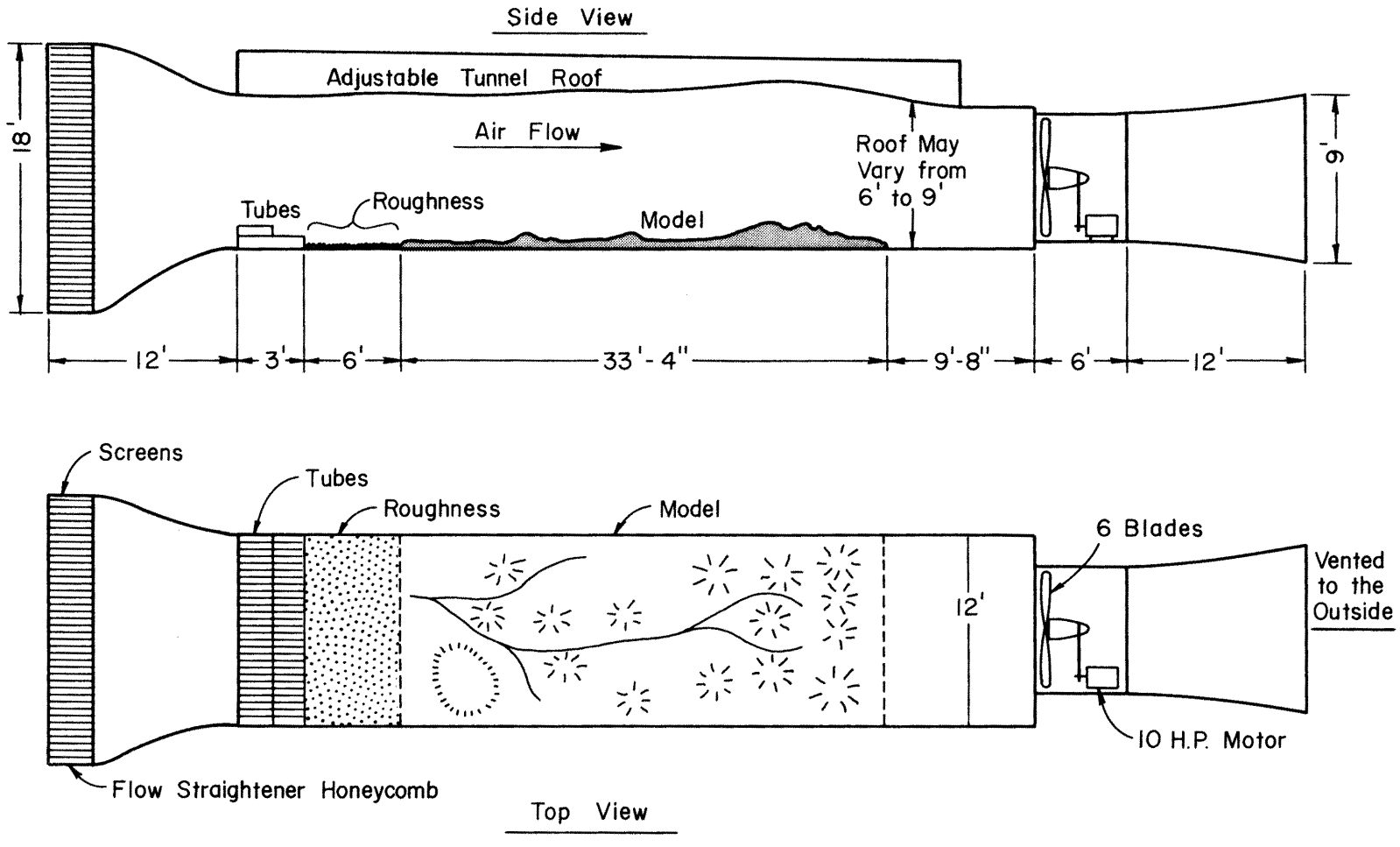

Fig. 5-4 Schematic diagrams of the Colorado State University environmental wind tunnel and upstream boundary conditions.

a) The average longitudinal (streamwise) velocity $\overline{U}$, the longitudinal and lateral turbulent intensities i_x and i_y were measured by means of a yawed or rotated single hot wire mounted over the model. The hot wire was operated at the normal position for obtaining $\overline{U}$ and i_x and at two yawed angles 45^o and 135^o for i_y. Average velocity and turbulent intensity profiles were obtained at 11 different locations over the model.

b) Concentration measurements over the topographic model was obtained by releasing radioactive Krypton from ground-level sources and using Geiger-Mueller tubes to determine the relative amount of Krypton in samples of the gas-air mixture. The sampling method was a modification of the original method used by Chaudhry (Ref. 9).

Only two sampling positions were selected for measurements because of the large number of sources (15). These were a line through Wolf Creek Pass - Mt. Hope and another through Pagosa Peak - Square Top Mountain.

In addition to these measurements some additional concentration measurements were obtained downstream from Oak Brush Hill--one of the field generator sites. The purpose of these latter measurements was to determine the possible terrain effects on tracer plumes released from different locations around this semi-isolated hill.

c) Visualization of the airflow over the topography was accomplished by using a chemical smoke. The chemical smoke, formed from titanium tetrachloride and compressed air, was released from special sources on the model. As the chemical smoke diffused downstream, photographs and movies of the smoke plumes were taken over the model.

d) Wind directions and speeds were measured in the west fork of the San Juan River Valley by means of a rotating hot-wire mechanism. These measurements were to show how the wind direction and speed varies with height in this particular valley which is upstream from many of the field sources.

In the case of the barostromatic airflow the following experiments were conducted:

a) Visualization of the airflow with chemical smoke;

b) Concentration measurements over the topographic model by the radioactive krypton method for three ground-level sources;

c) Temperature data with respect to height and time were obtained over the model;

d) Velocity profile data were obtained over the model.

Results of Wind-Tunnel Laboratory Experiments

1. Similitude conditions

a. Neutral airflow

According to Eq. 2-5 the concentration distribution over the model depends on 1) geometric, 2) dynamic (turbulence), and 3) wind velocity profile similarity.

The momentum boundary-layer thickness varied from 27 to 45 in. over the model which when scaled to the field is equivalent to 15,900 to 22,750 ft msl. These equivalent field

altitudes were high enough to suggest approximate similarity between model and field.

A vertical cross-sectional view of selected model wind velocity profiles and turbulent intensities is shown in Fig. 5-5. Three of the measurement sites, Carracas Mesa, Oak Brush Hill and Pagosa Springs are seeding generator locations. The wind velocity profile similarity was checked at one location by utilizing wind-tunnel velocity data obtained at the Pagosa Springs site on the model and wind velocity data obtained in the field at Durango. Figure 5.6 shows the comparison of the model wind velocity profiles for the different upstream conditions and a field velocity profile.

The results with upstream roughness indicate fairly good similarity with an exception in the lower 500 meters (prototype scale). A number of factors which may contribute to the disparity are 1) the differences in location - Durango is more sheltered than Pagosa Springs, 2) difference in the lower-level wind direction in the field, and 3) possible insufficient roughness on the model.

Dynamic similarity was based on the concept of an aerodynamically "rough" flow. In this case, the freestream velocity was set at a speed high enough to insure that the airflow over the model was turbulent. Under these conditions, the form drag prevails over the viscous drag and the flow is independent of the Reynolds number. For these experiments, a freestream between 2-3 mps was expected to satisfy these conditions.

Nemotos criteria for a distorted model, Eq. A-25 could not be checked because data on the eddy diffusion coefficients were not available for model or field. In this case the distortion factor is 1.4 and may be small enough that serious similarity differences may not occur. This subject is beyond the scope of this report but the problem needs further consideration and examination before definite statements can be made about the effects of scale distortion on modeling criteria.

The statistics of turbulence i_x , i_y (as well as i_z) correlate directly to the diffusing power of the model and field atmosphere. In the field, another wind fluctuation statistic often used in diffusion work is the variance, or standard deviation of the azimuth wind-direction angle σ_θ where θ is the angular direction of the horizontal wind (Ref. 34). This statistic is related to the intensity of turbulence in the cross-wind direction (i_y) by,

$$\sigma_\theta \sim \frac{\sigma_v}{\overline{U}} \qquad 5\text{-}1$$

According to Nemoto (Ref. 28) the model and field turbulent intensities should be matched or "similar" in neutral flow, i.e.,

$$\left[\frac{\sigma_i}{\overline{U}}\right]_M \equiv \left[\frac{\sigma_i}{\overline{U}}\right]_F \qquad 5\text{-}2$$

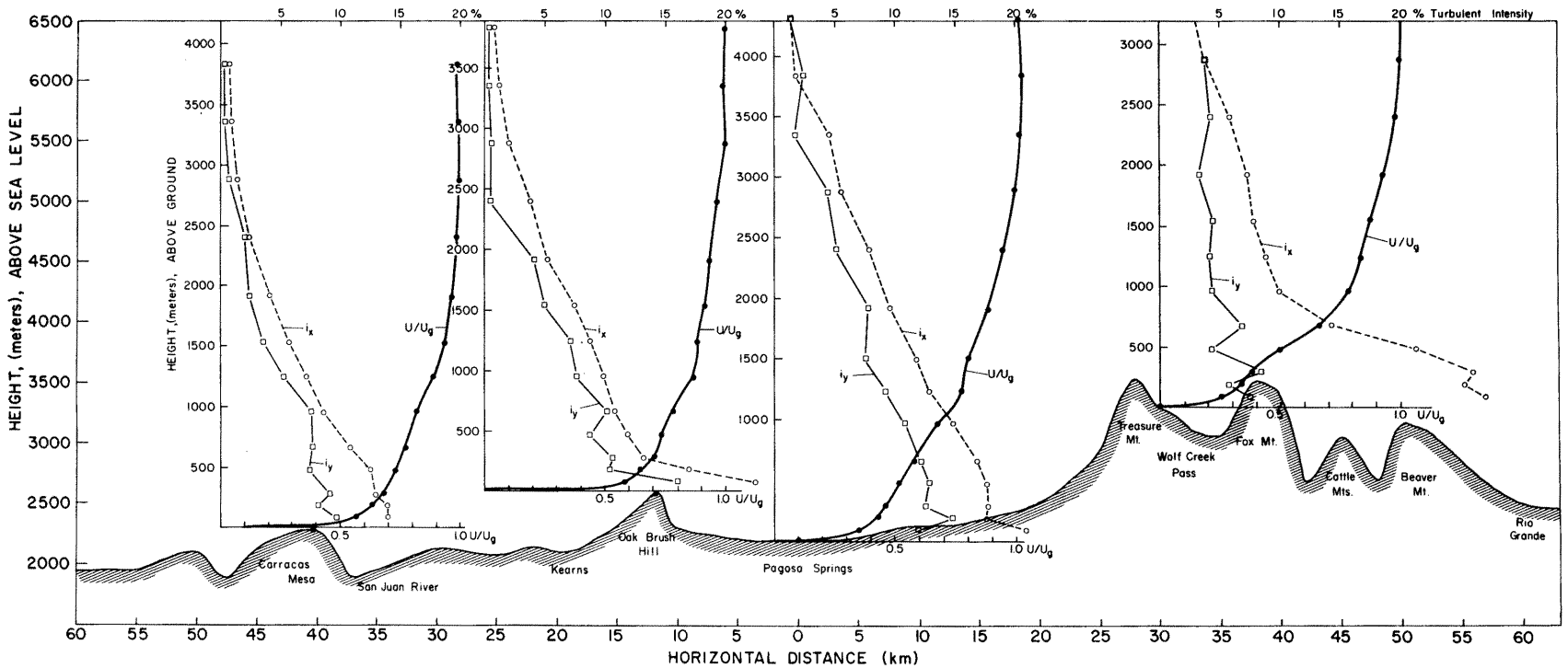

Fig. 5-5 Vertical cross-sectional view of the airflow and turbulence fields over the topographic model.

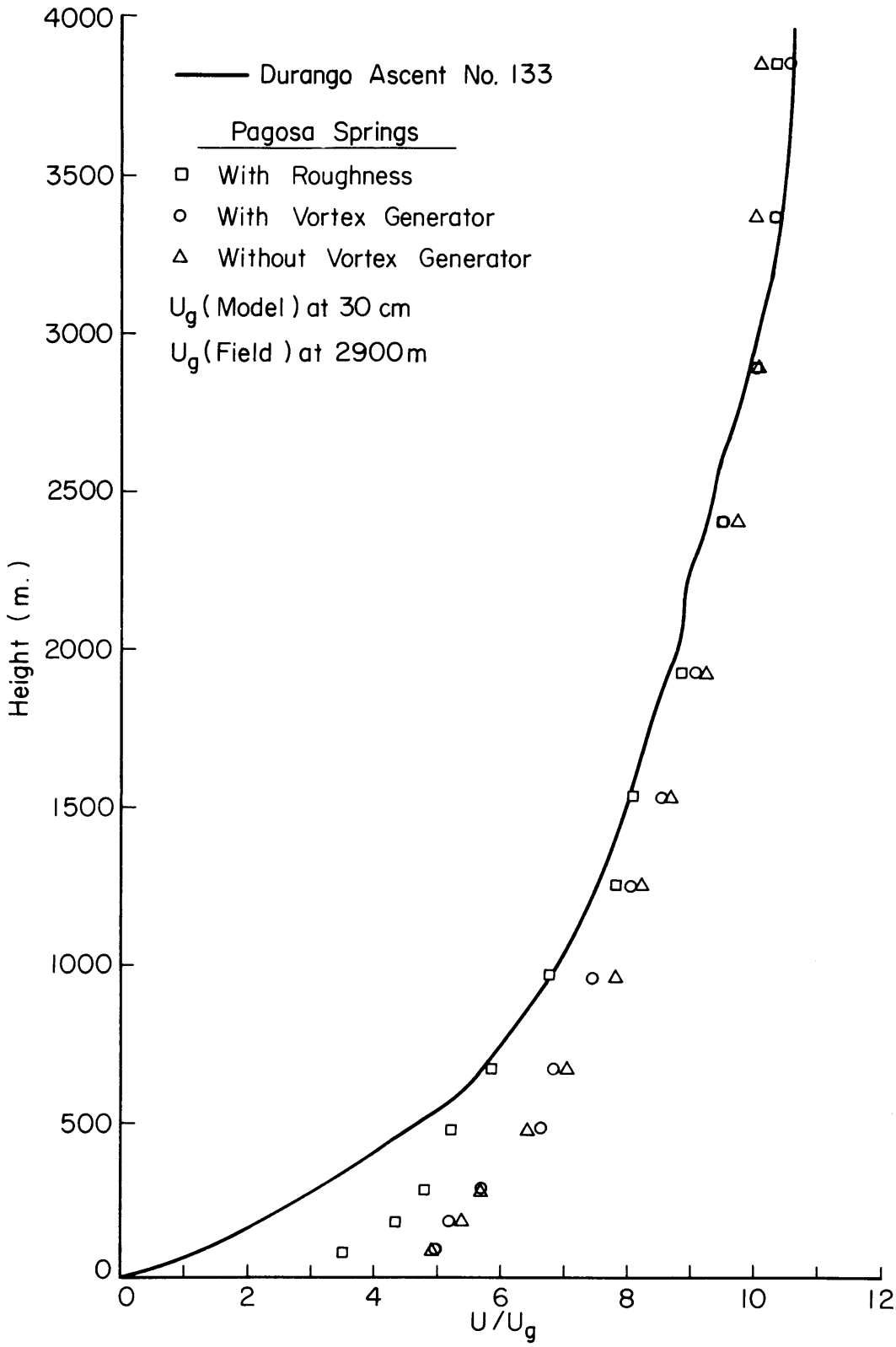

Fig. 5-6 Comparison of the model wind velocity profiles for different upstream conditions and a field velocity profile.

In the case of the longitudinal turbulent intensity, it is known from field measurements that under neutral stability conditions, the variance of longitudinal velocity $(\sigma_u)^2$ is proportional to the square of the windspeed at a fixed height. Since the wind speed increases with height, $\sigma_u/\overline{U}$ decreases upward in the boundary layer. It also seems to vary with terrain. One might expect a similar tendency in the lateral turbulent intensity (Ref. 24). The model results as shown in Fig. 5-5 suggest a similar behavior.

Estimates of the lateral and longitudinal turbulent intensity within the lower layers in mountainous terrain indicate numerical values between 15 and 60 percent (Ref. 30). Model numerical values for i_x and i_y were near the same magnitude but generally smaller than these field estimates. This might be expected since the numerical values of i_x, i_y, i_z, σ_θ, etc., are not constants for a particular set of meteorological conditions. Their values depend on sampling and averaging times that are inherent characteristics of a sample of data. The lower model turbulence values may be due to the longer "equivalent" field sampling time required to make the measurements over the model. This inherent characteristic of the turbulence data makes it difficult for making quantitative comparisons between model and field data. The whole problem needs a complete analytical examination.

b. Barostromatic airflow

In this type of airflow, as mentioned in the other sections, the concentration distribution depends on 1) geometric, 2) dynamic (thermal), 3) kinematic, and 4) time similarity.

The thermal stability and iregular terrain played a very important role in determining the diffusion of the tracer in this type of airflow. Unfortunately, model and field data were not adequate to check on the Richardson number criteria.

The vertical temperature distribution over the model was near-neutral or slightly unstable in the first 8 in. (~10,000 ft msl prototype per scale) then becoming slightly stable up to 16 in. (~12,000 ft msl) and then more stable above 16 in. This type of temperature profile was typical for the barostromatic airflow as was brought out by the other two studies.

The tracer material (Krypton-85) was cooled before entering the wind-tunnel sources so as to prevent any large buoyancy effects due to the cold environment of the wind tunnel.

2. Dispersion results

The visualization of airflow and diffusion was not totally satisfactory due to the inherent characteristics of the chemical smoke and the problems involved with dispensing it in the wind tunnel without disturbing the ambient airstream. However, this latter problem was minor once the smoke was approximately six inches from the source.

The principal results from the visualization study can be summarized as follows:

a) Meandering of the smoke plume - When the airstream conditions were appropriate a smoke plume entering the San Juan River Valley from a upstream source like Pagosa Springs, showed a tendency to meander from the east fork to the west fork valley. Figure 5-7 shows a series of pictures which illustrate this time variation of the plume.

b) Separation on the lee slopes - The separation of the airflow occurred consistently on the lee slopes of the ridge. This phenomena appeared to be most dominate in the west fork valley leading up to Wolf Creek Pass.

The separation phenomena was also illustrated by the rotating hot-wire measurements in the west fork of the San Juan River Valley. Figure 5-8 shows the turning of the wind direction and speed changes as measured in two locations in the valley.

The strong orographic effect of this valley had a definite influence on the concentration patterns measured the Wolf Creek Pass region. This orographic influence on the airflow was photographed and depicted in movies* of smoke plumes over the model.

c) Ground deposits of titanium dioxide - Figure 5-9 shows the ground deposit of titanium dioxide as the result of the chemical smoke released from several simulated ground sources. The pattern of the deposit resembles typical ground diffusion patterns of a time-mean plume.

A selection of results from the radioactive gas measurements will be considered next. Figures 5-10, 5-11 and 5-12 show the nondimensionalized concentration distribution at the Pagosa Peak and Wolf Creek Pass cross-sections for three sources at different distances from the Wolf Creek Pass target area. The sources were chosen so as to correspond to the field generator design setup.

Plume height and width for fifteen sources were estimated by using the criteria of 10 percent of the maximum concentration. Table 5-2 summarizes these data for different groups of sources for the two cross-sections. The nearest group of sources to the target area, Group 1, is approximately 20 mi from the Wolf Creek Pass target area. The farthest group, Group 4, is approximately 44 mi.

The results from Table 5-2 indicated that the horizontal dispersion under these stability conditions can be quite pronounced. The average model plume lateral dispersion was

$$D_y \sim 3\text{-}5\ 1/2 \text{ mi}/7 \text{ mi of horizontal transport}$$

when converted to prototype scale. Field measurements (Ref. 11) have indicated lateral plume dispersion on the order of

*A special edited movie entitled "Airflow and Dispersion over San Juan and Elk Mountains" shows this orographic effect on the airflow and dispersion.

Fig. 5-7 Pictures illustrating time variation of smoke plume in the wind tunnel.

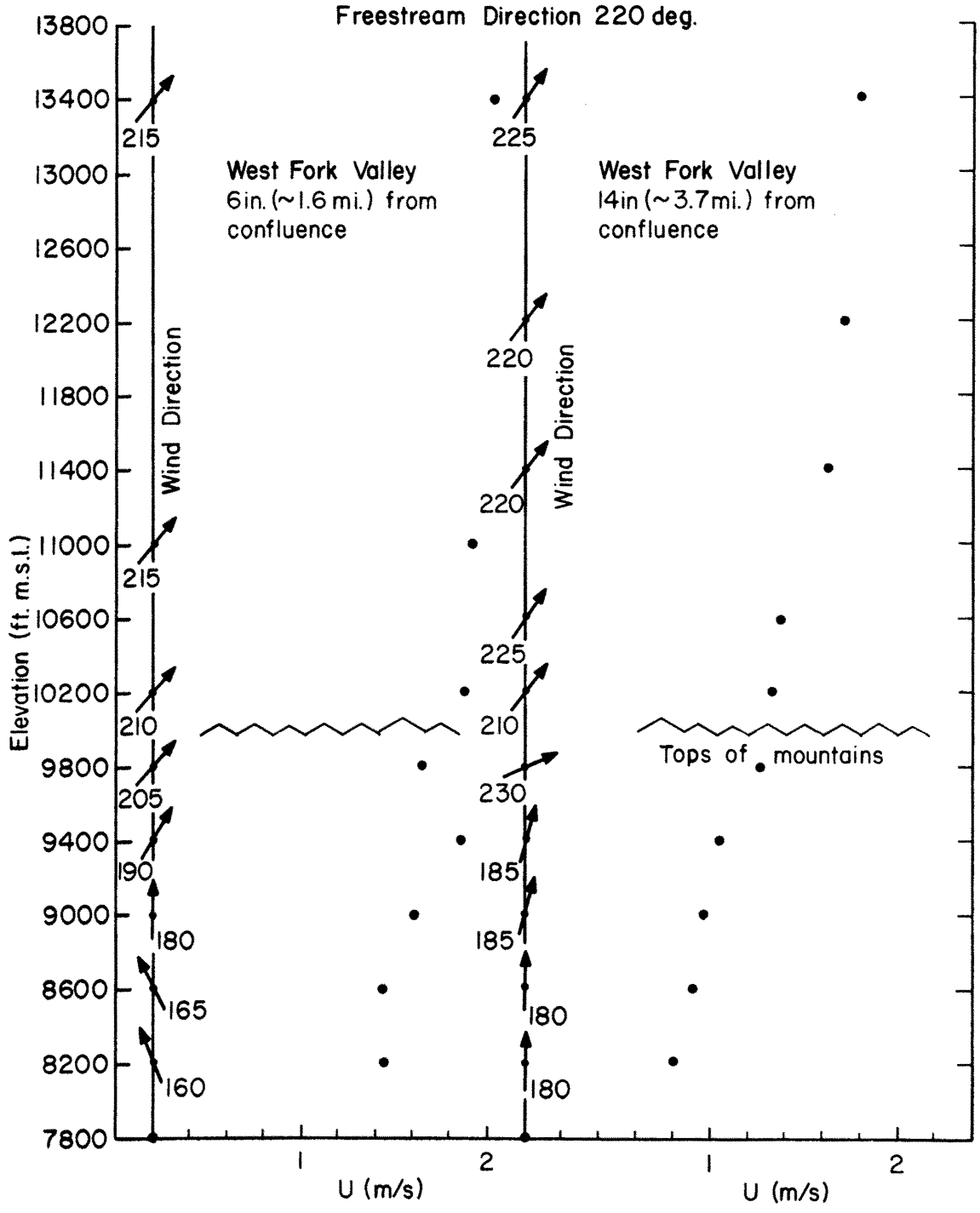

Fig. 5-8 Turning of the wind direction and speed changes as measured in the west fork of the San Juan River Valley.

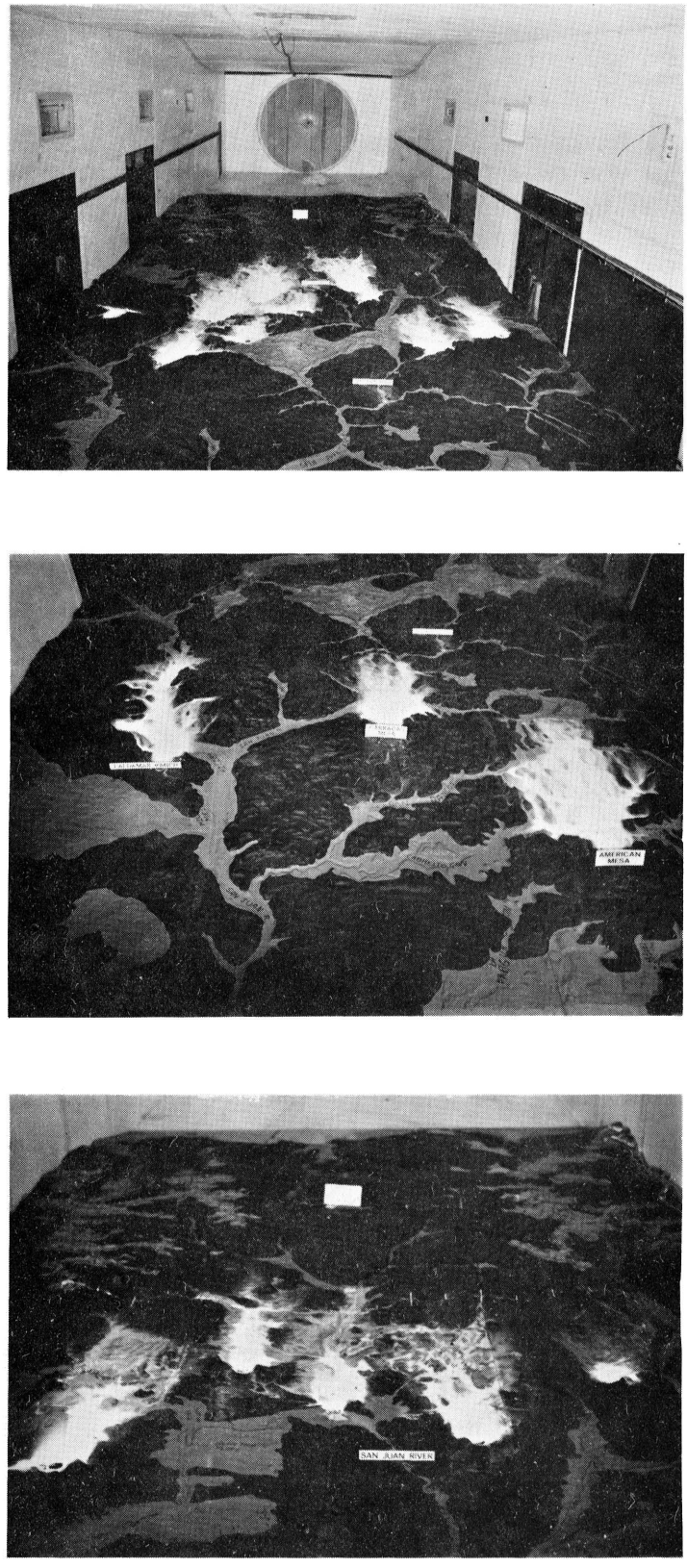

Fig. 5-9 Ground deposit as the result of chemical smoke from different simulated sources

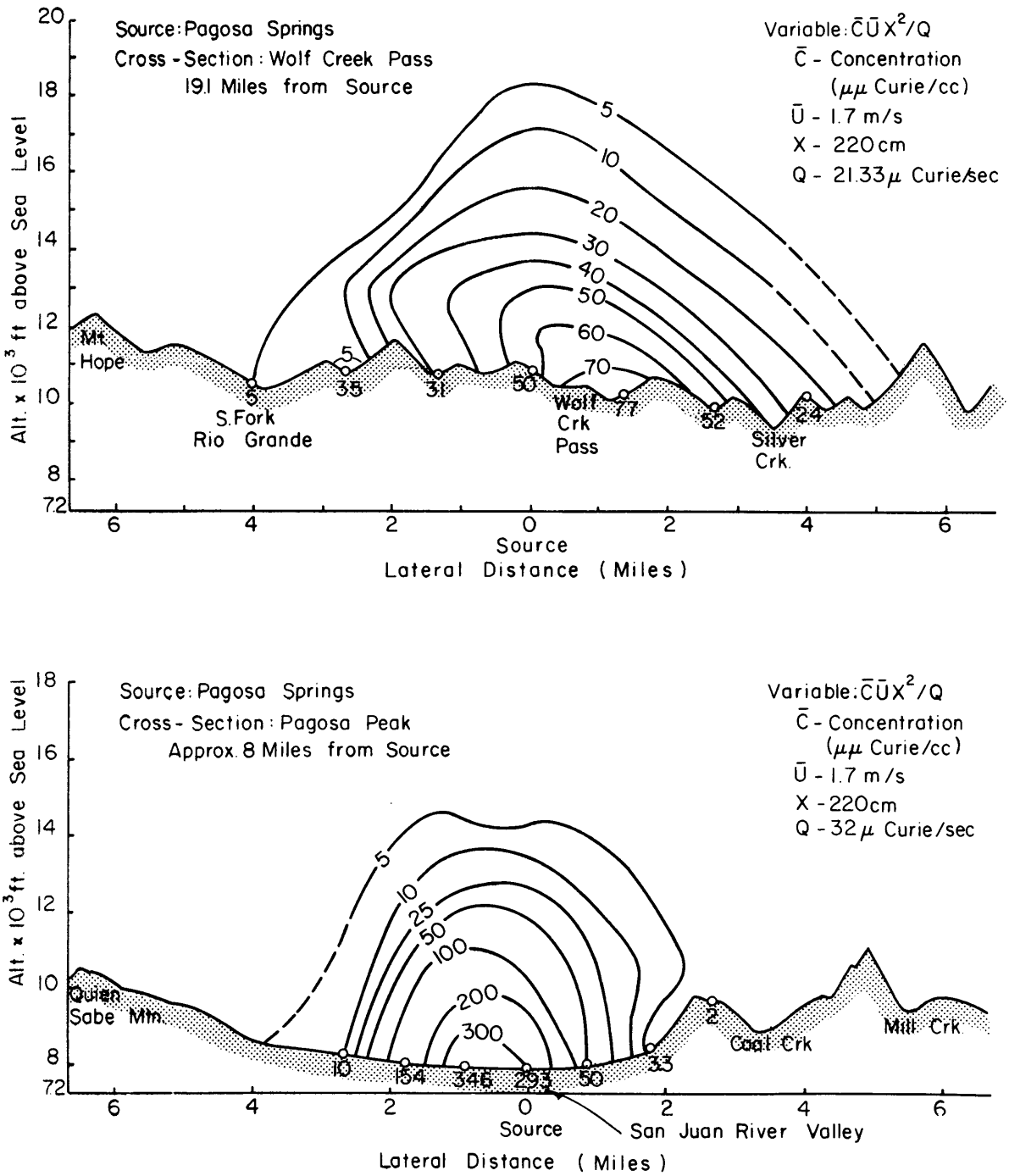

Fig. 5-10 Distribution of radioactive concentration for two lateral cross-sections over the model. Source: Pagosa Springs.

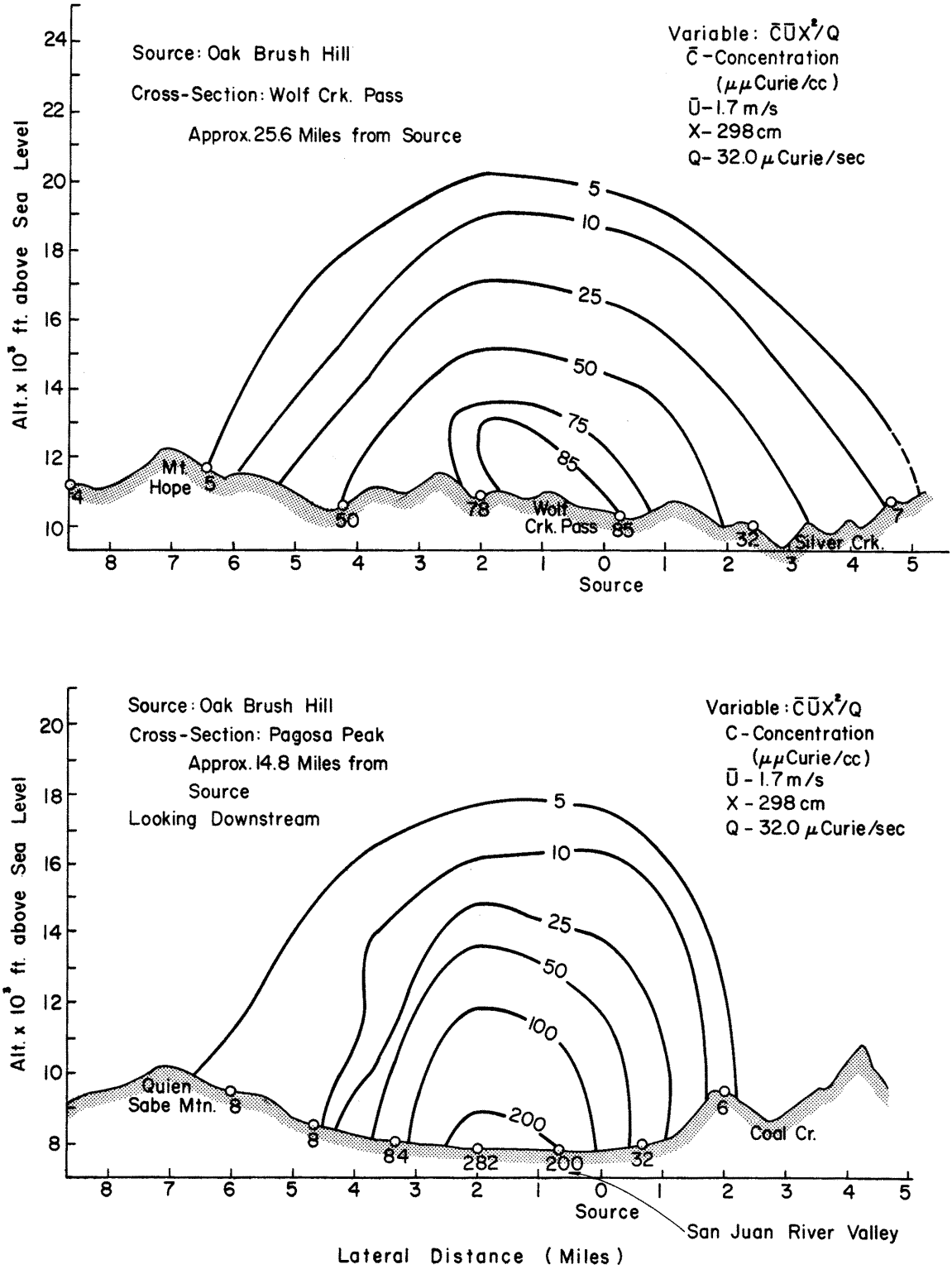

Fig. 5-11 Distribution of radioactive concentration for two lateral cross-sections over the model. Source: Oak Brush Hill.

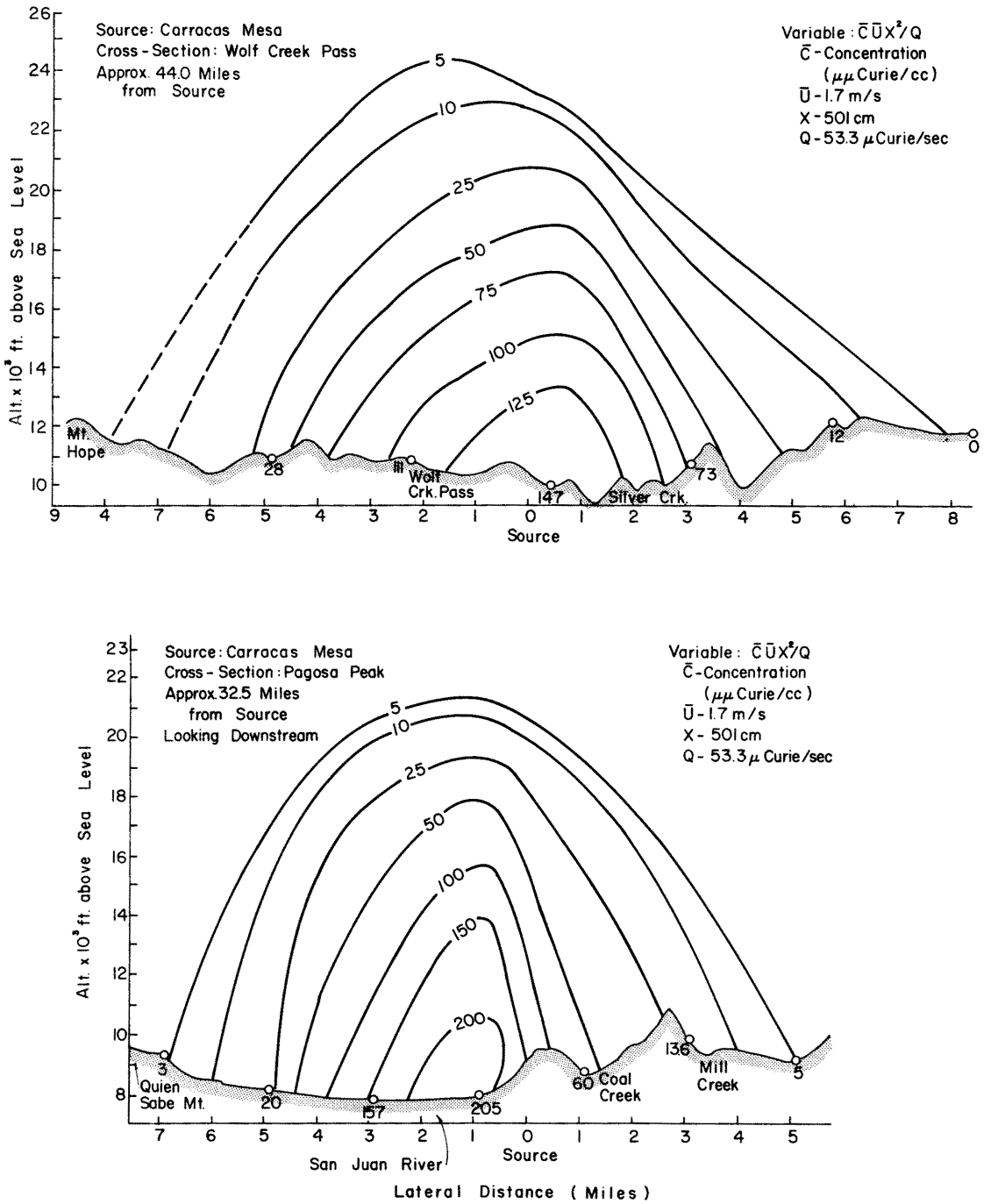

Fig. 5-12 Distribution of radioactive concentration for two lateral cross-sections over the model. Source: Carracas Mesa.

Table 5-2

Approximate Plume Widths and Heights at Two Downstream Cross-Sections for Different Groups of Sources San Juan Study. Distances and Heights Scaled to the Field

		Pagosa Peak Cross-Section		Wolf Creek Pass Cross-Section	
Group	Sources	Plume Width (mi)	Plume Height (ft msl)	Plume Width (mi)	Plume Height (ft msl)
#1	Hotts Ranch	3	11,750	9	17,500
	Pagosa Springs	3 1/2	12,250	8	18,500
	Hudson Ranch	5	14,750	9 1/2	18,000
	Blue Mountain	5 1/2	14,000	9	19,000
#2	Turkey Springs	5 1/2	15,500	7 1/2	22,500
	Harris Ranch	5	14,000	13	19,500
	Oak Brush Hill	5 1/2	15,000	11	19,750
	Eight Mile Mesa	6	15,750	10	20,000
#3	Kings Ranch	7 1/2	19,500	11 1/2	22,000
	Espinosa Ranch	6 1/2	15,500	12	20,000
	Chimney Rock	11 1/2	20,000	15	22,500
	Radcliff Ranch	6	18,000	11	22,000
#4	Baldamar Ranch	11	19,000	11 1/2	23,000
	American Mesa	11 1/2	22,500	13 1/2	24,000
	Carracas Mesa	7 1/2	19,750	11	22,000

D_y ~ 7-10 mi/6-7 mi horizontal transport.

If the total plume width is used for the criteria then the model plume dispersion compares more favorable with the field estimates. However, some of the field measurements were made during vertical directional wind-shear which evidently resulted in a wider plume in the field.

The model results show that the vertical dispersion was very rapid. Quite often the top of the plumes reached an "equivalent" field altitude of 20,000 ft msl approximately 25 mi from the source. The plume rise was

D_z ~ 4150-7350 ft agl/7-9 mi of horizontal transport.

The limited field measurements indicated a plume rise of

D_z ~ 4200 ft agl/5-7 mi of horizontal transport.

The model vertical dispersion appears to be a little exaggerated especially at the greater distances from the sources while the horizontal dispersion appears to be lacking in magnitude. The difference in stability conditions between the field and the model may explain part of the vertical dispersion difference. A strictly neutral-stability atmosphere through a deep layer is seldom, if ever, observed in the field.

The concentration distribution at the Wolf Creek Pass cross-section as the result of different combinations of ground-level sources is shown in Figs. 5-13 and 5-14. To obtain these results it was necessary to consider the respective concentration values from each source as an additive quantity. The tops of the model plumes were idealized. Effects of directional wind shear and Coriolis acceleration on the actual air motion would spread the upper region of the plumes more than was indicated in the model results. Turning of the wind due to the Coriolis acceleration would cause the plumes to spread more toward the east.

The dispersion of radioactive gas plumes was investigated from five ground-level sources near the semi-isolated Oak Brush Hill (Fig. 5-2) in attempt to determine any particular orographic effects.

The vertical dispersion from all five ground sources was much the same with no significant differences in vertical dispersion magnitude. The initial direction of the ground-level plumes were deflected to the left of the freestream direction as shown in Fig. 5-15. The latter affect was the only detectable orographic effect which, for weather modification purposes, was not significant.

Dispersion results with the barostromatic airflow model were limited due to the various problems. Figure 5-16 shows the concentration distribution over the Wolf Creek Pass cross-section as the result of two different ground-level sources. In this case, the affects of temperature stability

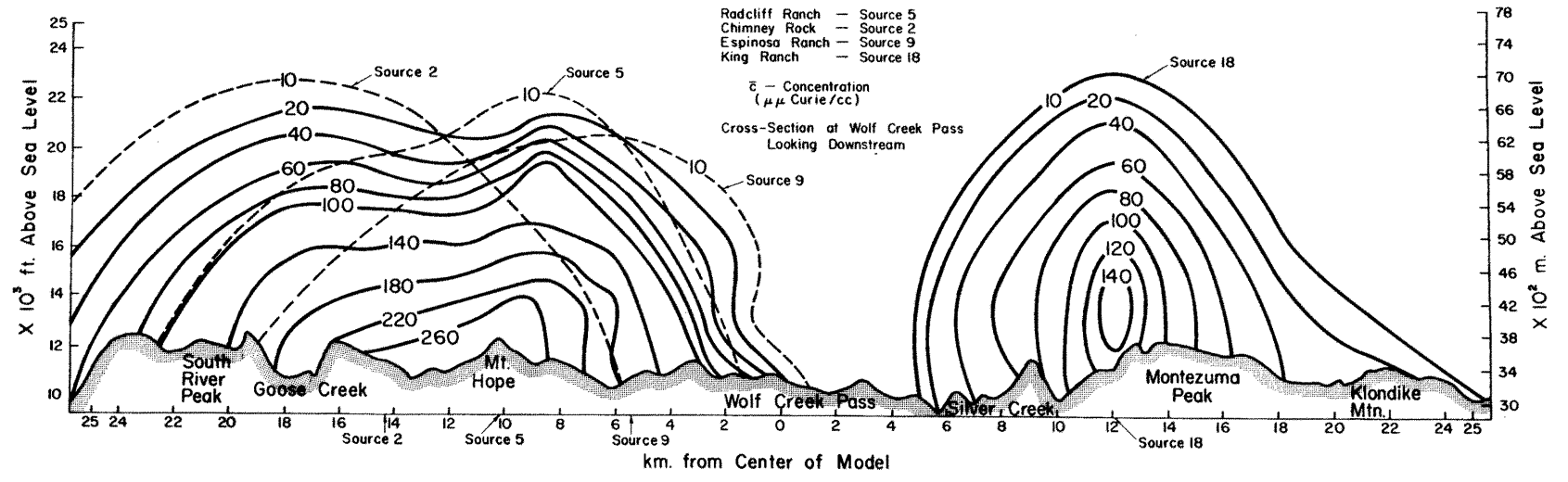

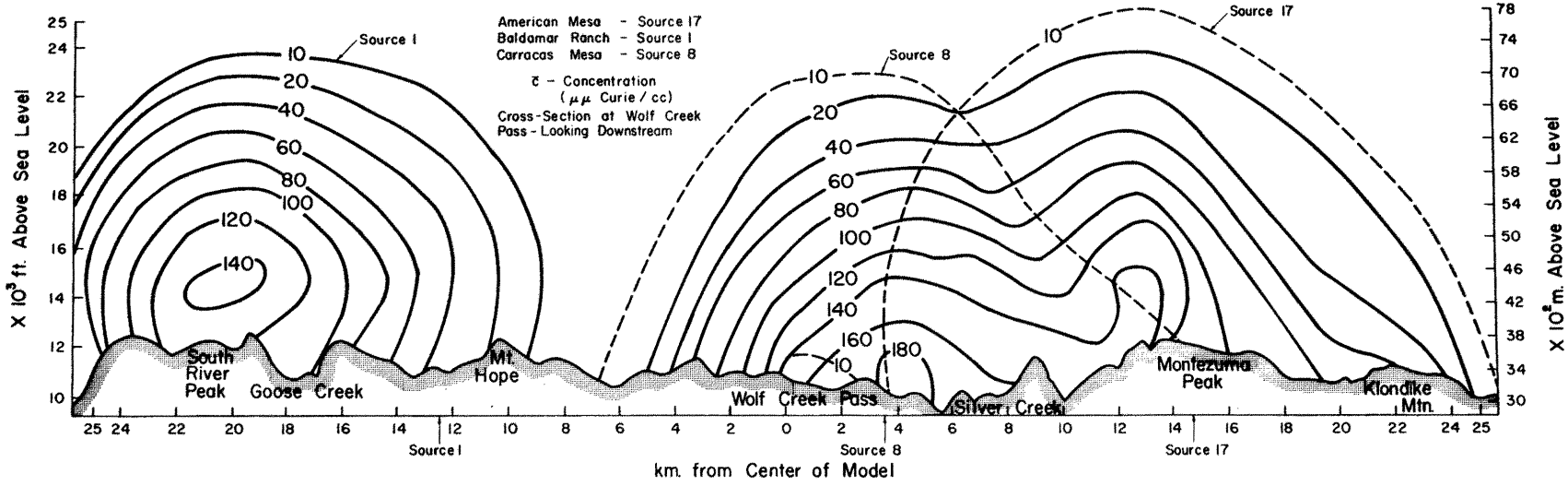

Fig. 5-13 Distribution of radioactive concentration over Wolf Creek Pass cross-section as the result of multiple sources.

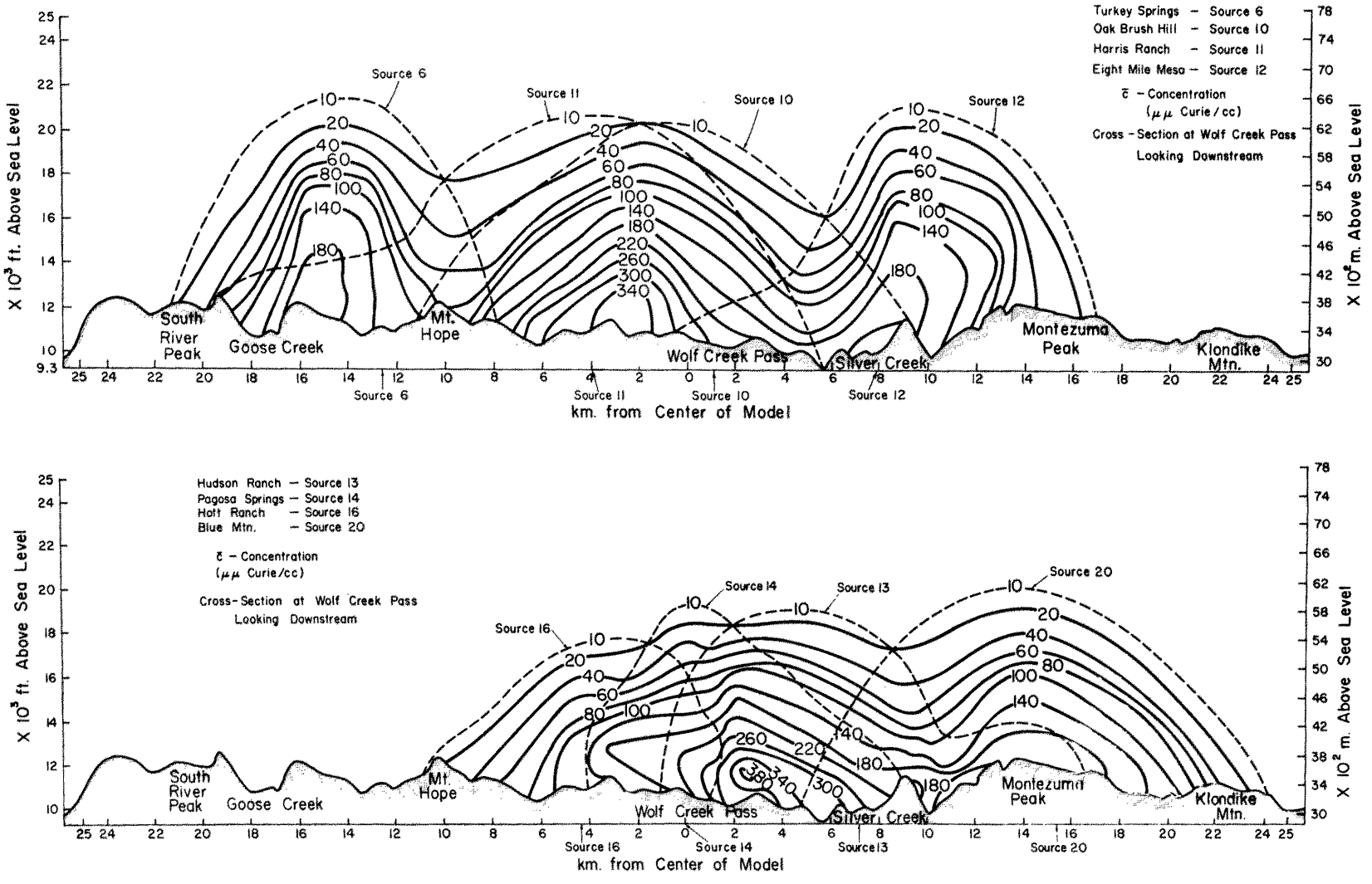

Fig. 5-14 Distribution of radioactive concentration over Wolf Creek Pass cross-section as the result of multiple sources.

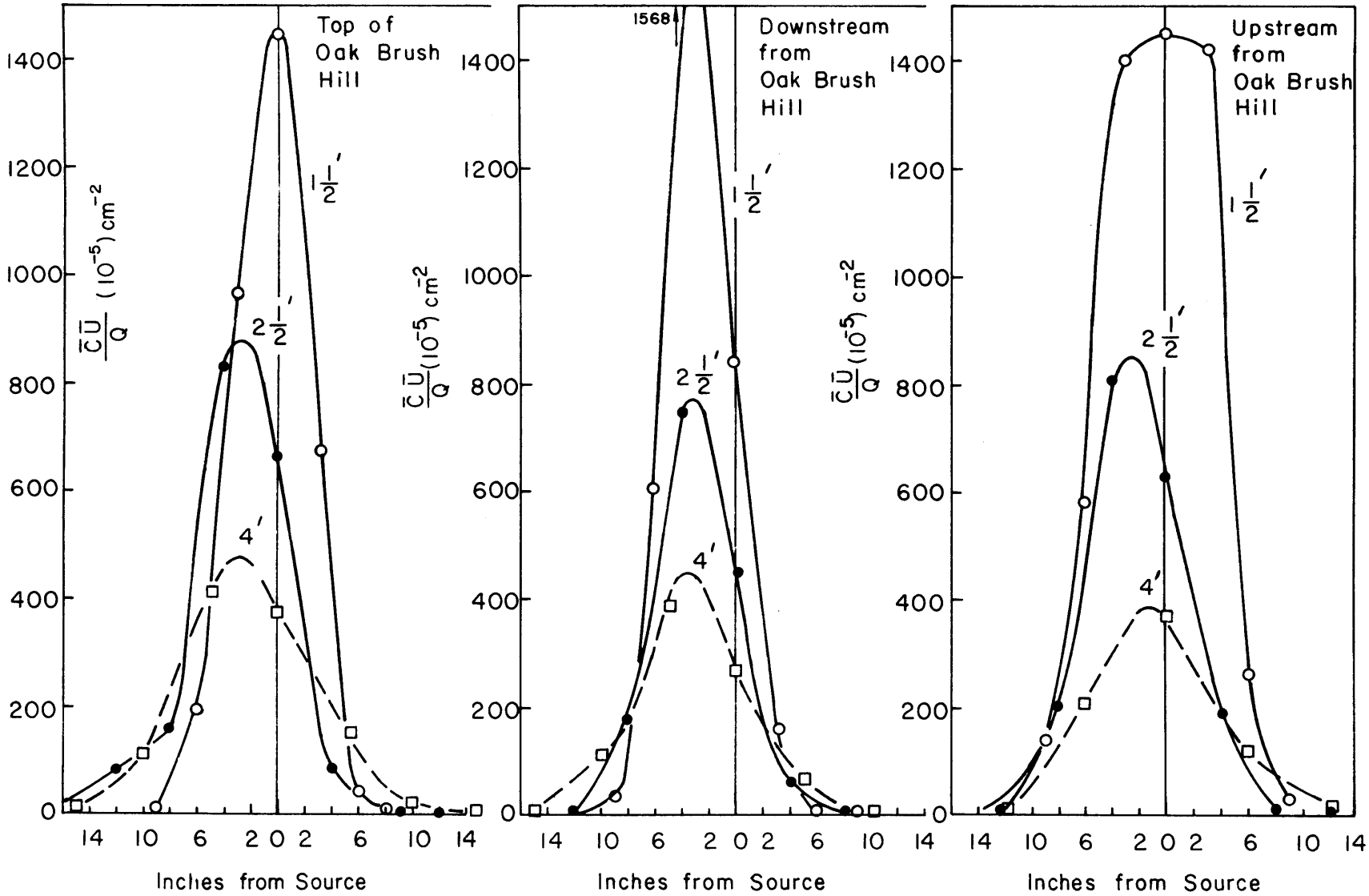

Fig. 5-15 Ground level plumes as affected by the airflow over Oak Brush Hill.

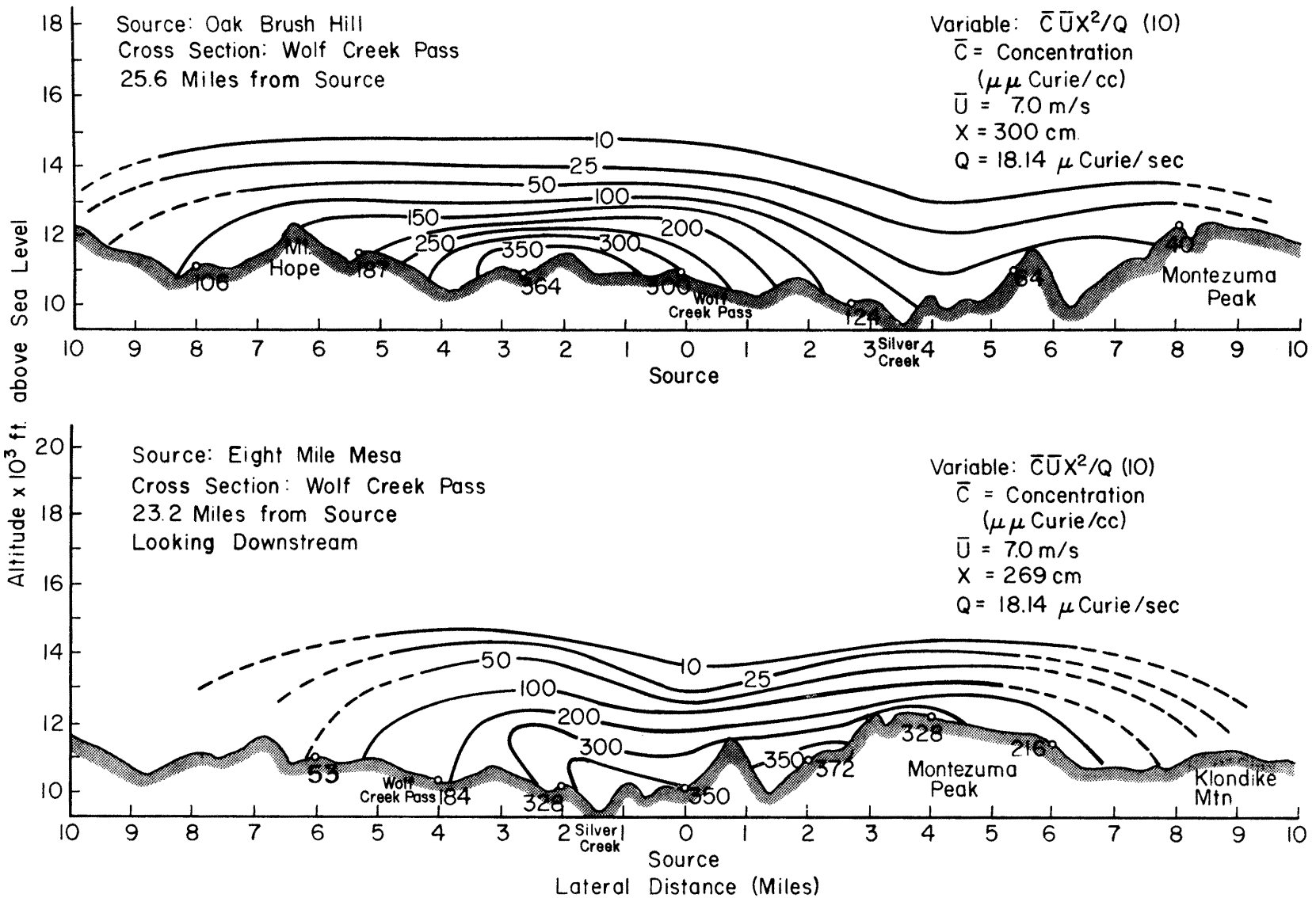

Fig. 5-16 Distribution of radioactive concentration over Wolf Creek Pass cross-section. Barostromatic airflow. Sources: Oak Brush Hill and Eight Mile Mesa.

and the irregular terrain were more apparent. Plume widths were on the order of 20 mi wide compared to the 10-13 mi wide plumes observed for the neutral case. The vertical dispersion was comparable to the neutral flow some 7-12 mi downstream from the source but at the longer distances the top of the plumes never exceeded a height of 16,000 ft msl in contrast to the 20,000 ft msl heights observed with the neutral case. The thermal stability in the levels above 16 cm (~12,000 ft msl) was an important factor in limiting the height of the plumes.

VI. SUMMARY, CONCLUSIONS AND RECOMMENDATIONS

Summary

The general purpose of this research was to develop laboratory physical models as a tool for modeling the atmospheric planetary boundary-layer over mountainous terrain. The simulated atmospheric flow was then to be applied to the investigation of transport-dispersion of a passive tracer material simulating silver-iodide seeding material used in weather modification programs.

This work was accomplished by developing two physical airflow models in wind tunnels with the assistance of long test sections, mechanical devices and low level cooling with dry ice. The dispersion measurements of a passive tracer gas were made over three different topographic models representing a large valley, isolated mountain and blocking mountain. These dispersion measurements were made with the aid of radioactive gas and a reliable detector instrument. A chemical smoke was used for visualization of the airflow.

A number of specific objectives were established and completed during this study. The first objective was to investigate and review the mathematical aspects of similarity for atmospheric transport and dispersion of particulate material, such as silver-iodide, over complex terrain. The investigation and review which was constantly updated throughout the study verifies that the problem of dispersion in mountainous terrain is a very complex problem due to the numerous variables involved in specifying the different aspects of the problem. It was found that several similarity criteria could be generated depending upon how much "fine" detail one wanted to simulate with a particular model.

The second objective was to determine the full capability for laboratory simulation of airflow over complex roughness features. It is well known that it is very difficult to produce a stably-stratified and turbulent airflow in a laboratory facility. In this study it was found that the limitations of the laboratory facilities and collection of field data required limiting the similarity criteria to where only "partial" similarity could be expected. However, this compromise did not appear to affect the results to a critical degree since the remaining similarity criteria appeared to describe the principal forces associated with the airflow and diffusion. The results confirm that partial similarity between atmospheric and simulated airflow in a laboratory facility was sufficient to give useful and practical data. At the present time, one is forced to use physical models which may approximate actual atmospheric conditions. In this study neutral and barostromatic airflow models were used for the purpose of obtaining airflow and dispersion results.

In investigations with the barostromatic airflow the following favorable aspects were discovered:

1) Large (~1°C/cm) vertical temperature gradients and low-speed (~10 cm/sec) airflow may be obtained by utilizing dry ice with a wind tunnel.

2) The resultant temperature and airflow conditions were sufficient for satisfying the gross requirements of Richardson and Froude number similarity with the atmosphere.

3) Richardson number equality was achieved primarily by means of thermal stratification since the addition of carbon-dioxide to the wind tunnel air does not effect the vertical density gradient to any large degree (~5%).

4) The airflow and thermal stratification of this physical model resembles similar aspects of mathematical models derived for studying airflow over terrain such as the "shallow-water" analogy.

5) The barostromatic physical model appears to simulate actual atmospheric conditions to a better degree than the neutral physical model. As a result, the airflow and resultant transport-dispersion correlates better with the actual atmospheric data.

6) Topographic effects play a major role in determining dispersion patterns with the barostromatic physical model.

In investigations with the neutral airflow the following aspects were discovered:

1) The separation phenomena which occurred downwind of many topographic features produced a turbulence field over the models which was highly nonhomogeneous and with large energy content in scales comparable to dimensions of the topographic features.

2) The neutral airflow model appears to exaggerate the vertical dispersion and, at times, to underestimate the horizontal dispersion.

3) The airflow and stability conditions of this physical model restricts the role of topography in determining dispersion patterns.

The third objective was to evaluate the use of laboratory simulation of airflow and transport for various types of orographic terrain as related to weather modification operations. The results indicate that laboratory experiments can assist development of field programs by providing the following types of pre-operational data:

1) Definition of the general direction of seeding plumes in mountainous terrain of different types.

2) Approximate estimates on the decrease of relative concentration with downstream distance for conditions of minimum depletion loss.

3) Approximate estimates on vertical and horizontal dispersion and the cloud volume occupied by the seeding material.

4) Relative dispersion characteristics for the evaluation of seeding generator sites.

5) Dispersion patterns from multiple sources.

The model and field results of this study also provide information on the use of ground-level generators as a method of seeding orographic clouds. The results suggest that ground-based generator sites are effective for distributing the seeding agent to orographic cloud systems for the following reasons:

1) The distribution of artificial nuclei with height is proper for optimum seeding, i.e., the largest number of nuclei are found in the lowest levels where the cloud temperatures are warmest and the least number is located where the cloud temperatures are coldest.

2) Ground generators operated over several hours can create a diversity of source regions (e.g., filling of valleys) where the seeding material can be distributed to a cloud system over a period of time by convection, orographic effects (advection) and turbulent mixing.

3) The ground-based generator is mobile and its location can be varied depending on the desired design conditions. However, the location may not be so critical during good orographic cloud situations when the atmospheric stability may be near neutral through a deep layer. The model and field results show that even valley locations of generators may be sufficient for distributing the seeding material to the cloud system under these atmospheric conditions.

4) Operation of multiple ground-level generators in mountainous terrain during near-neutral stability conditions and moderate winds provide seeding plumes which may cover a large volume of orographic cloud. A rough estimate on the cloud volume affected by effective artificial nuclei (neglecting depletion losses) based on model and field data is

$$\begin{aligned} \text{average depth} &\sim \tfrac{1}{2} \text{ mi} \\ \text{width} &\sim 30 \text{ mi} \\ \text{length} &\sim 20 \text{ mi} \\ \text{cloud volume} &\sim 300 \text{ mi}^3 \end{aligned}$$

The fourth objective was to obtain field information on the relative dispersion and transport characteristics of tracers with particle sizes ranging from meter to molecular sizes. The field data were primarily limited to the Eagle River Valley-Climax study. The following interesting data were found:

1) Aircraft sampling flights of the silver-iodide seeding material showed that the range of vertical transport seeding material was of the order

D_z 975-1740 meters agI/10 km of horizontal transport

with the larger values observed during near-neutral stability events. These vertical transport values exceeded the natural mean slope of the terrain which is 280 meters/10 km. The lateral transport varied as

$D_y \sim$ 7-15 km/10 km of horizontal transport.

Sampling of fluorescent zinc sulfide and sulfur hexafluoride was not successful. Only traces of zinc sulfide could be found over the area even at the lowest altitude (8-9,000 ft msl).

2) Dual constant-volume balloon flights showed that the total dispersion rate equaled and exceeded t^3 and t^4 for short periods. Zonal, meridional and vertical eddy diffusivities varied from 10^4 to 10^6 cm^2 sec^{-1}. The zonal and vertical eddy diffusivities increased in magnitude with height. Vertical motions of the order of ±2 m/s may not be uncommon near the ridge-top levels. Vertical motions greater than ±4 m/s may be prevalent near prominent ridges and during days with marked directional and speed wind-shear.

3) The atmospheric dispersion during orographic storm events was observed to be large enough to transport seeding materials from ground-based generators to orographic cloud systems. Mechanical turbulence enhanced by near-neutral stability conditions, orographically induced eddies, directional and speed wind-shear and convection were the various physical mechanisms acting to disperse the seeding material from the generators.

The fifth objective was to establish modeling criteria for future operational programs in weather modification. Probably, the best procedure in utilizing the laboratory model technique in weather modification and other diffusion oriented programs is to have a model study proceed for a selected area before extensive preparations have been completed on the physical location of seeding generators. Some preliminary meteorological data are needed on temperatures, winds and turbulence to guide the modeling program. With data from the model study, field program personnel could then proceed in a more objective manner for establishing the optimum field configuration for seeding operations. As the field program progressed any small-scale field problems regarding site locations or dispersion could also be evaluated in a laboratory facility.

The several limitations associated with the present laboratory modeling technique place some restrictions on the general use of this technique. These restrictions are:

1) Area limitations - Designated areas to be modeled would have to be less than 3200 sq. mi in order to not exceed the space requirements of present laboratory facilities. This limitation assures reasonable scaling of length for the model and reasonable confidence that the Coriolis accelerations can be neglected.
2) Scale-ratio limitations - With the area limitations noted above, length-scale ratios down to 1:10,000 can be utilized in the laboratory studies.
3) Wind direction limitations - In general, only one geostrophic or freestream wind direction can be simulated for a topographic model. Construction of extra model sections may alleviate this problem to a certain degree.
4) Low level trapping inversions.

Conclusions

On the basis of the laboratory simulation and field results of this study the following conclusions are made:

1) Partial similarity between physical variables in the field and laboratory physical airflow models was sufficient to obtain practical and useful data from the laboratory studies on atmospheric airflow and transport-dispersion over mountainous terrain.
2) The two laboratory physical airflow models, with their inherent limitations, are a practical tool for estimating airflow as well as dispersion characteristics over mountainous terrain. The laboratory studies can provide useful data for planning proposed field programs on weather modifications and other diffusion oriented problems.
3) Ground-based generators provide a practical and inexpensive method for seeding orographic cloud systems. The greatest potential of this type of generator is during near-neutral stability conditions and moderate winds.

4) The physical models and field results indicate that the atmospheric dispersion during orographic storm events is large enough to transport the seeding material from ground generators to cloud systems. Mechanical turbulence enhanced by near-neutral stability conditions and orographically induced eddies are principal physical mechanisms for dispersing the seeding material.
5) Current shortcomings of the modeling technique are due primarily to laboratory facility limitations. Improvement in facilities translates to improvement in model results.

Recommendations

On the basis of the results from this study the following recommendations are made:

1) The laboratory studies should attempt to improve model-field correspondence by creating a new generation of modeling techniques. Special attention should be given to modifying the boundary conditions in order to generate a variety of airflow, turbulence and temperature conditions.
2) Parallel field studies of the atmospheric boundary conditions should be used to provide data on vertical profiles of temperature, wind, turbulence and concentration taken under different atmospheric stability and wind conditions. Constant-volume balloon experiments and additional aircraft sampling can assist in obtaining information on atmospheric dispersion under these more precisely defined conditions. Additional sampling of particulate material may assist in defining the role of depletion variables in weather-modification program operations.
3) The relative merits of variable (vertical, distance, location) release points should be more precisely defined.

APPENDIX

APPENDIX

REVIEW OF SIMILITUDE CRITERIA

Basic Equations

The basic equations necessary for considering atmospheric motions and dispersion are the following:

equations of motion,
continuity equation,
equation of state,
Poisson's equation,
equation of turbulent heat transfer,
equation of heat transfer from the surface boundary, and
parabolic diffusion equation

In this study the continuity equation and equation of state are of little importance to the similarity analysis and will be omitted from further discussion. Therefore, the principal equations to be considered in determining similarity criteria for air motion and dispersion are:

1. Equation of motion

$$\frac{\partial \overline{U}_i}{\partial t} + \overline{U}_j \frac{\partial \overline{U}_i}{\partial x_j} + 2\varepsilon_{ijk}\Omega_j\overline{U}_k = -\frac{1}{\rho}\frac{\partial \overline{p}}{\partial x_i} + \frac{1}{\rho}\frac{\partial \overline{\sigma}_{ij}}{\partial x_j} + \frac{1}{\rho}\frac{\partial \sigma_{ij}}{\partial x_j} - \frac{\Delta\overline{T}}{\overline{T}} g\delta_{i3} \qquad \text{A-1}$$

2. Equation of Poisson

$$\theta = T\left(\frac{1000}{p}\right)^{R_d/C_{p_d}} \qquad \text{A-2}$$

3. Equation of turbulent heat transfer

$$\rho C_p\left(\frac{\partial \overline{T}}{\partial t} + \overline{U}_j \frac{\partial \overline{T}}{\partial x_j}\right) - \frac{\partial \overline{p}}{\partial t} - \overline{U}_j \frac{\partial \overline{p}}{\partial x_j} - \overline{U_j'} \frac{\partial p'}{\partial x_j}$$

$$= \frac{\partial}{\partial x_j}\left(k \frac{\partial \overline{T}}{\partial x_j}\right) - C_p\rho \frac{\partial}{\partial x_j}\left(\overline{T'u_j'}\right) + \overline{\Phi} \qquad \text{A-3}$$

4. Equation of heat transfer from the surface boundary

$$Q_T - Q_R + Q_{L\downarrow} - Q_{L\uparrow} = \pm Q_G \pm Q_H \pm Q_E \qquad \text{A-4}$$

5. Parabolic diffusion equation

$$\frac{\partial \overline{C}}{\partial t} = \frac{\partial}{\partial x_i}\left(\overline{C}\,\overline{U}_i\right) = \frac{\partial}{\partial x_i} K_{ii} \frac{\partial \overline{C}}{\partial x_i} + k_m \frac{\partial^2 \overline{C}}{\partial x_i \partial x_i} \qquad \text{A-5}$$

This set of equations may be simplified further depending upon the type of airflow under investigation and the boundary conditions. The fourth equation, the equation of heat transfer from the surface boundary

has not been used in deriving similarity criteria before and, because of the similarity difficulties this equation presented to the study, it was neglected except as a general tool for analyzing the similarity problem in depth.

For the set of equations to be complete, equations dealing with the physics of clouds should be included, but this aspect of the study cannot be considered in a laboratory physical model at the present time.

Boundary Conditions

The general boundary conditions for a study of air motion and dispersion over irregular terrain can be expressed mathematically as the following (see Fig. 2-1 also):

$$1.\quad \lim_{z\to z_o} \vec{U} = 0$$

$$2.\quad \lim_{z\to H} \vec{U} = \vec{U}_g$$

$$3.\quad \lim_{z\to z_o} \vec{\tau} = \vec{\tau}_o \qquad \text{A-6}$$

$$4.\quad \lim_{z\to H} \vec{\tau} \to \vec{\tau}_{min}$$

$$5.\quad \lim_{x,y,z\to\infty} C \to 0$$

$$6.\quad \lim_{x,y,z\to 0} C \to \infty$$

The continuity condition

$$\int_{-\infty}^{\infty}\int_{o}^{\infty} \overline{U}\, C(x,y,z)\,dz\,dy = Q \quad \text{for all} \quad x>0 \qquad \text{A-7}$$

will not be satisfied in the field because of the action of deposition and depletion variables.

Similitude Criteria

The similitude parameters governing the airflow and dispersion patterns may be derived by dimensional analysis, similarity theory and inspectional analysis. The purpose of this section is to give a review of the similarity criteria that several authors have derived that pertain to this particular problem and not to discuss the relative advantages and disadvantages of the similarity methods.

Sundaram (Ref. 25) derived the similitude requirements for the atmospheric boundary layer by applying similarity techniques to the differential equations governing the relevant flow processes. The

following mathematical expressions summarizes part of the similarity criteria derived by Sundaram for different airflow conditions:

1. Steady, turbulent, incompressible and neutral airflow:

$$\frac{u}{U_\infty} = f\left(\frac{z}{L_o}, \frac{U_\infty L_o}{\nu}, \frac{U_\infty L_o}{K_M}\right) \qquad \text{A-8}$$

2. Steady, uniform, turbulent flow (aerodynamically rough):

$$\frac{u}{U_\infty} = f\left(\frac{z}{z_o}, \frac{U_\infty z_o}{K_{M_o}}\right) \qquad \text{A-9}$$

3. Turbulent flow with temperature gradient (temperature gradient is sufficiently small so that deviation from neutral conditions are small; vertical gradients are more important than horizontal ones):

$$\left(\frac{u}{U_\infty}, \frac{\delta T}{\Delta T}\right) = f\left(\frac{z}{L_o}, \frac{U_\infty L_o}{\nu}, \frac{U_\infty L_o}{K_m}, \frac{U_\infty L_o}{K}, \frac{U_\infty L_o}{K_H}, g\frac{L_o}{U_\infty^2}\frac{\Delta T}{T_o}\right) \qquad \text{A-10}$$

with modifications

$$\left(\frac{u}{U_\infty}, \frac{\delta T}{\Delta T}\right) = f\left(\frac{z}{z_o}, Pr_t, Re_t, B\right) \quad \text{where} \quad B = g\frac{z_o}{U_\infty^2}\frac{\Delta T}{T_o} \qquad \text{A-11}$$

4. Turbulent flow with temperature gradient (fractional changes in potential temperature are not small):

$$\left(\frac{u}{U_\infty}, \frac{\delta T}{\Delta T}\right) = f\left(\frac{z}{z_o}, Pr_t, Re_t, B, \frac{\Delta T}{T_o}\right) \qquad \text{A-12}$$

5. Unsteady flows

$$\left(\frac{u}{U_\infty}, \frac{\delta T}{\Delta T}\right) = f\left(\frac{z}{L_o}, \frac{t}{t_o}, \frac{U_\infty t_o}{L_o}, \frac{U_\infty L_o}{\nu}, \frac{U_\infty L_o}{K_M}, \frac{U_\infty L_o}{K}, \frac{U_\infty L_o}{K_H}\right.$$

$$\left. g\frac{L_o}{U_\infty^2}\frac{\Delta T}{T_o}, \frac{u^*}{U_\infty}, -\frac{1}{ku^*}\frac{Q}{\rho C_p}\frac{1}{\Delta T}, \frac{\theta_o}{\Delta T}\right) \qquad \text{A-13}$$

6. Similarity of turbulent fluctuations:

$$\frac{u_o}{\sqrt{u_o'^2}}, \frac{(\Delta T)_o}{\sqrt{T_o'^2}}, \frac{L_o}{z_o}, \frac{U_o z_o}{K_{M_o}}, \frac{K_{M_o}}{K_{H_o}}, g\frac{z_o}{U_o^2}\frac{(\Delta T)_o}{T_o} \; . \qquad \text{A-14}$$

Nemoto (Refs. 28 and 29) derived the similitude requirements for the atmospheric boundary layer by using inspectional analysis and turbulence theory. A summary of his criteria are:

1. Turbulent and incompressible flow (neutral conditions)

$$\left[\frac{K_i}{L_o U_\infty}\right]_F \equiv \left[\frac{K_i}{L_o U_\infty}\right]_M \quad \left[\frac{\overline{u_i'^2}}{U_\infty^2}\right]_F \equiv \left[\frac{\overline{u_i'^2}}{U_\infty^2}\right]_M \qquad \text{A-15}$$

Nemoto modifies the eddy Reynolds number requirement by considering local isotropic turbulence theory and derives the following:

$$\frac{U_{\infty_M}}{U_{\infty_F}} = \left(\frac{\varepsilon_M}{\varepsilon_F}\right)^{1/3} \left(\frac{L_{M_o}}{L_{F_o}}\right)^{1/3} \qquad \text{A-16}$$

2. Thermal stratification-similarity based on equation of turbulent energy change:

$$\frac{U_{\infty_F}}{U_{\infty_M}} = \left(\frac{L_{o_F}}{L_{o_M}}\right)^{1/2} \left(\frac{\theta_M}{\Delta\theta_M} \Big/ \frac{\theta_F}{\Delta\theta_F}\right)^{1/2} \qquad \text{A-17}$$

3. Turbulent flow field with thermal stratification:

$$\left[\frac{K_i}{L_o U_\infty}\right]_F \equiv \left[\frac{K_i}{L_o U_\infty}\right]_M \quad \left[\frac{\overline{u_i'^2}}{U_\infty^2}\right]_F \equiv \left[\frac{\overline{u_i'^2}}{U_\infty^2}\right]_M \quad g\left[\frac{L_o}{U_\infty^2}\right]_M \equiv g\left[\frac{L_o}{U_\infty^2}\right]_F \qquad \text{A-18}$$

Nemoto indicates that the above three conditions can be simultaneously satisfied if the following relation holds among the sizes and velocities of the apparent mean eddies in the i-direction of model and prototype flows:

$$\frac{U_{miM}}{U_{miF}} = \left(\frac{L_{M_o}}{L_{F_o}}\right)^{3/2} \left(\frac{\Lambda_{miM}}{\Lambda_{miF}}\right)^{-1} \qquad \text{A-19}$$

Bernstein (Ref. 4) used the ordinary dimensional method and a generalized dimensional analysis to derive the similarity criteria for the atmospheric planetary layer. On the basis of of the equations of motion and boundary conditions he indicates that the variables relevant to flow in the atmospheric planetary layer are $\vec{U}$, $\vec{U}_g$, ρ, f, $\vec{\tau}$, $\vec{\tau}_o$, z, H and z_o. In this analysis he represents vectors as complex variables and assumes that relevant vectors lie in the horizontal plane and, therefore, are two-dimensional.

Bernstein used ordinary dimensional analysis to find the following functional relationship for neutral conditions,

$$\frac{\vec{U}}{\vec{U}_*} = f\left[\frac{\vec{U}_{*o}}{\vec{U}_g}, \frac{\vec{U}_g}{fz_o}, \frac{H}{z_o}, \frac{z}{z_o}, \frac{\vec{U}_*}{\vec{U}_{*o}}\right] \qquad \text{A-20}$$

and from his generalized dimensional analysis:

$$\frac{\vec{U}}{\vec{U}_g} = f\left[\frac{\vec{U}^2_{*o}}{fz_o\vec{U}_g}, \frac{H}{z_o}, \frac{z}{z_o}, \frac{\vec{U}_*}{\vec{U}*o}\right] \qquad \text{A-21}$$

Cermak et al., (Ref. 5) have used the inspectional method for deriving similarity criteria for atmospheric flows. These criteria are:

1. Turbulent and neutral airflow

$$\tau_{o_F} \equiv \tau_{o_M} \qquad \text{A-22}$$

$$C_{D_M}\rho_M\overline{U}^2_M \equiv C_{D_F}\rho_F\overline{U}^2_F$$

2. Turbulent flow with thermal stratification:

$$Re = \frac{U_o L_o}{\nu_o}$$

$$Ri = \frac{\Delta T_o}{\overline{T}_o}\frac{L_o}{U^2_o} g_o$$

$$Ro = \frac{U_c}{L_o \Omega_o} \qquad \text{A-23}$$

$$Pr = \frac{\nu_o}{k_o/p_o C_{p_o}}$$

$$Ek = \frac{U^2_o}{C_{p_o}\Delta\overline{T}_o}$$

3. Comparison of laminar laboratory airflow model to a turbulent atmospheric prototype airflow:

Model		Field
$Re = \frac{U_o L_o}{\nu}$	$\equiv$	$R_{e_t} = \frac{U_o L_o}{K_i}$
$Pr = \frac{\mu C_p}{k}$	$\equiv$	$P_{r_t} = \frac{K_M}{K_H}$

$$Ri \equiv \frac{g_o}{T_o} \frac{\Delta T_o L_o}{U_o^2} \qquad \text{A-24}$$

$$Eu = \frac{\Delta p_o}{\rho U_o^2}$$

$$Ek = \frac{U_o^2}{C_p \Delta T_o}$$

For dispersion similarity,

$$Pe = \frac{U_o L_o}{k_m} \equiv Pe_t = \frac{U_o L_o}{K_c}$$

Partial Simulation

One of the most important practical problems that arises in laboratory simulation is the effect of not satisfying exactly all the similarity requirements. The situation in which the modeling criteria are not completely fulfilled is called partial simulation. In practice partial simulation is unavoidable since many similarity criteria impose diametrically opposing requirements on the scaling parameters. Thus, it is well known that in fluids with the same kinematic viscosity, simultaneous modeling of both Reynolds and Froude number is nearly impossible.

Unfortunately, it is clear that in the flow problems of the type discussed above all the similarity criteria cannot be satisfied simultaneously and that partial simulation becomes unavoidable. When dealing with the simulation of the above class of flow problems on a different scale one has to decide which of the similarity parameters are more important for a satisfactory description of the physical processes governing the problems.

Sundaram (Ref. 25) listed the various questions that arise in connection with the practical application of laboratory modeling techniques. The ones important are:

1) "Of all the various similitude parameters occurring in a given problem which ones are the most important?
2) "How accurately should the similarity parameters be reproduced in the laboratory and what are the effects of relaxing them?

3) "What range of values of these similarity parameters should any facility be capable of reproducing?
4) "How accurately should quantities be measured in a facility?"

The area of modeling in which the greatest amount of experience is available and in which there is abundant evidence of successful partial simulation is in the modeling of flow about objects, buildings, and prominant features of terrain. The principal concern in these problems has been in the simulation of the streamlines of mean flow and the location of wakes and eddies.

In simulating the flow around sharp-edged terrain features, since Reynolds number is not expected to influence the gross flow features it has been possible to duplicate the mean streamline, the regions of turbulent eddies, and probably even the coarse structure of the turbulence by providing geometrical similarity in the models. Examples of successful modeling in this type of flow problem have been conducted by Field and Warden (Ref. 13), Garrison and Cermak (Ref. 14) and Halitsky et al., (Ref. 19).

In the case of terrain features, such as hills and valleys, viscous effects may become important for gross flow features in a model and it is necessary to consider Reynolds number effects. In this case, the procedure in model experiments has been to match a model Reynolds number to a "turbulent" Reynolds number for the atmosphere, a number obtained by using a representative value of eddy viscosity. Studies in which this type of reasoning has been applied are Abe (Ref. 1) and Cermak and Peterka (Ref. 6).

Scale Distortion

Distorted geometric models are common in hydraulics and ocean engineering laboratory studies, but have not been used to any great extent in wind-tunnel modeling. A recent study has examined the problem in relation to modeling urban areas (Ref. 9). A complete examination of the distorted similarity problem has not been considered, however, Nemoto (Ref. 28) has analyzed some aspects of the problem.

Nemoto examined the equations of motion of a turbulent atmosphere and found that in case of vertical exaggeration the degree of distortion is related to K_x and K_z, the eddy-diffusion (viscosity) coefficients in the longitudinal and vertical directions. He found that the relation,

$$\alpha = \left[\frac{\left(\frac{K_x}{K_z} \right)_F}{\left(\frac{K_x}{K_z} \right)_M} \right]^{1/2} \qquad \text{A-25}$$

should be satisfied between α and the eddy-diffusion coefficients for the mean flow patterns to be similar for prototype and model. At the present time the difficulty of obtaining measurements of the eddy-diffusion coefficients in the field and model have hindered efforts to check this relation. However, the recent urban area study (Ref. 9) was an attempt to examine this relation in terms of a fully-rough flow in the wind tunnel.

GLOSSARY OF TERMS

Eckert No. $Ek = \frac{U_o^2}{C_{p_o}(\Delta T)_o}$ -- Nondimensional ratio between inertia force and a compression force. Equivalent to the Mach number.

$Ek = (\gamma-1)M^2$

$\gamma = C_p/C_u$

Euler No. $Eu = \frac{\Delta P_o}{\rho_o U_o^2}$ -- Nondimensional ratio between the pressure force and the inertia force.

Froude No. $Fr = \frac{U_o}{\sqrt{g_o L_o}}$ -- Nondimensional ratio between the inertia force and force of gravity.

Peclet No. $Pe = \frac{U_o L_o}{K_c}$ -- Nondimensional ratio between inertial force and mass diffusivity.

Prandtl No. $Pr = \frac{C_p \mu}{k}$ -- Nondimensional ratio between the product of heat advection and viscous forces and the product of heat diffusion and inertia forces.

$Pr_t = \frac{K_M}{K_H}$

Reynolds No. $Re = \frac{U_o}{L_o \nu_o}$ -- Nondimensional ratio of the inertial force to the viscous force.

$Re_t = \frac{U_o}{L_o K_{M_o}}$

Richardson No. $Ri = g_o \frac{1}{\theta_o} \frac{(\partial\theta/\partial z)_o}{(\partial U/\partial z)_o^2}$ -- Nondimensional number arising in the study of shearing flows of a stratified fluid. Number expresses a characteristic ratio of work done against gravitational stability to energy transferred from mean to turbulent motion.

Rossby No.	$Ro = \frac{U_o}{f_o L_o}$	-- Nondimensional ratio of the inertial force to the Coriolis force.

REFERENCES

1. Abe, M., 1941: Mountain clouds, their forms and connected air currents. Part II Bull. Centr. Met., Obs. of Japan, 7(3), 93-145.

2. Auer, A. H., Jr., D. L. Veal and J. D. Marwitz, 1970: Some observations of silver-iodide plumes within the Elk Mountain water resource observatory. The Journal of Weather Modification, Vol. 2, No. 1 (May), 122-131.

3. Bergeron, T., 1949: The problem of artificial control of rainfall on the globe. Tellus, 1, 32-50.

4. Bernstein, A. B., 1965: Dimensional analysis applied to the wind distribution in the planetary boundary layer. Monthly Weather Review, Vol. 93, No. 10 (October), 579-585.

5. Cermak, J. E., et al., 1966: Simulation of atmospheric motion by wind-tunnel flows. Fluid Dynamics and Diffusion Laboratory Report No. CER66JEC-VAS-ESP-GIB-HC-RNM-SI17, Colorado State University

6. Cermak, J. E., and J. Peterka, 1966: Simulation of wind fields over Point Arguello, California, by wind-tunnel flow over a topographic model. Final Report, CER65-JEC-JAP64, Colorado State University.

7. Chappell, C. F., 1970: Modification of cold orographic clouds. Atmospheric Science Paper No. 173, Department of Atmospheric Science, Colorado State University.

8. Chaudhry, F. H., and R. N. Meroney, 1969: Turbulent diffusion in a stably stratified shear layer. Technical Report C-0434-5, Fluid Dynamics and Diffusion Laboratory, Colorado State University.

9. Chaudhry, F. H. and J. E. Cermak, 1971: Simulation of flow and diffusion over an urban complex. Technical Report ECOM-0423-7; CER70-71FHC-JEC24, Fluid Dynamics and Diffusion Laboratory, Colorado State University.

10. Corby, G. A., 1954: The airflow over mountains - A review of the state of current knowledge. Q. Jour. Royal. Meteor. Society, Vol. 80, 491-521.

11. EG and G, 1970: Installation and operation of an opportunity recognition and cloud seeding system for operational weather modification research in Colorado. Phase I Comprehensive Field Report. Bureau of Reclamation Contract No. 14-06-D-6963, Boulder, Colorado.

12. Fanaki, F. H., 1971: A simulation of heat flow in the lower troposphere by a laboratory model. Boundary-Layer Meteorology, Vol. 1, 345-367.

13. Field, J. H. and R. Warden, 1929-30: A survey of air currents in the Bay of Gibraltar. Geophysical Memoirs No. 59 (Rand M1563), Her Majesty's Stationery Office.

14. Garrison, J. A. and J. E. Cermak, 1968: San Bruno mountain wind investigation. A wind-tunnel model study. Fluid Dynamics and Diffusion Laboratory Report CER67-68JEC-JAG58, Colorado State University.

15. Grant, L. O., 1963: Indications of residual effects from silver-iodide released into the atmosphere. Proceedings of Western Snow Conference, 109-115 and Atmospheric Science Technical Paper No. 49, Colorado State University.

16. Grant, L. O., J. E. Cermak and M. M. Orgill, 1968: Delivery of nucleating materials to cloud systems from individual ground generators. Proceedings of the Third Sky Water Conference on the Production and Delivery of Cloud Nucleating Materials, Colorado State University, 99-134.

17. Grant, L. O., C. F. Chappell and P. W. Mielke, Jr., 1968: The recognition of cloud seeding opportunity. Proceedings of the First National Conferences on Weather Modification, 372-385.

18. Grant, L. O., et al., 1969: Weather modification - An operational adaptation program for the Colorado River Basin. Interim Report, Bureau of Reclamation Contract No. 14-06-D-6467, Department of Atmospheric Science, Colorado State University.

19. Halitsky, J., G. A. Magony and P. Halpern, 1965: Turbulence due to topographical effects. Geophysical Sciences Laboratory Report No. TR66-5, New York University.

20. Hanna, S. R., 1969: The thickness of the planetary boundary layer. Atmospheric Environment, Vol. 3, 519-536.

21. Houghton, D. D. and A. Kasahara, 1968: Nonlinear shallow fluid flow over an isolated ridge. Communications on Pure and Applied Mathematics, Vol. 21, 1023.

22. Kitabayski, K., M. M. Orgill and J. E. Cermak, 1971: Laboratory simulation of airflow and atmospheric transport-dispersion over Elk Mountain, Wyoming. Technical Report CER70-71KK-MMO-JEC-65, Fluid Dynamics and Diffusion Laboratory, Colorado State University.

23. Ludlam, F. H., 1955: Artificial snowfall from mountain clouds. Tellus, Vol. 7, 277-290.

24. Lumley, J. L. and H. A. Ranofsky, 1964: The structure of atmospheric turbulence. Interscience Publishers, New York.

25. McVehil, G. E., G. R. Ludwig and T. R. Sundaram, 1967: On the feasibility of modeling small scale atmospheric motions. CAL Report No. ZB-2328-P-1. Cornell Aeronautical Laboratory, Buffalo, New York.

26. Marwitz, J. D., D. L. Veal, A. H. Auer and J. R. Middleton, 1969: Prediction and verification of the airflow over a three-dimensional mountain. Technical Report 60, Natural Resources Research Institute, University of Wyoming.

27. Natural Resources Research Institute, 1969: Atmospheric water resources research. Final Report, Bureau of Reclamation Contract No. 14-06-D-6002, University of Wyoming.

28. Nemoto, S., 1961: Similarity between natural wind in the atmosphere and model wind in a wind-tunnel - Modeling criteria for a local wind. Papers in Meteorology and Geophysics, Vol. 12, Vol. 1, 30-52.

29. Nemoto, S., 1962: Similarity between natural wind in the atmosphere and model wind in a wind tunnel - Modeling criteria for a local wind. Papers in Meteorology and Geophysics, Vol. 13, No. 2, 171-195.

30. Orgill, M. M., J. E. Cermak and L. O. Grant, 1971: Laboratory simulation and field estimates of atmospheric transport - dispersion over mountainous terrain. Technical Report CER70-71MMO-JEC-LOG40. Fluid Dynamics and Diffusion Laboratory, Colorado State University.

31. Orgill, M. M., 1971: Research and development technique for estimating airflow and diffusion parameters in connection with the atmospheric water resources program. Interim Report. Fluid Dynamics and Diffusion Laboratory, Colorado State University.

32. Super, A. B., 1971: Some problems of winter weather modification in mountainous terrain. Paper presented at American Meteorological Conference on Atmospheric Waves. October 12-15, 1971, Salt Lake City, Utah.

33. Sutton, O. G., 1953: Micrometeorology. McGraw-Hill, New York.

34. U.S. Atomic Energy Commission, 1968: Meteorology and Atomic Energy. USAEC Division of Technical Information, Oak Ridge, Tennessee.

35. Willis, P. T., 1970: A parameterized numerical model of orographic precipitation. EG and G Report. Contract No. 14-06-D-5640, EG and G, Inc., Boulder, Colorado.

BIBLIOGRAPHY

List of Reports and Papers Written in Relation to This Project

1. Grant, L. O., J. E. Cermak and M. M. Orgill, 1968: Delivery of nucleating materials to cloud systems from individual ground generators. Proceedings of the Third Skywater Conference on the Production and Delivery of Cloud Nucleating Materials, Colorado State University, 99-134.

2. Cermak, J. E., M. M. Orgill and L. O. Grant, 1969: Research and development of techniques for estimating airflow and diffusion parameters in connection with the atmospheric water resources program. Interim Report CER68-69JEC-LOG-MMO27. Colorado State University.

3. Cermak, J. E., M. M. Orgill and L. O. Grant, 1969: Research and development of techniques for estimating airflow and diffusion parameters in connection with the atmospheric water resources program. Final Report CER69-70JEC-LOG-MMO11. Colorado State University.

4. Cermak, J. E., M. M. Orgill and L. O. Grant, 1970: Research and development of techniques for estimating airflow and diffusion parameters in connection with the atmospheric water resources program. Interim Report. Colorado State University.

5. Cermak, J. E., M. M. Orgill and L. O. Grant, 1970: Laboratory simulation of atmospheric motion and dispersion over complex topography as related to cloud seeding operations. Second National Conference on Weather Modification, Santa Barbara, California, 59-65.

6. Orgill, M. M., J. E. Cermak and L. O. Grant, 1970: Research and development of techniques for estimating airflow and diffusion parameters in connection with the atmospheric water resources program. Annual Report CER70-71MMO-JEC-LOG23. Colorado State University.

7. Orgill, M. M., J. E. Cermak and L. O. Grant, 1971: Laboratory simulation and field estimates of atmospheric transport-dispersion over mountainous terrain. Technical Report. CER70-71MMO-JEC-LOG40. Fluid Dynamics and Diffusion Laboratory, Colorado State University.

8. Orgill, M. M., J. E. Cermak and L. O. Grant, 1971: Research and development of techniques for estimating airflow and diffusion parameters in connection with the atmospheric water resources program. Interim Report. Contract No. 14-06-D-6842, Fluid Dynamics and Diffusion Laboratory, Colorado State University.

9. Kitabayshi, K., M. M. Orgill and J. E. Cermak, 1971: Laboratory simulation of airflow and atmospheric transport-dispersion over Elk Mountain, Wyoming. Technical Report CER70-71KK-MMO-JEC65, Fluid Dynamics and Diffusion Laboratory, Colorado State University.

10. Grant, L. O., C. F. Chappell and P. W. Mielke, Jr., 1971: The Climax experiment for seeding cold orographic clouds. Paper presented at the International Conference on Weather Modification. American Meteorological Society and Australian Academy of Sciences, September 6-11, 1971, Canberra, Australia.